Action of zona pellucida glycoproteins in mouse and human sperm

Dissertation

zur Erlangung des Doktorgrades (Dr. rer. nat.)

der Mathematisch-Naturwissenschaftlichen Fakultät

der Rheinischen Friedrich-Wilhelms-Universität Bonn

vorgelegt von

Melanie Balbach

aus

Bad Mergentheim

Bonn, 2017

Angefertigt mit Genehmigung der Mathematisch-Naturwissenschaftlichen
Fakultät der Rheinischen Friedrich-Wilhelms-Universität Bonn

1. Gutachter: Prof. Dr. D. Wachten
2. Gutachter: Prof. Dr. C. Thiele
3. Gutachter: Prof. Dr. O. Gruss
4. Gutachter: Prof. Dr. U. Vothknecht
Tag der Promotion: 19. 06. 2017
Erscheinungsjahr: 2017

Summary

For fertilization, sperm have to penetrate the oocyte's vestment, the zona pellucida (ZP). In mouse and human, the ZP consists of three or four different ZP glycoproteins, respectively. Binding of sperm to ZP glycoproteins evokes sperm hyperactivation and acrosome reaction, which enables sperm to penetrate the ZP. However, the ZP-induced signaling pathways underlying these behavioral responses are ill-defined. Therefore, in my thesis I investigated ZP signaling in mouse and human sperm. In both species, mixing with ZP glycoproteins evoked rapid changes in intracellular pH (pH_i) and intracellular Ca^{2+} concentration ($[Ca^{2+}]_i$). I was able to confirm that the sperm-specific Ca^{2+} channel CatSper mediates the ZP-evoked Ca^{2+} influx in mouse and human sperm. However, my experiments demonstrate that the molecular mechanism underlying CatSper activation by ZPs are distinctively different in mouse and human. In human sperm, CatSper activation does not require pH_i alkalization. Here, human ZP glycoproteins directly activate CatSper. However, in mouse sperm, the alkalization is essential for the ZP-evoked Ca^{2+} influx via CatSper. Moreover, my experiments reveal that ZP-induced alkalization is mediated by different proteins in mouse and human. In mouse sperm, ZP-evoked alkalization requires extracellular Na^+; however, the prominent candidate to control ZP-evoked alkalization, the sperm-specific Na^+/H^+ exchanger, is not fulfilling this function. My results rather demonstrate that another protein of the Na^+/H^+ exchanger family, the sodium-proton antiporter 1 (NHA1), controls ZP-evoked alkalization. In NHA1 KO mice, the ZP-evoked increase in pH_i and $[Ca^{2+}]_i$ was strongly attenuated. The mechanism underlying NHA1 activation remains, however, elusive. ZP-evoked alkalization was suppressed under depolarized membrane potentials, indicating that a polarized membrane potential is crucial for NHA1 activation. In human sperm, a polarized membrane potential was also required for ZP-evoked pH_i signaling, however, ZP-evoked alkalization is, in contrast to mouse sperm, not mediated by a Na^+/H^+ exchange. My work provides important new insights into the molecular mechanism underlying the action of ZP glycoproteins in mouse and human sperm and reveals fundamental differences between the two species, questioning the mouse as appropriate model system to study fertilization in human.

Zusammenfassung

Für die Befruchtung ist entscheidend, dass das Spermium die äußere Eihülle, die *Zona pellucida* (ZP) penetriert. In der Maus besteht die ZP aus jeweils drei, im Menschen aus vier verschiedenen ZP Glykoproteinen. Bindet ein Spermium an die ZP Glykoproteine, wird im Spermium eine Hyperaktivierung und die Akrosomreaktion ausgelöst. Das ermöglicht dem Spermium die ZP zu penetrieren. Der ZP-induzierte Signalweg, der diesen Verhaltensänderungen zu Grunde liegt, ist jedoch weitgehend unbekannt. In meiner Doktorarbeit habe ich die ZP-abhängigen Signalwege in humanen und murinen Spermien analysiert. In beiden Spezies induzieren ZP Glykoproteinen schnelle Änderungen des intrazellulären pH-Werts (pH_i) und der intrazellulären Calciumkonzentration ($[Ca^{2+}]_i$). Ich konnte zeigen, dass der spermienspezifische Calciumkanal CatSper für den ZP-induzierten Calciumanstieg in humanen und murinen Spermien verantwortlich ist, der molekulare Mechanismus der CatSper Aktivierung unterscheidet sich jedoch grundlegend zwischen Mensch und Maus. In humanen Spermien wird CatSper direkt durch ZP Glykoproteine aktiviert. In Mäusespermien ist dagegen eine Alkalisierung des pH_i essentiell für den CatSper vermittelten, ZP-induzierten Calciumanstieg. Darüber hinaus zeigen meine Experimente, dass die ZP-induzierte Alkalisierung in Mensch und Maus durch verschiedene Proteine vermittelt wird. In Mäusespermien ist die ZP-induzierte Alkalisierung abhängig von der extrazellulärem Na^+-Konzentration. Der Spermien-spezifische Na^+/H^+ Austauscher war der naheliegendste Kandidat, spielt jedoch für die Regulation der ZP-induzierten Alkalisierung keine Rolle. Verantwortlich hierfür ist ein anderes Mitglied aus der Na^+/H^+ Austauscher-Familie, der Natrium/Protonen-Antiporter 1 (NHA1). In NHA1 KO Mäusen ist der ZP-induzierte Anstieg in pH_i und $[Ca^{2+}]_i$ deutlich reduziert. Es ist jedoch unklar wie NHA1 aktiviert wird. Die ZP-induzierte Alkalisierung ist unter depolarisiertem Membranpotential unterdrückt, was darauf hindeutet dass die Aktivierung von NHA1 ein polarisiertes Membranpotential erfordert. Auch in humanen Spermien ist ein polarisiertes Membranpotential entscheidend für die ZP-induzierte Alkalisierung. Im Gegensatz zu Mäusespermien wird die ZP-induzierte Alkalisierung jedoch nicht über einen Na^+/H^+ Austauscher vermittelt. Meine Arbeit bietet wichtige neue Einblicke in den molekularen Mechanismus des ZP-induzierten Signalwegs in Spermien aus Maus und Mensch und enthüllt entscheidende Unterschiede im molekularen Mechanismus zwischen den beiden Spezies.

Index

List of figures

List of abbreviations

α	anti
µ	micro
8-Br-cAMP	8-bromoadenosine 3',5'-cyclic monophosphate
AR	acrosome reaction
BAPTA	1,2-bis(o-aminophenoxy)ethane-N,N,N',N'-tetraacetic acid
BCECF	2',7'-bis-(2-carboxyethyl)-5-(and-6)-carboxyfluorescein
BSA	bovine serum albumin
°C	degree celicus
$[Ca^{2+}]_i$	intracellular Ca^{2+} concentration
cAMP	cyclic adenosine monophosphate
CatSper	cation channel of sperm
CFCS	conserved furin cleavage site
$[Cl^-]_o$	extracellular chloride concentration
DMEM	Dulbecco's Minimal Essential Media
DMSO	dimethylsulfoxide
DTT	dithiothreitol
EC_{50}	half-maximal effective concentration
ECL	enhanced chemical luminescence
E. Coli	*Escherichia Coli*
EDTA	ethylenediamintetraacetic acid
EF	empty fraction
et al.	*et alibi*
$\Delta F/F_0$	relative change in fluorescence intensity

FCS	fetal calf serum
fig.	figure
g	gram
h	hour
HA-tag	hemagglutinin tag
hCG	human chorionic gonadotropin
HEK	human embryonic kidney cells
HEPES	2-(4-(2-hydroxyethyl)-1-piperazine)ethanesulfonic acid
HRP	horse-radish peroxidase
HSA	human serum albumin
HTF	human tubular fluid
IU	injection units
$[K^+]_o$	extracellular potassium concentration
K_D	dissociation constant
kDa	kilodalton
K8.6	depolarizing TYH with alkaline pH
l	liter
M	molar
MEM	Minimum Essential Media
$[Mg^{2+}]_o$	extracellular magnesium concentration
mM	millimolar
ms	millisecond
min	minutes
MW	molecular weight
mPIC	Mammalian Protease Inhibitor Cocktail

$[Na^+]_0$	extracellular sodium concentration
NHA1	sodium-hydrogen antiporter 1
NHE	sodium-proton exchanger
OD	optical density
p.A.	pro analysi
PAGE	polyacrylamide gel electrophoresis
PCR	polymerase chain reaction
PFA	paraformaldehyde
pH_i	intracellular pH
pH_o	extracellular pH
PKA	protein kinase A
PMCA	plasma membrane Ca^{2+} ATPase
PMSG	pregnant mare's serum gonadotropin
PVDF	polyvinylidene fluoride
ΔR/R	relative change in fluorescence ratio
RT	room temperature (about 21 °C)
s	seconds
SACY	soluble adenylate cyclase Y
SDS	sodium dodecyl sulfate
sNHE	sperm-specific sodium proton exchanger
STORM	stochastic optical reconstruction microscopy
TAPS	N-tris(hydroxymethyl)methyl-3-aminopropanesulfonic acid
TE	tris-EDTA
TEMED	tetramethylethylendiamine
Tris	tris(hydroxymethyl)aminomethane

TYH	Toyoda Yokoyama Hoshi
V_M	membrane potential
VSD	voltage-sensing domain
% v/v	percent by volume
% w/v	weight by volume
µM	micromolar
ZP	zona pellucida

Amino acids:

A	Alanine	L	Leucine
R	Arginine	K	Lysine
N	Asparagine	M	Methionine
D	Aspartic acid	F	Phenylalanine
C	Cysteine	P	Proline
Q	Glutamine	S	Serine
E	Glutamic acid	T	Threonine
G	Glycine	W	Tryptophan
H	Histidine	Y	Tyrosine
I	Isoleucine	V	Valine

1 Introduction

1.1 Fertilization in mammals

In sexual reproduction, fusion of a male and a female gamete is the beginning of new life. The immotile oocyte provides the maternal genome and contains the inventory required to initiate and maintain embryo development. In mouse and human, the oocyte has a diameter of about 70 µm and 120 µm, respectively (Griffin *et al.*, 2006; van den Hurk & Zhao, 2005). The mammalian oocyte is surrounded by two vestments: the zona pellucida (ZP), a matrix of glycoproteins, and the cumulus oophorus (fig. 1.1a). The ZP protects the oocyte and the developing embryo against the environment (Yanagimachi, 1994), mediates the first interaction between gametes during fertilization, and prevents polyspermy (Wassarman, 2008). The cumulus oophorus, a multilayered mass of cumulus cells embedded in a hyaluronic acid-rich matrix, supports oocyte development and maturation (Huang & Wells, 2010; Van Soom *et al.*, 2002).

The motile sperm harbor the paternal genome and deliver this good to the oocyte. Human and mouse sperm differ considerably in size: human sperm are about 55 µm long, while mouse sperm are about 125 µm in length. Sperm can be divided structurally into the head containing the tightly packed DNA, and the flagellum, conveying sperm motility. The flagellum is subdivided into midpiece, principal piece, and endpiece. Typical for rodents, mouse sperm have a sickle-shaped head with a small apical hook (fig. 1.1b), whereas the head of human sperm is spatual-shaped (fig. 1.1c). The acrosome, a Golgi-derived vesicle, occupies the anterior region of

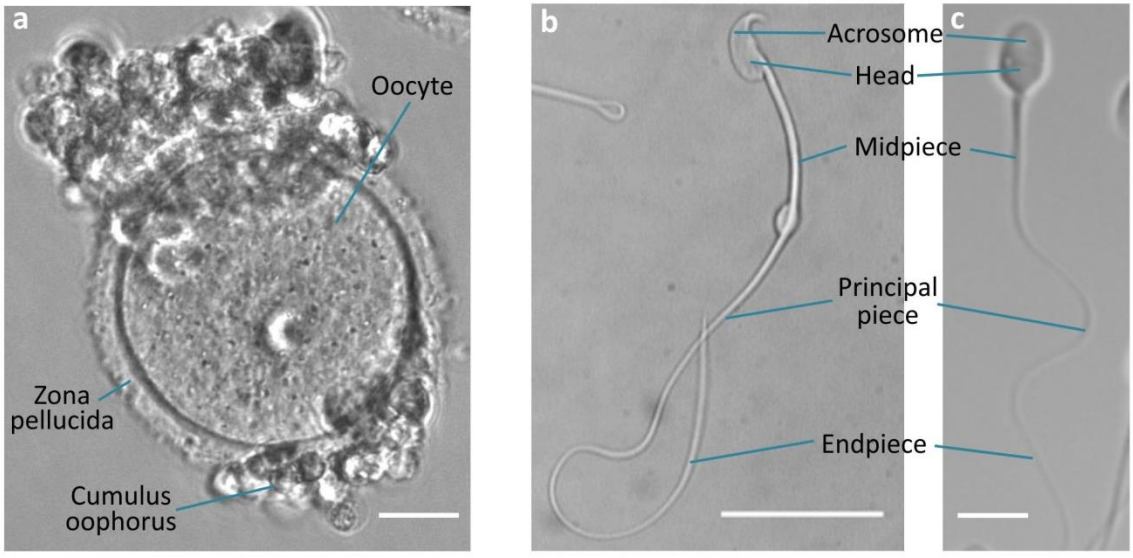

Fig. 1.1: Male and female gamete

(a) Murine oocyte; scale bar: 20 µm. **(b**) Murine sperm; scale bar: 20 µm. **(c)** Human sperm; scale bar: 10 µm.

the mammalian sperm head and is surrounded by the outer and inner acrosomal membrane, respectively.

Sperm acquire the ability to swim during their passage across the epididymis (Dacheux & Dacheux, 2013; Soler *et al.*, 1994; Yeung *et al.*, 1993). Upon ejaculation, mammals release millions of sperm into the vagina. Freshly ejaculated sperm are unable to fertilize the oocyte. The fertilization competence is acquired inside the female genital tract, a process termed capacitation. *In vitro*, bicarbonate (HCO_3^-), albumin, and Ca^{2+} (Visconti *et al.*, 1995) are required for capacitation, which involves an ill-defined signaling cascade, resulting in complex changes in the biochemical, physiological, and cellular properties of sperm. A Na^+/HCO_3^- cotransporter transports HCO_3^- across the plasma membrane (Demarco *et al.*, 2003), where it activates the atypical soluble adenylate cyclase (SACY), which synthesizes cyclic adenosine monophosphate (cAMP) (Buck *et al.*, 1999; Okamura *et al.*, 1985; Wandernoth *et al.*, 2010). cAMP drives a signaling cascade mediated by protein kinase A (Nolan *et al.*, 2004; Visconti *et al.*, 1995), which in turn activates tyrosine kinases (Alvau *et al.*, 2016; Baker *et al.*, 2006; Battistone *et al.*, 2014; Varano *et al.*, 2009), resulting in tyrosine phosphorylation of ion channels, metabolic enzymes, and structural proteins (Chung *et al.*, 2014; Ficarro *et al.*, 2003; Visconti *et al.*, 1995). Concurrently, plasma membrane phospholipids are redistributed (Boerke *et al.*, 2008; Flesch *et al.*, 2001; Gadella & Harrison, 2000) and cholesterol and glycoproteins are removed (Osheroff *et al.*, 1999; Visconti *et al.*, 1999), which in turn alters the physiochemical properties of the plasma membrane. Moreover, capacitation increases the intracellular pH (pH_i), (Vredenburgh-Wilberg & Parrish, 1995; Zeng *et al.*, 1996), the intracellular Ca^{2+} concentration ($[Ca^{2+}]_i$) (Baldi *et al.*, 1991; Ruknudin & Silver, 1990), and hyperpolarizes the sperm membrane potential (V_M) (Arnoult *et al.*, 1999; Zeng *et al.*, 1995).

During the transit trough the female reproductive tract, sperm undergo a vigorous selection process and only about 10-20 sperm arrive at the oocyte in the distal part of the oviduct (Chang & Suarez, 2012; Ishikawa *et al.*, 2016). How mammalian sperm navigate inside the female genital tract is a matter of debate. Sperm guidance is presumably regulated by thermotaxis and rheotaxis, which refers to a directed movement up a temperature gradient and swimming against a fluid flow, respectively (Bahat *et al.*, 2003; Kantsler *et al.*, 2014; Miki & Clapham, 2013; Oliveira *et al.*, 1999). Additionally, sperm chemotaxis in response to a gradient of chemoattractants released by the oocyte and the cumulus oophorus was proposed as guiding mechanism (Kaupp *et al.*, 2008; Oliveira *et al.*, 1999; Ralt *et al.*, 1994).

After reaching the oocyte, sperm have to penetrate trough the cumulus oophorus and the ZP. This is facilitated by sperm hyperactivation and the acrosome reaction. Hyperactivated sperm display a high-amplitude, asymmetrical flagellar beat with increased flagellar force (Bastiaan & Franken, 2007; Chiu *et al.*, 2008b; Morales *et al.*, 1988). Where exactly hyperactivated motility

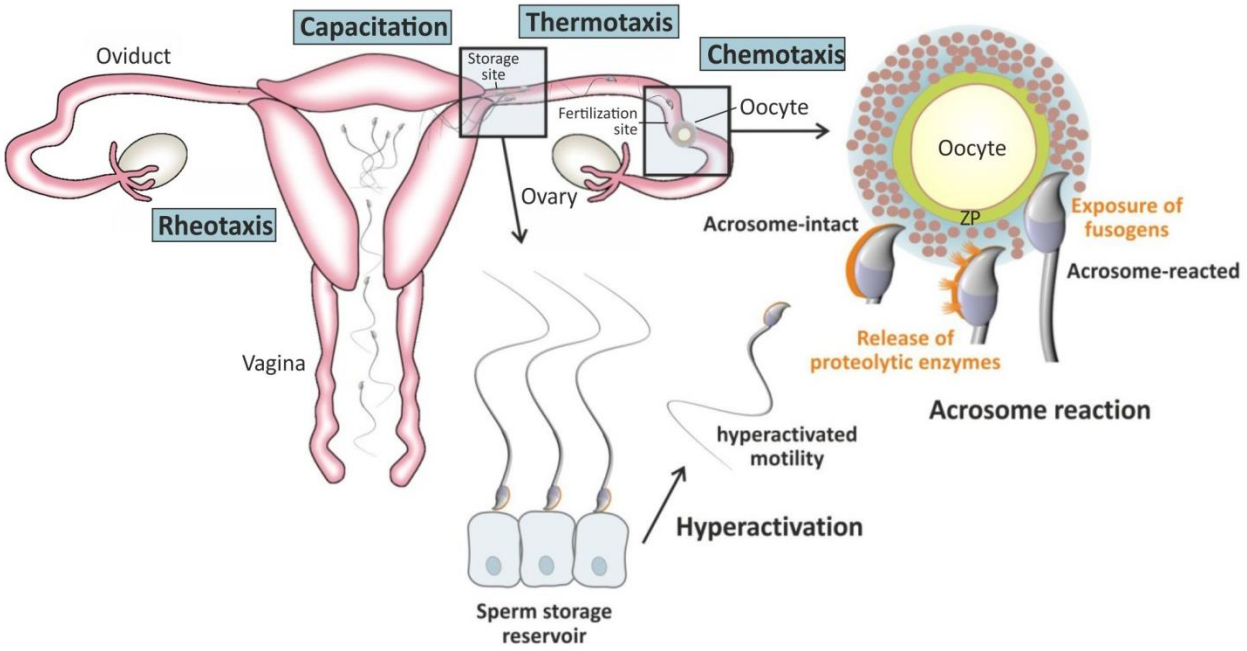

Fig. 1.2: Mammalian fertilization

Freshly ejaculated sperm are not able to fertilize. Sperm develop fertilization competence during transit trough the female reproductive tract. This maturation process is termed capacitation. Sperm localize the oocyte in the oviduct presumably by rheotaxis, thermotaxis, and chemotaxis. After entering the oviduct, sperm are trapped in a sperm storage reservoir by binding to the oviductal epithelium. Sperm are hyperactivated while releasing themselves from this reservoir now displaying more vigorous, assymetric flagellar beating. The site of the acrosome reaction has been located to the cumulus oophorus and the ZP. During acrosomal exocytosis hydrolytic enzymes are released, which loosen the cumulus oophorus and the ZP. In parallel, fusogens on the inner acrosomal membrane are exposed, which enables sperm to fuse with the oocyte`s plasma membrane.

is evoked during the transit trough the female genital tract is a matter of debate. It has been suggested that sperm undergo hyperactivation to detach from the oviductal epithelium (Chang & Suarez, 2012; Demott & Suarez, 1992; Pacey *et al.*, 1995). Moreover, in human sperm, ZP glycoproteins and follicular fluid induce hyperactivated motility (Bastiaan & Franken, 2007; Chiu *et al.*, 2008b; Mbizvo *et al.*, 1990).

The acrosome reaction is triggered by a sustained Ca^{2+} increase evoked by oocyte-associated factors. These factors seem to activate phospholipase C (PLC) (Fukami *et al.*, 2003), which hydrolyses PIP2 resulting in IP3 and diacylglycerol. Reportedly, IP3 mobilizes Ca^{2+} from the acrosome (Rossato *et al.*, 2001), which further increases $[Ca^{2+}]_i$ through store-operated Ca^{2+} entry (Florman, 1994; Jungnickel *et al.*, 2001; O'Toole *et al.*, 2000), resulting in fusion and vesiculation of the outer acrosomal membrane and the sperm plasma membrane. Thereby, proteolytic enzymes such as acrosin and hyaluronidase are released (Bleil & Wassarman, 1983;

Chiu *et al.*, 2010; Florman *et al.*, 1999; Liu *et al.*, 2007b), which loosen the cumulus oophorus and digest the ZP (Adham *et al.*, 1997; Kawano *et al.*, 2010; Kimura *et al.*, 2009). In parallel, sperm fusogens on the inner acrosomal membrane are exposed or activated, converting the sperm into a fusion-competent state (Saling *et al.*, 1979; Yanagimachi, 1994). One example for these fusogens in mouse and human sperm is Izumo1, a sperm-specific protein of the immunoglobulin family (Inoue *et al.*, 2005). Izumo1 interacts with its oocyte surface receptor Juno, a member of the folate receptor family (Bianchi *et al.*, 2014). After fusion of sperm and oocyte, the paternal DNA is released into the oocyte and forms the male pronucleus. With the fusion of male and female pronuclei, fertilization is complete.

1.2 Zona pellucida glycoproteins

The ZP surrounds the oocyte and the embryo up to the early blastocyst stage of development. Composed of a meshwork of long, interconnected filaments, the ZP has a porous, elastic structure (Fig. 1.3a) (Wassarman, 2008). In mouse and human, the ZP is ~6 µm and ~19 µm thick, respectively (Bertrand *et al.*, 1995; Wassarman *et al.*, 1998) and consists of heavily glycosylated ZP glycoproteins (Jiménez-Movilla *et al.*, 2004; Wassarman, 2008). In mouse, there are three different ZP glycoproteins: ZP1 (~200 kDa), ZP2 (~120 kDa), and ZP3 (~83 kDa) (Wassarman, 1988), whereas in humans, there are four ZP glycoproteins: ZP1 (~100 kDa), ZP2 (~120 kDa), ZP3 (~58 kDa), and ZP4 (~65 kDa) (Bauskin *et al.*, 1999; Chiu *et al.*, 2008b; Lefievre *et al.*, 2004). In mouse, *ZP4* is a pseudogene (Goudet *et al.*, 2008). Ultrastructural analysis of mouse oocytes has demonstrated that ZP2 and ZP3 polymerize into 2-3 µm long filaments, which are crosslinked by ZP1 dimers (Fig. 1.3b) (Green, 1997; Wassarman & Mortillo, 1991). Thereby, ZP2 and ZP3 are equally abundant, but four-times more frequently present than ZP1 (Epifano *et al.*, 1995). In mice lacking ZP1, the ZP is more loosely organized, considerably thinner, and less well associated with oocytes (Rankin *et al.*, 1999). In ZP2-deficient mice, a thin ZP, consisting of ZP1 and ZP3, was detected in early follicles, which is not sustained in pre-ovulatory oocytes (Rankin *et al.*, 2001). Follicles of ZP3-deficient mice do, however, not develop a ZP at all (Liu *et al.*, 1996). These data suggest that two ZP glycoproteins are sufficient for ZP formation in mouse. One must be ZP3, the other one can be either ZP1 or ZP2. The ultrastructure of human ZP is unknown. An infertile female patient, carrying a homozygous deletion of *ZP1*, did not form of a ZP (Huang *et al.*, 2014), suggesting a difference in the ZP structure of mouse and human oocytes.

The ZP in mouse and human is required for oocyte and early embryo development. ZP1-deficient females are subfertile because the structure of the ZP is compromised causing precocious hatching of oocytes and early embryos (Rankin *et al.*, 1999). The loss of ZP2 or ZP3 results in a considerable decrease in the amount of oocytes after ovulation and impaired early embryo development resulting in female infertility (Liu *et al.*, 1996; Rankin *et al.*, 1996; Rankin *et al.*, 2001). In humans, ZP dysmorphology could be correlated with compromised oocyte

development, impaired embryo implantation and subsequent reduction in pregnancy rates (Huang *et al.*, 2014; Sauerbrun-Cutler *et al.*, 2015).

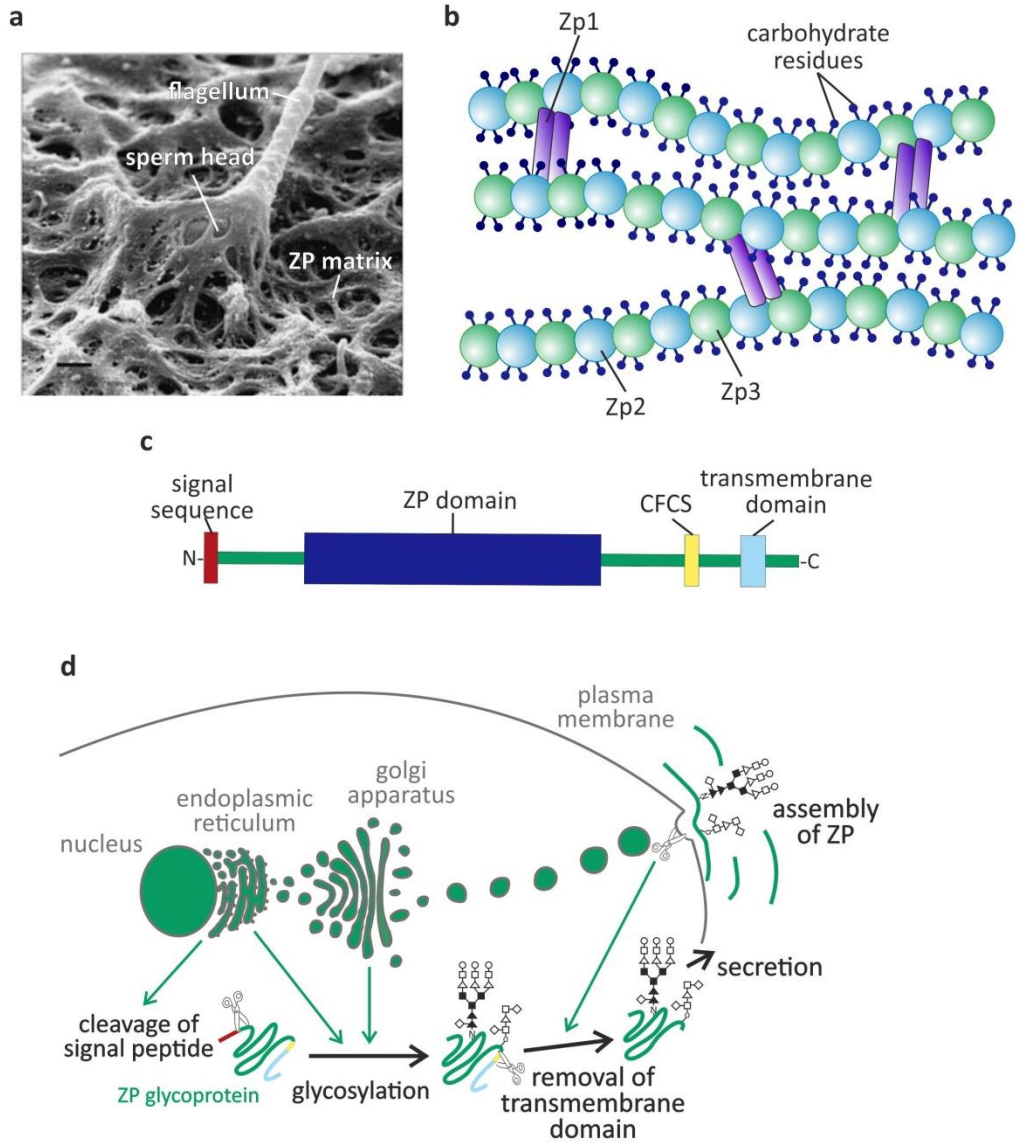

Fig. 1.3: Structure and assembly of the zona pellucida

(a) Mouse sperm penetrating the filamentous zona pellucida (from Michelmann *et al.*, 2006). **(b)** In mouse, ZP2 and ZP3 form long filaments that are interconnected by ZP1 dimers (adapted from Wasserman, 1988). **(c)** The polypeptide chains of ZP glycoproteins in mouse and human include an amino-terminal secretory signal peptide (red), a ZP-domain (blue), a consensus furin cleavage site (CFCS; yellow), and a transmembrane domain (light blue); adapted from Wassarman *et al.*, 2004. **(d)** Posttranscriptional processing of ZP glycoproteins comprises cleavage of the secretory signal peptide, glycosylation and removal of the transmembrane domain prior to secretion and assembly into ZP; modified from Kiefer *et al.*, 2002.

ZP glycoproteins are generated as precursor polypeptides, possessing an amino-terminal secretory signal peptide, a ZP domain, and a consensus furin cleavage site upstream of the carboxy-terminal transmembrane domain (Fig. 1.3c) (Callebaut *et al.*, 2007; Jovine *et al.*, 2005; Jovine *et al.*, 2002). Following cleavage of the secretory signal peptide, ZP precursors are heavily glycosylated in the endoplasmic reticulum and the Golgi (Fig. 1.3d). The membrane-anchored ZP precursors are then packaged into vesicles, which fuse with the plasma membrane of the oocyte. At the oocyte plasma membrane, ZP precursors are proteolytically cleaved, removing the transmembrane domain, allowing secretion of ZP glycoproteins and assembly into the ZP (Kiefer & Saling, 2002; Qi *et al.*, 2002). It is still a matter of debate, whether ZP glycoprotein secretion is facilitated by cleavage at the consensus furin cleavage site (Litscher *et al.*, 1999; Williams & Wassarman, 2001) or by a different mechanism (Zhao *et al.*, 2002).

The ZP plays a pivotal role during critical steps of fertilization by facilitating 1) species-specific gamete recognition, 2) primary sperm-oocyte interaction, 3) induction of the acrosome reaction, and 4) post-fertilization block to avoid polyspermy (Fig. 1.4).

To prevent cross-species fertilization, a species-specific interaction between sperm and oocyte is required. Removal of the ZP allows for fertilization by foreign sperm (Hanada & Chang, 1978; Yanagimachi *et al.*, 1976), demonstrating that the ZP acts as barrier for cross-species sperm-oocyte fusion. Mouse sperm are able to bind to the human oocyte, but cannot penetrate it, whereas human sperm are not able to bind to mouse oocytes and fail to penetrate the ZP (Bedford, 1977).

After sperm overcome the cumulus oophorus, the ZP mediates the primary interaction between sperm and oocyte. This initial adhesion is a high-affinity event, involving about 30.000 binding sites within the ZP (Thaler & Cardullo, 1996), tethering sperm to the surface of the oocyte. However, it is still a matter of debate, which ZP glycoprotein serves as the oocyte`s sperm receptor. When mouse sperm were pre-incubated with purified ZP glycoproteins *in vitro*, only ZP3 inhibited binding between sperm and the ZP. Therefore, it has been proposed that ZP3 serves as the primary sperm binding protein (Beebe *et al.*, 1992; Bleil & Wassarman, 1980, 1983; Gupta & Bhandari, 2011). ZP2 was suggested to be involved in secondary binding of acrosome-reacted sperm (Bleil *et al.*, 1988; Tsubamoto *et al.*, 1999). However, human sperm bind to the ZP of humanized transgenic mouse oocytes only when expressing human ZP2, but not human ZP1, ZP3, or ZP4 (Baibakov *et al.*, 2012). Moreover, when mouse ZP2 was substituted by human ZP4, ZP binding was abolished and mice were infertile (Avella *et al.*, 2014). The sperm binding region in mouse and human ZP2 could be narrowed down to a species-specific domain near the N-terminus (Avella *et al.*, 2014). Altogether, these results suggest that ZP2 rather than ZP3 serves as the primary sperm binding protein in both species.

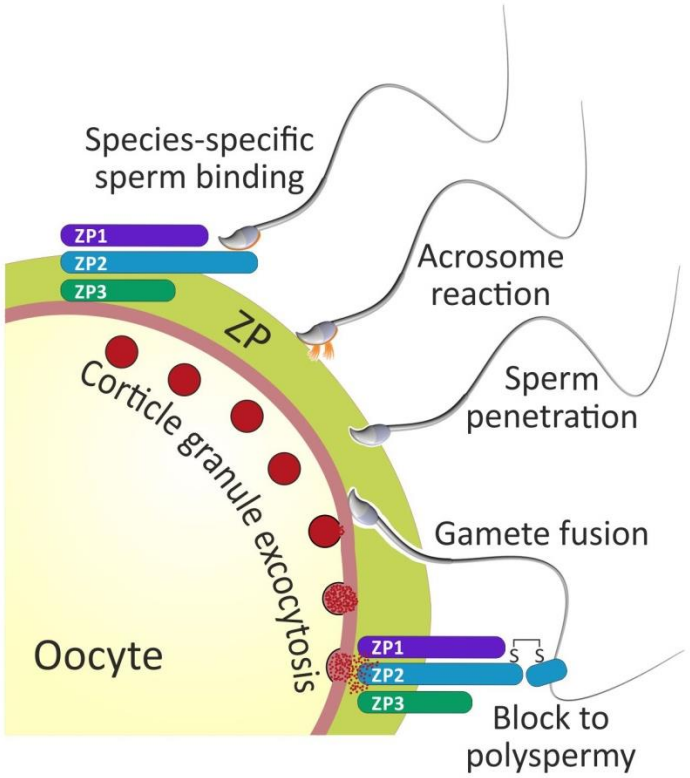

Fig. 1.4: The zona pellucida plays a pivotal role during fertilization

Species-specific interaction between sperm and oocyte is mediated by the zona pellucida (ZP). Sperm have been proposed to bind to an N-terminal domain of ZP2. Sperm undergo the acrosome reaction, penetrate the ZP, and fuse with the oocyte`s plasma membrane. Fertilization triggers cortical granule exocytosis, which leads to cleavage of ZP2 and ZP hardening. This postfertilization block to polyspermy prevents additional sperm from penetrating trough the ZP matrix.

Moreover, the ZP plays a role in the postfertilization block of polyspermy, avoiding the formation of non-viable, polyploid embryos. In mouse, fertilization triggers the release of proteases and glycosidases from membrane-bound, secretory organelles termed cortical granules. Cortical granule exocytosis causes mechanical hardening of the ZP (Wolf & Hamada, 1977), which renders the ZP impassable for sperm (Braden *et al.*, 1954). ZP hardening is caused by proteolytic cleavage of ZP2 (120 kDa) into its “fertilized” form $ZP2_f$ (90 kDa), mediated by the metalloproteinase ovastacin (Burkart *et al.*, 2012; Moller & Wassarman, 1989). Human ZP2 is also cleaved into $ZP2_f$ after fertilization, presumably also due to the release of cortical granules (Bauskin *et al.*, 1999).

1.3 Ion channels and transporters required for sperm fertility

In mouse and human sperm, navigation and fertilization of the oocyte are triggered and coordinated by changes in pH_i, V_M, and $[Ca^{2+}]_i$, mediated by a unique interplay of ion channels and transporters.

1.3.1 CatSper, the principal sperm Ca^{2+} channel

CatSper (cation channel of sperm) is the principal Ca^{2+} channel in human and mouse sperm (Lishko & Kirichok, 2010; Quill *et al.*, 2001; Ren *et al.*, 2001). CatSper is localized in the principal piece of the flagellum in mouse and human sperm (Ren *et al.*, 2001; Tamburrino *et al.*, 2015). The heteromeric CatSper channel complex is made up of at least nine different subunits. The four homologous α subunits (CatSper 1-4) (Navarro *et al.*, 2008; Qi *et al.*, 2007) form the channel pore, whereas CatSper β, γ, δ, ε, and ζ represent auxiliary subunits that associate with the pore-forming complex (Chung *et al.*, 2017; Chung *et al.*, 2011; Liu *et al.*, 2007a; Wang *et al.*, 2009). Characteristic for voltage-gated ion channels, each pore-forming subunit harbors six transmembrane repeats (S1 - S6) with positively charged amino acid residues in S4. The pore motif is located between S5 and S6 and carries the signature sequence of Ca^{2+}-selective channels, TxWxD. The flagella of CatSper ζ-deficient sperm are inflexible from the midpiece midway down the principal piece and male are subfertile (Chung *et al.*, 2017). Male mice deficient for CatSper 1-4 or CatSper δ display normal sperm morphology and basal motility but are infertile (Carlson *et al.*, 2005; Chung *et al.*, 2011; Jin *et al.*, 2007; Ren *et al.*, 2001). In humans, mutations in CatSper 1 and CatSper 2 are associated with male infertility (Avenarius *et al.*, 2009; Avidan *et al.*, 2003). The CatSper channel complex forms a quadrilateral arrangement along the sperm flagellum, which serves as a platform to organize Ca^{2+} signaling domains (Chung *et al.*, 2014). Knocking out any of the CatSper subunits destroys the organization of these Ca^{2+} signaling domains and impairs hyperactivated motility (Carlson *et al.*, 2003; Chung *et al.*, 2017; Chung *et al.*, 2014; Quill *et al.*, 2003). Sperm lacking these Ca^{2+} signaling domains are, therefore, unable to penetrate and fertilize the oocyte, unless the ZP is manually removed (Quill *et al.*, 2001; Ren *et al.*, 2001). Moreover, rheotaxis is abolished in CatSper1 and CatSper ζ knockout sperm (Chung *et al.*, 2017; Miki & Clapham, 2013).

The monovalent CatSper current $I_{CatSper}$ is controlled by the V_M and by pH_i (Carlson *et al.*, 2003; Kirichok *et al.*, 2006; Lishko *et al.*, 2011; Lishko & Kirichok, 2010; Strünker *et al.*, 2011; Xia *et al.*, 2007). Increasing pH_i shifts the voltage-dependence of CatSper activation to more negative, physiological membrane potentials (Fig. 1.5) (Kirichok *et al.*, 2006). Therefore, stimulation of sperm with an alkaline-depolarizing medium (K8.6) serves as a faithful trigger of CatSper-mediated Ca^{2+} influx (Carlson *et al.*, 2003).

In addition, CatSper is also a ligand-gated channel. Nanomolar concentration of the female sex hormones progesterone and prostaglandins activate human, but not mouse CatSper channels (Brenker *et al.*, 2012; Lishko *et al.*, 2011; Strünker *et al.*, 2011). Recently, the orphan enzyme

α/β hydrolase domain-containing protein 2 (ABHD2) has been identified as the progesterone receptor in human sperm (Miller *et al.*, 2016). Upon activation by progesterone, the lipid hydrolase ABHD2 cleaves the endocannabinoid 2-arachidonoylglycerol (2-AG) into free glycerol and arachidonic acid. 2-AG inhibits CatSper; 2-AG depletion by ABHD2 relieves the inhibition and activates CatSper. In human, ABHD2 and CatSper are both localized in the principal piece, whereas in mouse, ABHD2 is located in the acrosome and not in the principal piece, which might explain why progesterone does not evoke a Ca^{2+} influx in mouse sperm. The activation of CatSper by prostaglandin is, however, not mediated by ABHD2 and still elusive (Miller *et al.*, 2016).

The human CatSper channel is rather promiscuous and can be activated by a number of non-physiological ligands, for example endocrine disrupting chemicals (EDCs). EDCs mimic the action of progesterone and prostaglandins and, thereby, stimulate a Ca^{2+} influx in human sperm (Schiffer *et al.*, 2014). In mouse and human sperm, CatSper-mediated Ca^{2+} influx is also evoked by cyclic nucleotides. Brenker *et al*. demonstrated that cyclic nucleotide analogs activate human CatSper directly by binding to an extracellular site (Brenker *et al.*, 2012).

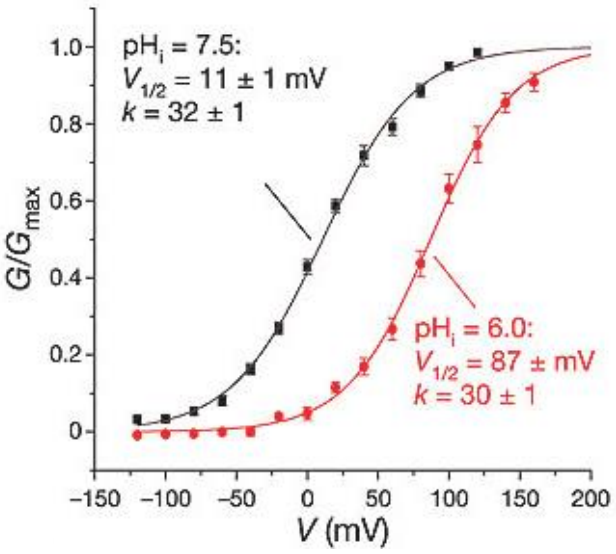

Fig. 1.5: **Activation curves of CatSper at pHi 7.5 and pHi 6.0**

Little $I_{CatSper}$ current is active at pH 6.0 in the physiological range of the membrane potential. Upon alkalization to pH 7.5, the activation curve is shifted to more permissive potentials. From Kirichok *et al*., 2006.

1.3.2 Slo3 potassium channel

The membrane potential in mouse and human sperm is set by the K^+-selective ion channel Slo3, which is exclusively expressed in the principal piece of the flagellum (Brenker *et al.*, 2014; Santi *et al.*, 2010; Schreiber *et al.*, 1998; Zeng *et al.*, 2011). In human, the K^+ current is weakly pH_i- but strongly Ca^{2+}-dependent and inhibited by progesterone (Brenker *et al.*, 2014; Mannowetz *et al.*, 2013). In contrast, mouse Slo3 is activated at $pH_i > 6.0$ and depolarized membrane potentials > 0 mV, but not regulated by Ca^{2+} (Brenker *et al.*, 2014; Navarro *et al.*, 2007; Schreiber *et al.*, 1998; Zeng *et al.*, 2011). In Slo3-deficient sperm, the capacitation-induced hyperpolarization is abolished and the membrane potential is depolarized (Zeng *et al*., 2001). The loss of Slo3 causes defects in sperm motility, osmoregulation, and acrosome reaction, resulting in male infertility (Santi *et al.*, 2010; Zeng *et al.*, 2011). In humans, a depolarized V_M is also associated with lower fertilization success (Brown *et al.*, 2016).
In mouse and human, the Slo3 channel complex contains the auxiliary subunit leucine-rich repeat-containing 52 (LRRC52) (Brenker *et al.*, 2014; Yang *et al.*, 2011). Knocking out Slo3 results in the concomitant loss of LRRC52, indicating that LRRC52 expression is critically dependent on the presence of Slo3 (Yang *et al.*, 2011). LRRC52 regulates the gating behavior of Slo3, allowing the activation of the channel at physiological pH_i and V_M (Zeng *et al.*, 2015). In LRRC52-deficient sperm, Slo3 activation requires more positive voltages and higher pH (Zeng *et al.*, 2015), resulting in infertility.

In mouse sperm, Slo3 together with CatSper regulate V_M and Ca^{2+} influx in response to alkalization (Zeng *et al.*, 2013). It has been suggested that Slo3 and CatSper work in concert during mouse sperm capacitation. The increase in pH_i during capacitation shifts the conductance-voltage relationship of CatSper and Slo3 to more hyperpolarized V_M (Kirichok *et al.*, 2006; Santi *et al.*, 2010; Zeng *et al.*, 2011). Thereby, Slo3 maintains a hyperpolarized V_M to promote a Ca^{2+} influx via CatSper (Navarro *et al.*, 2007). In human sperm, the activation of Slo3 by Ca^{2+} suggests that Slo3 might act downstream of CatSper. Slo3-mediated hyperpolarization might serve as negative feedback-loop, reducing the open probability of CatSper, which curtails rather than enhances the CatSper-mediated Ca^{2+} influx (Brenker *et al.*, 2014).

1.3.3 The proton channel Hv1

In human sperm, the voltage-gated proton channel Hv1 mediates proton (H^+) export, leading to intracellular alkalization. (Lishko *et al.*, 2010). Hv1 is confined to the principal piece of the human flagellum and appears as a homodimer with a H^+-selective pore formed by the four transmembrane segments of the protein (Lee *et al.*, 2008; Ramsey *et al.*, 2010; Tombola *et al.*, 2008). Hv1 is activated by depolarization, regulated by pH, and inhibited by Zn^{2+} (Ramsey *et al.*, 2010; Sasaki *et al.*, 2006). Sperm harbor an N-terminally cleaved Hv1 isoform, termed Hv1Sper, which not only carries outward but also inward H^+ currents (Berger *et al.*, 2016). Because mouse sperm do not express a functional Hv1 channel (Lishko *et al.*, 2010; Ramsey *et al.*, 2009) and

infertile patient with mutations in Hv1 have so far not been identified, the role of Hv1 for sperm function is ill-defined. Capacitation is accompanied by intracellular alkalization and suppressed by Zn^{2+}; thus Hv1 could play a role in sperm maturation during the transit trough the female genital tract (Lishko *et al.*, 2010).

1.3.4 Sodium-proton exchanger family

Proteins of the sodium proton exchanger (NHE) family have been proposed to set the pH_i in mouse and human sperm (Garcia & Meizel, 1999).

2.3.4.1 The sperm-specific sodium proton exchanger

One member of the NHE family is the atypical, sperm-specific sodium proton exchanger (sNHE), encoded by *Slc9c1*. The sNHE is expressed in the principal piece of mouse sperm (Wang *et al.*, 2003). The protein harbors 14 transmembrane segments with a cyclic nucleotide-binding domain close to its intracellular C-terminus. The sNHE also harbors a putative voltage-sensor motif, similar to that of voltage-gated ion channels (Catterall, 2000). The unique characteristics of the sNHE suggest that it may be regulated by cyclic nucleotides and changes in V_M (Wang *et al.*, 2003).
However, the physiological function of the sNHE in sperm is enigmatic. It has been suggested that the sNHE extrudes protons upon hyperpolarization of the membrane potential during capacitation (Chávez *et al.*, 2014). Knocking out sNHE in mice renders male mice infertile due to a defect in sperm motility (Wang *et al.*, 2003). However, this phenotype is not caused by the loss of sNHE, but rather to the concomitant loss of SACY (Jansen *et al.*, 2015; Wang *et al.*, 2003), which is found in a signaling complex with the sNHE and whose function is essential for sperm motility (Wang *et al.*, 2007). SACY is the predominant source for cAMP production in sperm (Harrison, 2003; Hess *et al.*, 2005; Wuttke *et al.*, 2001) and loss of cAMP synthesis in SACY-deficient mice results in immotile sperm, which are not able to fertilize the oocyte (Esposito *et al.*, 2004; Xie *et al.*, 2006). Thus, it is difficult to determine the physiological function of sNHE in sNHE-deficient mice.

2.3.4.2 Sodium-proton antiporter 1 and 2

Two proteins of the sodium/proton antiporter (NHA) subfamily, NHA1 and NHA2, encoded by *Slc9b1* and *Slc9b2*, respectively, were shown to be expressed in the principal piece of mouse sperm (Chen *et al.*, 2016; Liu *et al.*, 2010). The expression of a human orthologue in male testis was also reported (Ye *et al.*, 2006). The NHAs feature 12 transmembrane segments, but no voltage-sensor domain or CNBD (Liu *et al.*, 2010). The mRNA level of NHA1 was significantly increased in NHA2-deficient sperm and *vice versa*, indicating that the two *Slc9b* genes are functionally redundant (Chen *et al.*, 2016). NHA1- and NHA2-deficient mice are subfertile, whereas elimination of both proteins caused infertility. Reportedly, in NHA1- and NHA2-knockout sperm, cAMP signaling and sperm motility is impaired, which can be rescued by

incubating sperm with cAMP analogs (Chen *et al.*, 2016; Liu *et al.*, 2010). Although the proteins seem to be important for sperm function, a functional role in pH regulation still has to be revealed.

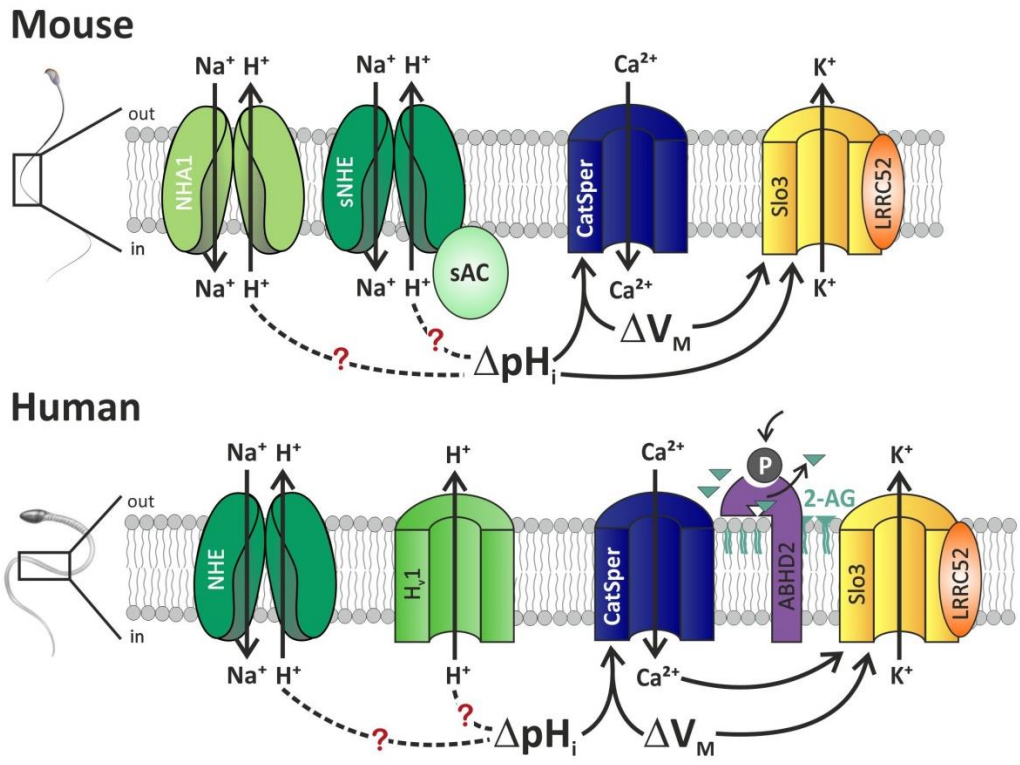

Fig. 1.6: Ion channels and exchanger in mouse and human sperm

The principal Ca^{2+} channel in mouse and human sperm is CatSper, which is regulated by changes in intracellular pH (ΔpH_i) and changes in membrane potential (ΔV_M). In human sperm, CatSper is activated by binding of progesterone (P) to the lipid hydrolase ABHD2. ABHD2 hydrolyses the endocannabinoid 2-AG, which relieves CatSper from inhibition by 2-AG. pH_i regulation is presumably mediated by sNHE and NHA1 in mouse sperm, and Hv1 and a protein of the NHE family in human sperm. The pH-dependent mouse and Ca^{2+}-dependent human Slo3 K^+ channel with its accessory subunit LRRC52 controls the membrane potential. Dotted lines present signaling pathways with weak experimental evidence; question marks indicate hypothetical signaling pathways that have not been confirmed experimentally. Modified after Wachten *et al.*, 2017.

1.4 ZP signaling

Although binding of sperm to the ZP has been studied for decades, very little is known about the signaling pathways underlying the action of ZP glycoproteins in sperm. Stimulation of mouse sperm with isolated ZP glycoproteins depolarizes the membrane potential, alkalizes pH_i, and

increases $[Ca^{2+}]_i$ (Arnoult *et al.*, 1996a). Following ZP binding, two phases of ZP-evoked intracellular Ca^{2+} responses were observed. A rapid, transient Ca^{2+} response (Arnoult *et al.*, 1999; Wassarman *et al.*, 2001) and a second, slow, and rather sustained elevation of $[Ca^{2+}]_i$ (Arnoult *et al.*, 1996c; Brewis *et al.*, 1996b; Florman *et al.*, 1989). In mice, the first, rapid Ca^{2+} response is mediated by CatSper (Xia & Ren, 2009). The ZP-evoked Ca^{2+} response originates from the principal piece and progresses towards the sperm head in ~3 s. It is not known how ZP binding induces the second sustained Ca^{2+} increase, which does not depend on CatSper. It was reported that the sustained Ca^{2+} increase is facilitated by an IP_3-induced Ca^{2+} release from intracellular stores (Jungnickel *et al.*, 2007; O'Toole *et al.*, 2000).

The molecular mechanism underlying CatSper activation by ZPs in mouse sperm is ill-defined. In patch-clamp recordings from mouse sperm, ZPs did not enhance CatSper currents (Xia & Ren, 2009), arguing against a direct activation of the channel by ZPs. Furthermore, it is unknown, which proteins underlie the ZP-evoked alkalization and depolarization and how these proteins are activated. Based on the data published so far, the following model was developed for mouse sperm (Fig. 1.7): Upon interaction with the ZP, the unknown ZP-binding protein leads to depolarization of the membrane potential. This activates Slo3, whereby the membrane potential hyperpolarizes. In turn, the sNHE is activated, resulting in proton export and an increase in sperm pH_i. The alkalization activates CatSper, resulting in a Ca^{2+} influx.

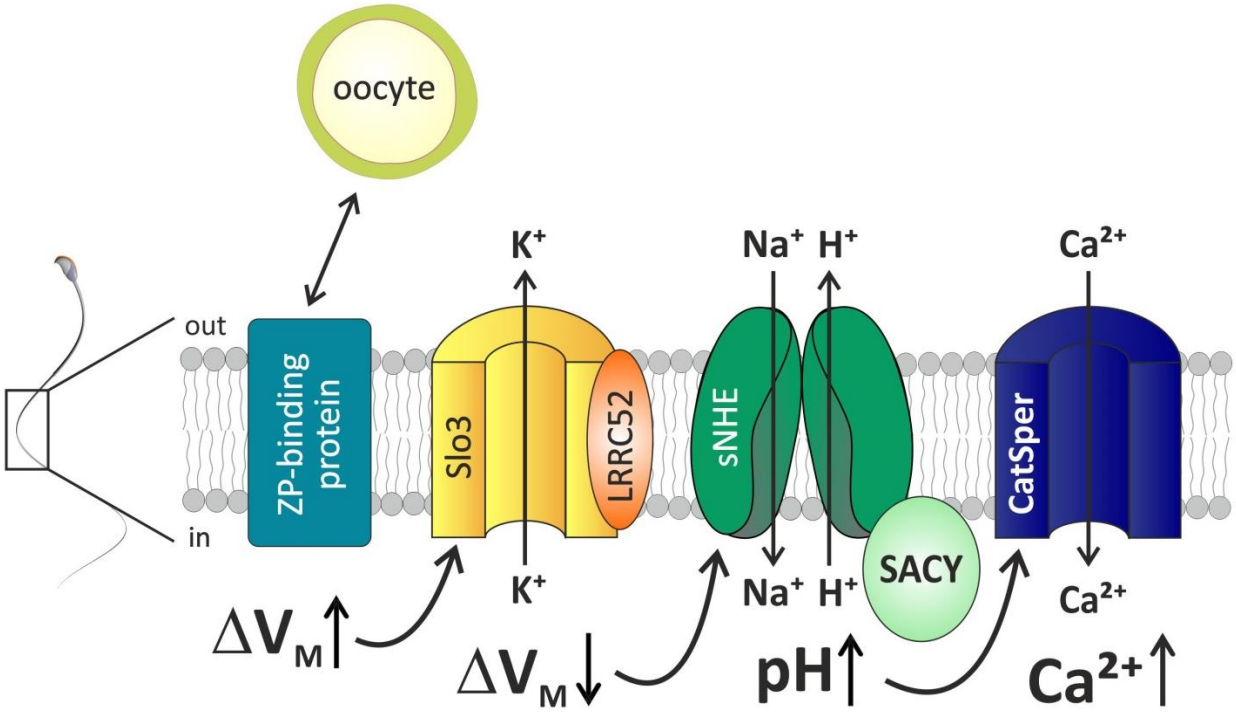

Fig. 1.7: Model of the ZP-induced signalling pathway

Interaction of an unknown ZP-binding protein in sperm with the oocyte`s zona pellucida depolarizes V_M which activates Slo3. Slo3 hyperpolarizes V_M and, thereby, activates the sperm-specific Na^+/H^+ exchanger (sNHE). The sNHE alkalises sperm pH_i, which ultimately triggers a Ca^{2+} influx via CatSper.

For human sperm, much less is understood about the action of ZP. Here, ZPs also evoke an increase in $[Ca^{2+}]_i$ (Bray *et al.*, 2002; Brewis *et al.*, 1996b; Patrat *et al.*, 2006). Whether the Ca^{2+} increase is mediated by CatSper is unknown. Moreover, it is unknown whether ZPs evoke changes of pH_i and/or V_M in human sperm. In mouse and human sperm, the inventory and control of ion channels is considerably different (see 1.3). Thus, the molecular mechanism underlying ZP signaling in sperm has to be unraveled in a species-specific manner.

1.5 Aim of this PhD thesis

In my PhD thesis, I aimed to:

- Unravel the molecular mechanism underlying ZP-induced pH_i signaling and CatSper activation in mouse sperm
- Investigate ZP-induced pH_i and Ca^{2+} signaling in human sperm and elucidate the mechanism of ZP action
- Determine the role of different ZP glycoproteins in ZP signaling in mouse and human sperm

2 Materials and methods

2.1 Materials

2.1.1 Chemicals

All chemicals were obtained in pro analysis grade from the companies AAT Bioquest (Sunnyvale, USA), Applichem (Darmstadt), BioRad (Munich), Biozym (Hess. Oldendorf), Fluka (Steinheim), Eppendorf (Hamburg), GE Healthcare (Solingen), Intervet GmbH (Unterschleißheim), Merck Millipore (Darmstadt), Qiagen (Hilden), Roth (Karlsruhe), Serva (Heidelberg), Sigma-Aldrich (St. Louis, USA), Semrock (Rochester, USA) and Thermo Fisher Scientific (Waltham, USA). Enzymes and corresponding buffers were purchased from Novagen (Darmstadt), Ambion (Austin, USA), MBI Fermentas (Vilnius, Lithuania), New England Biolabs (Frankfurt) and Roche (Mannheim). Oligonucleotides were purchased from Eurofins MWG Operon (Ebersberg). For the cultivation of bacterial cultures, media purchased from Roth (Karlsruhe) were used. Chemicals for use in cell culture were purchased from Thermo Fisher Scientific (Waltham, USA). Primary and secondary antibodies were purchased from abcam (Cambridge, UK), Biorbyt (Cambridge, UK), Dianova (Hamburg), LI-COR Biosciences (Bad Homburg), SantaCruz Biotechnology (Heidelberg), and Thermo Fisher Scientific (Waltham, USA). Cell lines were purchased from ATCC, Eucomm and GE Healthcare (Little Chalfont, UK). RNA was obtained from Zyagen (San Diego, USA). Proteins were blotted on Immobilon-P and Immobilon-FL PVDF-membranes from Merck Millipore (Darmstadt). Microscope slides were purchased from Menzel (Braunschweig).

All solutions were prepared with double-distilled water. If necessary, solutions were sterilized by autoclavation (20 min, 121 °C).

2.1.2 Antibodies

All monoclonal and polyclonal primary antibodies were commercially acquired or produced in collaboration with Dr. Kremmer (Institute for Molecular Immunology, Helmholtz-Zentrum München) by immunizing animals with peptides. ZP-antibodies were additionally purified by Dr. Kremmer after collecting the cell supernatant from hybridoma cells. All applied primary antibodies are listed in Table 1, secondary antibodies are summarized in Table 2. The species and manufacturers are indicated and it is noted in which dilutions the antibodies were used in Western blot (WB) or immunocytochemistry (ICC).

Table 1: Primary antibodies

Antibody	Species	Dilution		Manufacturer
		ICC	WB	
HA	rat	1:500	1:100	E. Kremmer (HZ München)
HIS	mouse	1:100	1:1000	Millipore
hZP2	mouse		1:1000	ATCC/Kremmer
hZP2	mouse		1:1000	ATCC/Kremmer
mCatSper	goat	1:100		Santa Cruz
mZP1	rat	1:100	1:1000	ATCC/Kremmer
mZP2	rat	1:100	1:1000	ATCC/Kremmer
mZP3	rat	1:100	1:1000	ATCC/Kremmer
NHA1	rabbit	1:100	1:1000	Biorbyt
tubulin	mouse	1:500	1:5000	Sigma

Table 2: Secondary antibodies

Antibody	Species	Conjugate	Dilution		Manufacturer
			ICC	WB	
anti-goat	donkey	A647	1:500		Life technologies
anti-mouse	donkey	Cy3	1:1000		Dianova
anti-mouse	donkey	Cy5	1:500		Dianova
anti-mouse	sheep	HRP		1:5000	Dianova
anti-mouse	donkey	RDye680		1:10000	Li-Cor Biosciences
anti-mouse	donkey	RDye800		1:10000	Li-Cor Biosciences
anti-rabbit	goat	A488	1:500		Life technologies
anti-rabbit		RDye800		1:10000	Li-Cor Biosciences
anti-rat	donkey	Cy3	1:500		abcam
anti-rat	donkey	A488	1:500		Dianova
anti-rat	goat	HRP		1:5000	Dianova
anti-rat	goat	RDye680		1:10000	Li-Cor Biosciences
anti-rat	goat	RDye800		1:10000	Li-Cor Biosciences

2.2 Escherichia coli culture

2.2.1 Bacterial strains and vectors

For the amplification of plasmid-DNA, the *E. coli* strain K12 with the following genotype was used:
XL1-Blue (Bullock *et al.*, 1987; Stratagene, La Jolla, USA), genotype: *rec*A1*, end*A1*,gyr*A96*, thi*-1*, hsdR*17 (rK-, mK+), *supE*44, *rel*A1, *lac* [F' *proAB, lacI*qZΔ*M15,*Tn*10* (Tetr)].

The plasmid vectors used for recloning as well as transient gene expression are listed in Table 3:

Table 3: Plasmid vectors

Plasmid (Reference)	Applied for
pcDNA3.1(+) / pcDNA3.1Zeo(+) (Life Technologies)	Transient gene expression in cell line HEK293
pHLsec (Jones et al., 2006)	Transient gene expression in cell line HEK293T
Mouse ZP1 (Epifano et al., 1995)	Recloning of pHLsec-mZP1intHis
Mouse ZP2 (Liang et al., 1990)	Recloning of pHLsec-mZP2intHis
Mouse ZP3 (Ringuette et al., 1988)	Recloning of pHLsec-mZP3intHis

2.2.2 Composition and preparation of *E. coli* culture media

E. coli bacteria cultures were amplified in in LB-medium (10 g/l tryptone, 5 g/l yeast extract, 5 g/l NaCl, pH 7.0), single clones were multiplied on LB-agar dishes. For the preparation of LB-agar dishes, 15 g/l agar was added to the LB-medium. Both medium and the medium-agar suspension were autoclaved for 20 min at 212 °C and stored at RT. The medium-agar suspension was cooled down to about 50 °C and poured into sterile agar dished. If needed, antibiotics were added to the medium to a final concentration of 100 µg/ml (ampicillin) or 30 µg/ml (kanamycin). Until used, agar plates were stored at 4 °C.

2.2.3 Amplification of E. *coli* cultures for plasmid preparation

E. coli bacteria in single colony were incubated for at least 8 h in LB-medium at 30 °C in a rotation incubator or warm air shaker. For selection of transformed plasmids, media were supplemented with a suitable antibiotic.

2.2.4 Generation of competent E. coli cells

Competent *E. coli* cells were generated according to a modified protocol based on the $CaCl_2$ method (Mandel and Higa, 1970). 0.5 ml of an E. coli overnight culture were cultured in 50 ml LB medium at 37 °C until an optical density (OD) of 0.4 was reached, representing a cell number of approximately 2 x 10^8 cells/ml. The OD was measured at 600 nm. The culture was chilled on ice for 30 min. During subsequent working steps, cells were kept constantly in ice. Cells were centrifuged (10 min, 5.000 x g, 4 °C), the pellet was resuspended in 1 ml cold 0.1 M $CaCl_2$ solution and brought to a final volume of 25 ml. After incubation on ice for 20 min, the cells were pelleted again (10 min, 5.000 x g, 4 °C), resuspended in 1 ml cold 0.1 M $CaCl_2$ solution containing 25 % glycerin and brought to a final volume of 5 ml. After two more hours on ice, aliquots were prepared and stored at - 80 °C until further use.

2.3 Preparation of nucleic acids

DNA was solubilized in TE or TE_{RNase}

TE: 10 mM Tris/HCl, pH 8.0, 1 mM EDTA

$TE_{RNase:}$ TE supplemented with 4 µg/ml RNase cocktail (Amibon)

2.3.1 Mini-preparation of plasmid DNA via alkaline lysis

The mini-preparation of plasmid DNA was carried out using alkaline cell lysis (Birnboim & Doly, 1979). A volume of 1.5 ml of *E. coli* overnight culture was pelleted by centrifugation (1 min, 10.000 x g, RT) and resuspended in 150 µl solution I (25 mM Tris/HCl, 10 mM EDTA, pH 7.5). 180 µl solution II (0.2 M NaOH, 1% SDS) were added and the suspension was carefully inverted to lyse the cells. Cell debris and proteins were denatured by adding 225 µl solution III (3 M KAc, pH 4.7). After centrifugation (7 min, 18.000 x g, 4 °C), the supernatant was extracted and nucleic acids were precipitated by adding 700 µl ethanol. The solution was centrifuged (7 min, 18.000 x g, 4 °C) and the resulting pellet was washed with 500 µl 70 % ethanol before it was centrifuged again (7 min, 18.000 x g, 4 °C) to collect the purified plasmid DNA. The DNA pellet was dried in air to remove the ethanol and finally taken up in 20 µl TE_{RNase}.

2.3.2 Midi- and maxi-preparation of plasmid DNA

For the generation of larger amounts of plasmid DNA, the NucleoBond Xtra kit (Macherey-Nagel) was used. *E.coli* cells of a 200 - 500 ml culture were collected by centrifugation (15 min, 5.000 x g, 4 °C) and resuspended in 20 ml resuspension buffer + RNase A. For cell lysis, 20 ml lysis buffer was added and the suspension was inverted for mixing, before it was incubated for 5 min at RT. A filter column was prepared by washing with 25 ml equilibration buffer. A volume of

20 ml neutralization buffer was added to the cell suspension and mixed by inversion. The suspension was transferred to the filter column, which was allowed to empty via gravity flow. The column was washed with 25 ml equilibration buffer and 25 ml wash buffer. The plasmid DNA was eluted by adding 15 ml elution buffer to the column. For DNA precipitation, a volume of 10.5 ml isopropanol was added, and the suspension was mixed thoroughly. After centrifugation (15.000 x g, 45 min, 4 °C), the pellet was washed with 5 ml 70 % ethanol and centrifuged again (15.000 x g, 15 min, 4 °C). The plasmid DNA was air dried and resuspended in a volume of 200 – 300 µl TE.

2.3.3 Preparation of genomic DNA from mouse tissue

Three week old mice were anesthetized with Isoflurane (Curamed Pharma) to amputate the tail tip. After placing the earmarks, a 0.5 cm long tail piece was amputated. For lysis, the tissue was incubated in 500 µl lysis buffer (10 mM Tris/HCl, 100 mM EDTA, 0.5 % SDS, 1 mg/ml Proteinase K, pH 8.0) overnight at 56 °C in a water bath. The next day, the solution was inverted multiple times and centrifuged (18.000 x g, 5 min, RT) before the supernatant was transferred to a fresh tube. To precipitate DNA from the supernatant, 500 µl isopropanol were added. Subsequently to centrifugation (18.000 x g, 30 min, 4°C), the supernatant was discarded and the pellet was washed with 300 µl 70 % ethanol. The dried pellet was dissolved in 100 µl TE.

2.4 Separation, purification and quantification of plasmid DNA and DNA fragments

2.4.1 Agarose-gel electrophoresis

DNA molecules were separated according to their size via agarose gel electrophoresis for analytical as for preparative issues. For the separation of DNA molecules of 500 – 10.000 bp size, gels containing 1 % agarose were used. Agarose was completely dissolved in 1 x TAE-buffer (Table 4) by boiling. After cooling down to 60 °C, 1 µg/ml EtBr was added and the solution was poured into a gel carrier with comb. The samples were mixed with 10 x loading buffer (Table 4) and applied onto the hardened agarose gel. Electrophoresis was performed for 20 min in 1 x TAE as running buffer with a constant voltage of 120 V. Subsequently, the nucleic acid bands were analyzed using UV-light. As size standard, the GeneRuler 1 kb DNA ladder (Thermo Fisher Scientific) was used.

Table 4: Buffer for agarose-gel electrophoresis

TAE (50 x)	loading buffer (10 x)
2 M tris/acetate, pH 7.5	10 x TAE
50 mM EDTA	50 % glycerol
	0.25 % xylene

2.4.2 Elution of DNA from agarose gels

For purification of DNA from agarose gels, the NucleoSpin Gel and PCR Clean-up kit (Macherey-Nagel, Düren) was used. A gel slice containing the DNA fragment of interest was excised from the gel, a volume of 200 µl binding buffer per 0.1 g gel was added, and the sample was incubated for 10 min at 50 °C. After solubilizing the gel slice, the sample was transferred to a filter column, centrifuged (11.000 x g, 1 min, 4 °C), and the flow-through was discarded. The sample was washed two times with 700 µl washing buffer and subsequently centrifuged (11.000, 1min, x g, 4 °C). After a final centrifugation step (11.000 x g, 1 min, 4 °C), the DNA was eluted in 25 µl ddH2O.

2.4.3 Ethanol precipitation

Ethanol precipitation was used to concentrate DNA or to exchange the sample buffer the DNA is dissolved in. Sodium acetate was added to the DNA solution to a final concentration of 0.3 M (pH 4.8) before a threefold volume of ethanol was added. After centrifugation (30 min, 17.000 x g, 4 °C), the precipitated DNA pellet was washed with 70 % ethanol, dried on air and dissolved in TE buffer or H_2O.

2.4.4 Purification with SureClean

For the purification of DNA before further subcloning, the SureClean reagent (Bioline, Luckenwalde) was used. DNA was mixed with an equal volume of the reagent and incubated for 10 min at RT. After centrifugation (10 min, 14.000 x g, RT), the supernatant was removed carefully, and 70 % ethanol were added in a volume 2x larger than the original sample volume. The sample was mixed thoroughly and centrifuged again (10 min, 14.000 x g, RT). The resulting pellet was dried on air and resuspended in 30 µl TE buffer.

2.4.5 Photometric quantification of nucleic acid concentration

Before photometric analysis, the DNA sample was diluted in TE buffer. The absorption was measured at 260 nm (OD_{260}) in an absorption spectrometer against TE buffer as a reference. An OD_{260} of 1 resembles a nucleic acid concentration of 50 µg/ml. Contaminations with proteins or phenol residues can be determined by calculating the ratio between 260 nm and 280 nm, the value should not be smaller than 1.8. The quantification with the Nanodrop ND-1000 (NanoDrop Products) was performed in a similar fashion.

2.4.6 Quantification of nucleic acid concentration by agarose-gel electrophoresis

By comparing the DNA band intensities on an agarose gel with a simultaneously applied size standard with known DNA quantities, the amount of DNA in one sample can be estimated. The gel was stained with ethidium bromide to visualize the DNA bands using a UV-transilluminator.

2.5 Modification of nucleic acids

2.5.1 Restriction digest of plasmid DNA

In preparation for cloning, plasmid DNA was digested using restriction endonucleases. The digest was prepared in the appropriate buffer recommended for optimal activity of the endonuclease at 37 °C. Digestion with more than one enzyme at once was carried out only if the according buffer conditions were matching. Otherwise, the digests were performed subsequently, including fragment purification using preparative agarose gel electrophoresis. Per µg DNA, 1-3 units of the restriction enzyme were used. Each digest was incubated for 1 - 2 h at 37 °C. The entire digest was separated by gel electrophoresis and the desired band was eluted from the gel with the NucleoSpin Extract II-Kit (Macherey-Nagel).

2.5.2 Ligation of DNA fragments

For ligation, 50 ng of digested vector DNA and a 2 – 5 fold molar excess of insert were prepared in a total volume of 10 µl, containing 1 x ligase buffer (Roche) and 0.5 µl T4-DNA-ligase (Roche). The ligation reaction mixture was incubated for at least 60 min at RT.

2.5.3 Transformation

For bacterial transformation, 5 µl ligation product was mixed with 5 µl 10 x CM-buffer (100 mM $CaCl_2$, 400 mM $MgCl_2$), filled up to a final volume of 50 µl using ddH_2O and pre-cooled on ice. 50 µl competent XL1-blue *E. coli* cells were thawed on ice, carefully mixed with the DNA/CM-buffer solution and incubated on ice for 20 min. After a 1 min heat shock at 42 °C, the mixture was incubated for 10 min on ice, before 200 µl LB-medium were added. The mixture was incubated

for 30 min at 37 °C on a shaker. Finally, the cells were plated on agar dishes with respective antibiotics and incubated overnight at 37 °C.

2.6 Polymerase chain-reaction (PCR)

The polymerase chain reaction (PCR) was used for the amplification of DNA fragments with specific length and sequence. Using consecutive cycles, the matrix-DNA was denatured and hybridized with oligonucleotides (primers), which were then elongated using a heat stable polymerase (Mullis *et al.*, 1986).

2.6.1 Primer synthesis

Primer were synthesized by Eurofins MWG Operon and send as lyophilisate. Primer were dissolved with TE to a concentration of 100 µM and stored at -20 °C.

2.6.2 PCR conditions

All PCR reactions were carried out in a thermocycler (Perkin Elmer, Waltham, USA) using KOD Hot Start DNA Polymerase and the according buffer (Table 5).
In preparation for the first cycle, the DNA was denatured for 2 min at 94 °C. During cycles, the periods for denaturation and hybridization were set to 45 sec, followed by a final extension of 2 min at 70 °C. The annealing temperature was chosen according to the lowest melting temperature (Tm) of both primers used, calculated by the following formula:

$$Tm = (G/C) \times 4\ °C + (A/T) \times 2\ °C - (\text{basepair mismatches}) \times 4\ °C - 4\ °C$$

The duration of the elongation phase at 72 °C was adjusted to the length of the amplified fragment (1 min per 1000 bp). Dependent on the sample, 30 – 45 cycles were carried out.

For genotyping of transgenic mice, the DreamTaq PCR mastermix (Thermo Fisher Scientific) was applied. Here, 30 µl PCR mixture, 1.5 µl tail DNA and 1.5 µl of each primer were used.

Table 5: Pipetting scheme for PCR reactions

PCR mixture
50 ng plasmid DNA
5 µl KOD Hot Start DNA Polymerase buffer
5 µl dNTPs (2mM)

2 µl $MgSO_4$ (25 mM)
3 µl primer I (5 pmol/ml)
3 µl primer II (5 pmol/ml)
1 µl KOD Hot Start Polymerase I (1 U/µl) (Novagen)

2.7 Mammalian cell culture

2.7.1 Sterile work

All cell culture work was performed under safety work benches (Herasafe, Thermo Scientific) with gloves. Cells were cultured in an incubator (SanyO) at 37 °C, 7.5 % CO_2 and 95 % humidity.

2.7.2 Cell lines

The mammalian cell lines used in this thesis for heterologous protein expression, α-ZP antibody production, and transgenic mouse line generation and are listed in Table 6.

Table 6: Mammalian cell lines

Cell line (ATCC cell line number)	Organism	Medium
HEK293 (ATCC-CRL-1573)	*Homo sapiens*	MEM + 1 % NEAA
HEK293T (ATCC-CRL-3216)	*Homo sapiens*	DMEM
M1.4 (ATCC-CRL-2464)	*Rattus norvegicus* (B cell); *Mus musculus* (myeloma)	DMEM
IE-3 (ATCC-CRL-2464)	*Rattus norvegicus* (B cell); *Mus musculus* (myeloma)	DMEM
IE-10 (ATCC-CRL-2462)	*Rattus norvegicus* (B cell); *Mus musculus* (myeloma)	DMEM
H2.8 (ATCC-CRL-2568)	*Mus musculus* (B cell); *Mus musculus* (myeloma)	DMEM
H3.1 (ATCC-CRL-2569)	*Mus musculus* (B cell); *Mus musculus* (myeloma)	DMEM
JM8.N4	*Mus musculus*	KnockoutDMEM + GlutaMAX

2.7.3 Continuous culture of HEK293, HEK293T cells, and hybridoma cells

HEK293 and HEK293T cells were cultured in medium supplemented with 10 % FCS on 9 cm petri dishes, hybridoma cells were cultured in 20 % FCS. At a confluency of about 75 %, cells were detached and distributed onto new petri dishes. To this end, cell medium was removed and cells were washed with 3 – 5 ml sterile phosphate-buffered saline (PBS) (137 mM NaCl, 2.7 mM KCl, 6.5 mM Na_2HPO_4, 1.5 mM KH_2PO_4, pH 7.4). Cells were detached by incubation with 0.8 ml 0.05 % trypsin-EDTA (Life technologies) for 2 – 3 min at 37°C on a heating plate. The reaction was stopped by adding 4.2 ml of medium. The cells were resuspended and the cell number was determined using a Neubauer chamber. 4 x 10^5 cells per 9 cm dish were seeded for maintenance of the culture. After 30 – 40 passages, cells were discarded and a fresh aliquot of cells was taken into culture.

2.7.4 Cryopreservation of mammalian cell lines

For cryopreservation, cells were harvested and centrifuged (200 x g, 5 min, RT). 2 x 10^6 cells in 900 µl fresh medium were mixed with 100 µl DMSO in cryogenic vials (Nunc A/S, Thermo Scientific). Overnight, cells were cooled down in a cryo container (Mr. Frosty, Thermo Scientific) and subsequently stored in liquid nitrogen. To take frozen cells back into culture, cells were slowly heated up in a 37°C water bath and mixed with 10 ml culture medium. To remove the DMSO, cells were centrifuged (200 x g, 5 min, RT), suspended in fresh culture medium and seeded on petri dishes.

2.7.5 Transient transfection

70 % confluent HEK cells were transiently transfected using polyethyleneimine (PEI), a stable cationic polymer (Boussif *et al.*, 1995). PEI condenses DNA into positively charged particles that bind to anionic cell surfaces. Consequently, the DNA:PEI complex is endocytosed by the cells and the DNA released into the cytoplasm (Sonawane *et al.*, 2003). For protein preparation, 9 cm plates were transfected. For immunocytochemical analysis, cells were seeded on polylysine-coated coverslips in 4-well plates. Appropriate DNA concentrations were diluted in OptiMEM medium (Thermo Fisher Scientific) and mixed with 1 µg/ml PEI (Sigma-Aldrich). In the meantime, cell medium was replaced with fresh medium containing 2 % FCS to suppress proliferation. After 10 min, the DNA:PEI mixture was dropwise added to the cells. 4 hours post transfection, cells were treated with 5 mM butyrate to increase the transfection efficiency. After 24 h, ICC was performed or cells were harvested for protein preparation.

2.7.6 Stem cell culture

JM8.N4 embryonic stem cells mutant for Slc9b1 were cultured in KnockOut DMEM supplemented with 10 % FCS, 1 % GlutaMAX, 0.007 % β-mercaptoethanol, 0.1 % murine LIF and 50 µg G418. As feeder layer, cell culture plates were coated with 0.1 % gelatin for 30 min before use. For bringing frozen cells into culture, mineral oil was removed when cells were still frozen. Thawing cells were mixed with 1 ml pre-warmed medium, centrifuged at 1200 x g for 5 min and resuspended in fresh medium. Cells were plated out and the medium was exchanged every day until cells reached 80 % confluency. For splitting, cells were washed in 1 x PBS and carefully detached by adding EDTA-free trypsin. After around 3 min, the reaction was stopped with medium and cells were washed at 1200 x g for 5 min. After dispersing cells in new medium, they were seeded on fresh gelatin-coated cell culture plates.

2.8 Immunofluorescence

2.8.1 Immunocytochemistry

For the immunocytochemical analysis of mammalian cells, 24 to 48 h after transfection, cells seeded on PLL-coated coverslips were washed with PBS and fixed for 5 min in 4 % paraformaldehyde (PFA). To saturate unspecific binding domains and to permeabilize the cells, coverslips were incubated for 30 min with 5 % (v/v) Chemiblocker (Millipore) and 0.5 % (w/v) Triton-X100 (CT). Primary antibodies diluted in CT were used for 1 h to specifically detect the protein of interest. Then, secondary antibodies coupled to a fluorescent dye diluted in CT were added for 1 h to detect the complex between antigen and primary antibody. In parallel, DNA was stained using 4’,6-diamidino-2-phenylindole (DAPI) (Invitrogen, final concentration 1:10.000). In between the single incubation steps, cells were thoroughly washed with PBS-T. All incubation steps were carried out at RT. After staining, cells were mounted on microscope slides using Aqua-Poly/Mount (Polyscience) and examined with a confocal laser-scanning microscope (Fluoview FV 1000, Olympus) Olympus FV10 microscope; images were captured with an Olympus DP71 camera using the FV10-ASW 3.0 Viewer software (Olympus, Japan). Immunocytochemistry of mouse oocytes was performed with the similar protocol; however staining and washing was performed by transferring oocytes into drops of antibody solution or PBS-T.

2.8.2 Sectioning of frozen tissue

Adult male mice were anesthetized with Isoflurane (Curamed Pharma) and killed by cervical dislocation. The testis were prepared, punctured twice with a cannula and incubated overnight at RT in 4 % PFA. After a single washing step in PBS for 10 min, testis were transferred in a 10 %

sucrose solution for 1 h and subsequently incubated overnight in 30 % sucrose. On the next day, testis were embedded in Tissue TEK (Sakura Finetek) and stored in -80°C. Testis was sectioned in 16 - 20 µM thick cross sections using a 2800 Frigocut-E cryostat (Reichert-Jung, Nussloch) at an ambient temperature of -30°C. The knives temperature was set to -22°C. Sections were stored on SuperFrost Plus microscope slides (Menzel) at -20°C until further use.

2.8.3 β-galactosidase staining of testis sections

To confirm the expression of β-galactosidase in testis, sectioned tissue was surrounded with a hydrophobic pen (ImmEdge Hydrophobic Barrier Pen, Vector Laboratories) and washed three times for 5 min at RT with the LacZ wash solution (Table 7). 150 - 200 µl LacZ substrate (Table 7) was added to each microscope slide and the cells were incubated overnight in the darkness at 37°C in an incubator without CO_2. Slices were shortly washed twice with H_2O and mounted with coverslips using Aqua-Poly/Mount (Polyscience).

Table 7: Buffer used for β-galactosidase staining

LacZ basis solution	LacZ wash solution	LacZ substrate solution
0.2 M Na_2HPO_4	LacZ basis solution	LacZ basis solution
0.2 M NaH_2PO_4	10 % Deoxycholate	50 mM $K_3[Fe(CN)_6]$
50 mM $MgCl_2$ Stock	Nonidet P40	50 mM $K_4[Fe(CN)_6]$
0.5M EGTA Stock pH 8.0		8 ‰ X-Gal

2.9 Protein preparation

2.9.1 Protein preparation from mammalian cells

To prepare total lysates from cell culture lines, the medium was removed, cells war washed in PBS and then scraped off the plate bottom with a rubber scraper in 1 ml PBS. Cells were pelleted at 700 x g for 5 min and resuspended in 100 to 200 µl lysis buffer (?). After incubation for 30 min on ice, cell debris was removed by centrifugation (10.000 x g, 5 min, 4°C) and the supernatant was stored at -80 °C.

2.9.2 Protein preparation from mouse tissue

Mice were anesthetized with Isoflurane (Curamed Pharma) and killed by cervical dislocation. The desired organs were prepared and either directly used for protein preparation or stored at

-80°C until further use. For protein preparation, organs were cut into small pieces and then homogenized in 1 to 3 ml lysis buffer using a Potter homogenizer at 300-500 U/min. After 30 min on ice, tissue remnants were removed by centrifugation (10.000 x g, 5 min, 4°C) and the supernatant was stored at -80 °C

2.9.3 Protein quantification with bicinchoninic acid

The amount of protein in a solution was determined using the Pierce® BCA Protein Assay Kit (Thermo Scientific). The sample was diluted 1:5 and 1:10 in lysis buffer, the measurement was performed in duplicates. 10 µl sample were mixed with 190 µl color reagent (reagent A mixed with reagent B in proportion 50:1) in a 96 well plate and incubated at 37 °C for 30 min. Subsequently, the absorption was detected at 570 nm using a microplate reader (Fusion Microplate Reader; Perkin Elmer). To obtain a standard curve, defined concentrations of BSA (Thermo Scientific) between 0 and 2 mg/ml were used.

2.10 Purification of proteins from cell supernatant

2.10.1 Batch purification via Ni-NTA agarose

Heterologously expressed ZP proteins were purified by immobilized metal affinity chromatography via their His-tag using Ni-NTA agarose (Qiagen). To this end, 200 µl resin were equilibrated with 1 ml cell medium for 5 min at RT. After centrifuging at 700 x g for 2 min, the medium was removed and 1 ml cell supernatant were added. Incubation overnight on a rotating wheel ensured efficient binding between agarose and proteins. On the next day, the supernatant was removed by centrifugation (700 x g, 2 min) and the resin was washed four times with washing buffer (Table 8). For elution, the agarose was incubated for 10 min with 200 µl elution buffer (Table 8). Analysis was performed by SDS-PAGE and Western blotting with 40 µl supernatant of each working step including input.

Table 8: Buffer used in batch and ÄKTA purification

Washing buffer	Elution buffer
20 mM NaP	20 mM NaP
500 mM NaCl	500 mM NaCl
10 mM Imidazole	500 mM Imidazole
pH 7.4	pH 7.4

2.10.2 Large-scale protein purification using the ÄKTA system

In larger scale, proteins were purified from 70 ml cell supernatant using the ÄKTA Protein Purification System (GE Healthcare). The whole system was rinsed with H_2O, a 1 ml HiTrap Chelating HP column (GE Healthcare) was inserted and loaded with 3 mM $CoCl_2$. The column was washed with 5 ml washing buffer, 5 ml elution buffer and subsequently, 5 ml washing buffer (Table 8) using a flow rate of 0.5 ml/s. The supernatant was applied to the column with a flow rate of 0.4 ml/s never exceeding a pressure of 0.5 MPa. After removing unbound proteins using 5 ml washing buffer (flow rate 0.3 ml/s), proteins were eluted with a continuous gradient of 10 to 500 mM imidazole using a flow rate of 0.5 ml/s. The eluate was collected in fractions of 0.5 ml which were analyzed by Western blotting. The four fractions with the highest amount of protein were used for further experiments.

2.10.3 Buffer exchange

Eluted ZP-fractions were buffer exchanged using Illustra NaP-5 columns (GE Healthcare) to remove imidazole. Excess storage buffer was removed from the column, then the column was equilibrated with 10 ml sperm buffer. Subsequently, 0.5 ml sample was added to the column. Shortly after the liquid had passed through the column, the purified sample was eluted with 1 ml sperm buffer.

2.10.4 Protein quantification

The concentration of heterologous ZP proteins was determined by measuring the absorption at 280 nm using a UV/Vis spectrophotometer (Hitachi, Tokio, Japan). The concentration was then calculated using the Beer-Lambert Law:

$$c\ (\text{concentration}) = \frac{A\ (\text{absorbance})}{\varepsilon\ (\text{absorptivity coefficient}) * d\ (\text{path length})}$$

2.10.5 PNGase digestion

To analyze the glycosylation pattern of ZP proteins, N-linked glycosidic residues were removed by digestion with PNGase-F (New England BioLabs). 20 µg of protein, 1 µl Glycoprotein Denaturing Buffer and H_2O were combined to make a 10 µl total reaction volume. The proteins were denatured by heating the sample to 100°C for 10 min. Then, 2 µl GlcoBuffer II, 2 µl 10 % NP-40 and 5 µl H_2O were mixed with 1 µl PNGase F. The reaction was incubated at 37°C for 1 h, deglycosylation was analyzed by SDS-PAGE and Western blotting using 4 - 12 % gradient gels.

2.11 Separation and detection of specific proteins

2.11.1 Reducing SDS-polyacrylamide gel electrophoresis

The electrophoretic separation of proteins was performed using SDS-polyacrylamide gel electrophoresis (SDS-PAGE) after Laemmli (Laemmli, 1970). The SDS-PAGE was performed using the Minigel-Twin system (Biometra, gel size: 0,1 x 8 x 10 cm) with a 7.5 % running and 5 % stacking SDS-gel. The gel composition is summarized in Table 9. Samples were mixed with 4 x SDS sample buffer (Table 10) and boiled up for 5 min at 95°C. The electrophoretic separation in 1 x SDS running buffer (Table 10) was performed at 12 - 15 mV for the stacking and at 20 - 25 mV for the running gel.
To separate PNGase-digested proteins, 4 - 12 % NuPAGE Novex Bis-Tris gradient gels (Life Technologies) with a thickness of 1.5 mm were used. Electrophoresis was performed in MOPS running buffer (Table 10) in an XCell SureLock mini gel chamber (Life Technologies) at 200 mV.

Table 9: Pipetting scheme for SDS-PAGE gels

	Running gel (7.5 %)	**Stacking gel (5 %)**
1.5 M Tris HCl, pH 6.8/8.8	0.5 ml (pH 6.8)	1.5 ml (pH 8.8)
10 % SDS	20 µl	60 µl
10 % APS	40 µl	40 µl
Acrylamide	340 µl	1.5 ml

Table 10: Buffer used in SDS-PAGE

4 x SDS sample buffer	**SDS running buffer (20 x)**	**MOPS running buffer**
8 % SDS	250 mM Tris	50 mM MOPS
200 mM Tris/HCl	1 % SDS	50 mMTris base
50 % Glycerol	1.92 M Glycine	0.1% SDS
4 % ß-mercaptoethanol		1 mM EDTA
0.04 % Bromphenol blue		

As molecular weight marker, the Protein Marker VI (PanReac AppliChem) was used. The marker contains prestained proteins from 10 to 250 kDa with two reference bands at approx. 25 and 75 kD, coupled with a green and a red dye, respectively.

2.11.2 Mass spectrometry

In preparation of protein analysis via liquid chromatography–mass spectrometry (LCMS), proteins isolated from sperm were separated on SDS gels and stained with Coomassie. Per lane, 14-17 gel slices were excised and proteins were in-gel digested with trypsin (Promega). Peptides were separated in a 90 or 180 min gradient by a nanoAcquity LC System equipped with a HSS T3 analytical column (1.8 µm particle, 75 µm x 150 mm) (Waters), and analyzed by ESI-LC-MS/MS using an LTQ Orbitrap Elite mass spectrometer (Thermo Scientific). All database searches were performed using SEQUEST as well as MS Amanda (Mechtler lab, Vienna, Austria) algorithm, embedded in Proteome DiscovererTM (Rev. 1.4, Thermo Electron© 2008-2011), with a NCBI protein database (mouse, accession number NP_766280.2, accessed June 13, 2013). Only fully tryptic peptides with up to two missed cleavages were accepted. Oxidation of methionine was permitted as variable modification. The mass tolerance for precursor ions was set to 10 ppm; the mass tolerance for fragment ions was set to 0.4 amu. To filter the results, a peptide FDR threshold of 0.01 (q-value) according to Percolator was set in Proteome Discoverer, two peptides per protein and peptides with search result rank 1 were required.

2.11.3 Transfer and immobilization of proteins by Western blotting

Proteins separated by SDS-PAGE were transferred to a PVDF membrane (Immobilon-P or Immobilon-FL, Millipore) with the semi-dry approach using a milliblot-graphite electroblot-system (Millipore). The membrane was activated in MeOH, whatman paper were incubated in the respective blotting buffers. The experimental setup is shown in Fig. 2.1. Proteins were blotted for 40 min at 2.4 mA/cm^2 gel area.

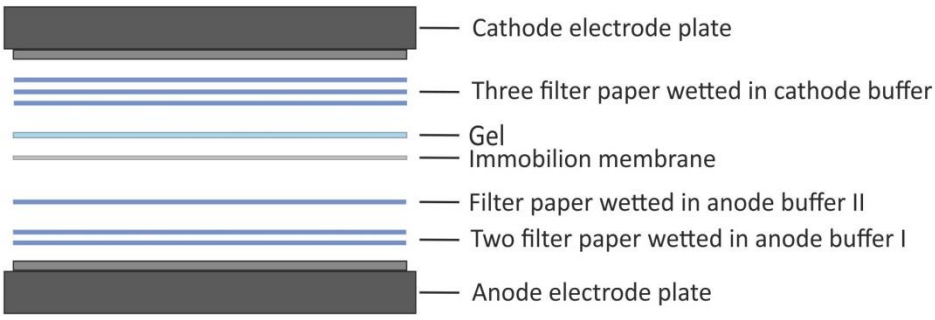

Fig. 2.1: Protein transfer using the semi-dry approach

Proteins separated by gradient gels were transferred via the wet blot procedure using the XCell II Blot Module (Thermo Fisher Scientific). PVDF membrane was activated with MeOH. Subsequently, six blotting pads, two whatman paper and the membrane were incubated in blotting buffer. Three blotting pads, one whatman paper, the gel and the PVDF membrane were

stacked into the cathode module. Air bubbles were removed, filter paper and three botting pads were added and the chamber was closed with the anode module. Transfer buffer was filled into the blotting chamber, the outer part was filled with H_20. Proteins were then transferred for 2 h at 30 mV. A successful transfer for both blotting approaches was indicated by the presence of marker bands on the PVDF membrane.

Semi-dry anode I buffer	Semi-dry anode II buffer	Semi-dry cathode buffer	Wet blot transfer buffer
300 mM Tris	25 mM Tris	25 mM Tris	5 % NuPage transfer buffer
20 % MeOH	20 % MeOH	20 % MeOH	10 % MeOH
pH 10.4	pH 10.4	40 mM Glycin	0.1 % NuPAGE antioxidant
		pH 9.4	

2.11.4 Immunostaining of immobilized proteins

For the immunological detection of protein on PVDF membranes, unspecific binding sites were saturated by incubating the membrane with Bløk blocking buffer (Millipore). After incubating the membrane with a specific primary antibody to verify the protein of interest, excessive antibody was removed by washing in PBS + 0.05 % Tween (PBS-T). Specific antigen-antibody complexes were detected with a secondary antibody coupled to a horseradish peroxidase (HRP) or near-infrared fluorophores. Before detection of the secondary antibody, the membrane was washed again in PBS-T and stored in PBS. During all incubation and washing steps, the membrane was slightly panned. All working steps including the applied solutions are summarized in Table 11.
If the antibody was coupled to HRP, the membrane was incubated with the ECL (enhanced chemiluminescence) detection reagent (Sigma-Aldrich) in the dark. The signal was detected using the LAS-3000 Luminescent Image Analyzer (FUJIFILM). Fluorophor-coupled antibodies were visualized using the Odyssey Infrared Imaging System (Li-Cor Biosciences).

Table 11: Immunological detection of immobilized proteins

Working step	Incubation time and temperature	Incubation solution
Blocking	40 min, RT	Blök blocking buffer
Primary antibody detection	Overnight, 4°C	Primary antibody in Blök / PBS-T (1:1)
Washing	3 x 10 min, RT	PBS-T

Secondary antibody detection	60 min, RT	Secondary antibody in Blök / PBS-T (1:1)
Washing	3 x 10 min, RT	PBS-T
Storage	4 °C	PBS

2.12 Laboratory animals

2.12.1 Captive care and breeding

The mice used for this thesis were kept in the mouse facility of the research center caesar in Bonn. Mice were *ad libitum* supplied with drinking water and a breeding diet for rat and mice (1314 Standard, Altromin). After three weeks, offspring was weaned from their mother, sorted according to sex and genotyped by PCR. Mice used in this thesis were 2 - 4 months of age. To analyze the mating behavior, male and female mice were mated for one night. Early the next morning, female mice were checked for vaginal plugs. After at least ten days it was examined if female mice were pregnant. If so, the number of offspring was documented after birth.

CatSper-null mice

CatSper knockout mice were kindly provided by Dr. David Clapham, Howard Hughes Medical Institue (Boston, USA)

Slo3-null mice

Slo3 knockout mice were kindly provided by Prof. Dr. Christopher Lingle, Washington University (St. Louis, USA).

LRRC52-null mice

LRRC52 knockout mice were kindly provided by Prof. Dr. Christopher Lingle, Washington University (St. Louis, USA).

sNHE-null mice

sNHE knockout mice were purchased from the Jackson Laboratory (B6; 129S6-Slc9a10tm1Gar/J, stock number: 007661).

bPAC transgenic mice

Transgenic bPAC mice were generated by Vera Jansen and Dagmar Wachten using pronuclear injection of a bPAC-HA fragment cloned into a pPrCExV-1 vector (Robert E. Braun, Jackson Laboratories, Maine, USA) (see Jansen *et al*., 2015)

NHA1-null mice

NHA1-null mice were generated by blastocyst injection of Slc9b1 mutant ES cells (EPD0187_1_D11, EUCOMM) into albino BL6 females performed by the transgenic service of the LIMES institute in Bonn. The offspring was genotyped by PCR using NHA1-specific primers. and the individual founder animals further mated with wildtype animals.

2.12.2 Isolation of native mouse zona pellucida

To increase the number of ovulated oocytes per mice, female mice were superovulated. To this end, 10 U pregnant mare's serum gonadotropin (PMSG) (ProSpec, Rehovot, Israel) was injected intraperitoneally which increases oocyte production. After 48 hours, mice were treated with human chorionic gonadotropin (hCG) to induce ovulation (ProSpec, Rehovot, Israel). 14 hours later, oocyte isolation was performed. As shown in Fig. 2.2a, the oviduct was prepared from the genital tract of the mice. The ampulla was ruptured, and cumulus-enclosed oocytes were released in Toyoda Yokoyama Hoshi (TYH) medium (Toyoda & Chang, 1974) (Table 12) containing 300 µg/ml hyaluronidase (Fig. 2.2b). After 15 min, cumulus-free oocytes were transferred into fresh buffer and washed twice (Fig. 2.2c). Zona pellucidae and oocytes were separated by shear forces generated by expulsion from 50 nm pasteur pipettes. Zona pellucidae were counted, transferred into fresh buffer (Fig. 2.2d) and solubilized for 30 min at 70°C.

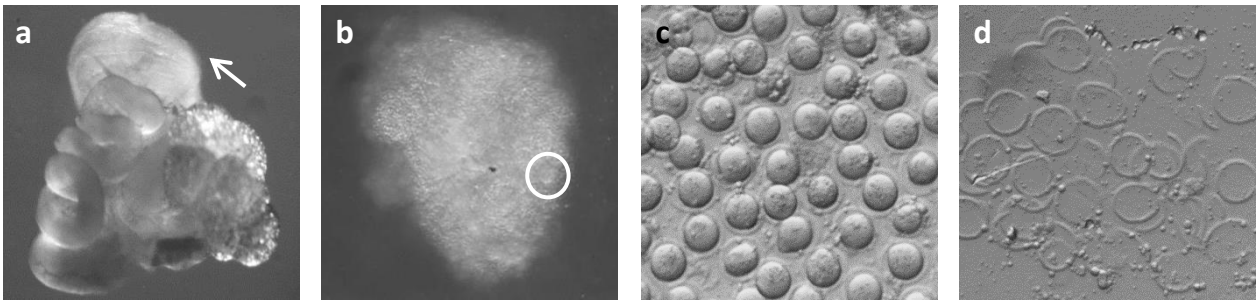

Fig. 2.2: Isolation of oocytes and zona pellucida from superovulated mice

(a) Oviduct with swollen ampulla (indicated by white arrow) dissected from superovulated mouse. **(b)** Oocytes surrounded by cumulus cells released from ampulla, one oocyte is highlighted with a white circle**. (c)** Cumulus-free mouse oocytes. **(d)** Mouse zona pellucidae.

2.13 Mouse and human sperm experiments

2.13.1 Mouse sperm preparation

Adult male mice were anesthetized with Isoflurane (Curamed Pharma) and killed by cervical dislocation. Buffer used for mouse sperm preparation and experiments are summarized in Table 12. Cauda epididymis were excised, separated from fat tissue and each transferred into 500 µl TYH medium. Five small incisions were made and sperm were allowed to disperse for 15 min. The supernatant was collected, and the sperm number was determined using a hemocytometer. For capacitation, sperm were incubated for 90 min in TYH buffer with 113 mM NaCl containing 25 mM $NaHCO_3$ and 3 mg/ml bovine serum albumin (BSA). To activate CatSper, a high K^+ TYH buffer with 138 mM KCl as well as alkaline pH (K8.6) was used. Measurements under depolarized membrane potential were performed in TYH with 138 mM KCl at pH 7.4 (TYH high K^+). For experiments without $[Na^+]_{ex}$, Na^+ was replaced in the buffer by N-methyl-D-glucamine (NMDG) (TYH Na^+ free).

Table 12: Buffer used for mouse sperm preparation and experiments

TYH	K8.6	TYH high K^+	TYH Na^+ free
138 mM NaCl	4.8 mM NaCl	4.8 mM NaCl	138 mM NMDG
4.8 mM KCl	138 mM KCl	138 mM KCl	4.8 mM KCl
2 mM $CaCl_2$	2 mM $CaCl_2$	2 mM $CaCl_2$	2 mM $CaCl_2$
1.2 mM KH_2PO_4	1.2 mM KH_2PO_4	1.2 mM KH_2PO_4	1.2 mM KH_2PO_4
1.0 mM $MgSO_4$	1.0 mM $MgSO_4$	1.0 mM $MgSO_4$	1.0 mM $MgSO_4$
5.6 mM Glucose	5.6 mM Glucose	5.6 mM Glucose	5.6 mM Glucose
0.5 mM Sodium pyruvate	0.5 mM Sodium pyruvate	0.5 mM Sodium pyruvate	
10 mM L- lactate	10 mM L- lactate	10 mM L- lactate	10 mM L- lactate
10 mM HEPES	10 mM TAPS	10 mM HEPES	10 mM HEPES
pH 7.4	pH 8.6	pH 7.4	pH 7.4

2.13.2 *In-vitro* fertilization

KSOM medium (EmbryoMax Modified M16 Medium, Millipore) was mixed with mineral oil and equilibrated overnight at 37°C. On the day of the in-*vitro* fertilization experiment, 100 µl drops of fresh KSOM medium were placed into multiple wells of a multi-well plate and overlaid with 1 ml medium-oil mixture. Oocyte-cumulus complexes (COC) were isolated from superovulated mice and placed into the drop. 1 x 10^5 capacitated sperm were added to each COC. After

4 hours of incubation at 37°C and 5 % CO_2, oocytes were transferred into fresh KSOM medium. On the next day, the amount of two-cell stage oocytes was quantified.

2.13.3 Human sperm preparation

Motile human sperm were isolated from the ejaculate using the "swim-up" technique: 0.5 to 1 ml of liquefied semen was layered in a 50 ml falcon tube below 4 ml human tubular fluid (HTF). Buffer used for human sperm preparation and experiments are summarized in Table 13. The tubes were incubated in a tilted angle of 45 degree at 37°C and 10 % CO_2 for 60 - 90 min. Motile sperm were allowed to swim up into the HTF layer, while immotile sperm, as well as other cells or tissue debris, did remain in the ejaculate fraction. A maximum of 3.5 ml of the HTF layer was transferred to a fresh falcon tube and washed twice in HTF by centrifugation (700 x g, 20 min, RT). The purity and vitality of each sample was controlled via light microscopy, the cell number was determined using a Neubauer counting chamber. Per ejaculate, a sperm count of 0.5 – 8 x 10^7 cells was obtained. For capacitation, sperm were incubated in HTF with 72,8 mM NaCl containing 25 mM $NaHCO_3$ and 3 mg/ml HSA (Irvine Scientific) for 90 min. Measurements under depolarized membrane potential were performed in HTF with 97.8 mM KCl at pH 7.4 (HTF high K^+). For experiments without $[Na^+]_{ex}$, Na^+ was replaced in the buffer by N-methyl- D-glucamine (NMDG) (HTF Na^+ free). For experiments under Mg^+-free conditions, $MgCl_2$ was omitted (HTF Mg^+ free). In HTF without Cl^-, the ion was replaced by gluconate (HTF Cl^- free).

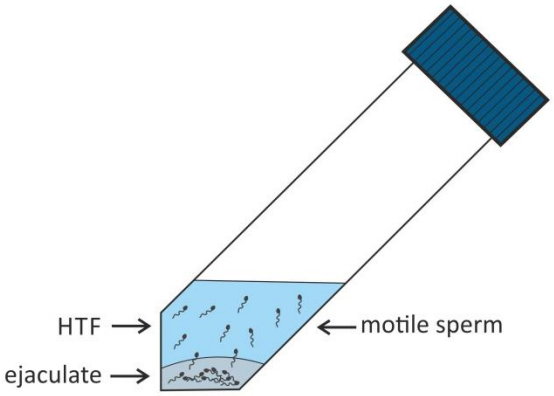

Fig. 2.3: "Swim-up" technique for the preparation of motile human sperm

Liquefied semen was layered in a 50 ml falcon tube below 4 ml of HTF. The sample was incubated at 37 °C, 10 % CO2 for 60 - 90 min to enable motile sperm to swim up into the HTF buffer.

Table 13: Buffer used for human sperm preparation and experiments (in mM)

HTF	HTF high K^+	HTF Na^+ free	HTF Mg^+ free	HTF Cl^- free

97.8 mM NaCl	4.7 mM NaCl	97.8 mM NMDG	97.8 mM NMDG	97.8 mM NaGluocate
4.7 mM KCl	97.8 mM KCl	4.7 mM KCl	4.7 mM KCl	4.7 mM KGluconate
2.04 mM $CaCl_2$	2.04 mM $CaCl_2$	2.04 mM $CaCl_2$	2.04 mM $CaCl_2$	2.04 mM CaGluconate
0.37 mM KH_2PO_4	0.37 mM KH_2PO_4	0.37 mM KH_2PO_4	0.37 mM KH_2PO_4	0.37 mM KH_2PO_4
0.2 mM $MgSO_4$	0.2 mM $MgSO_4$	0.2 mM $MgSO_4$		0.2 mM $MgSO_4$
2.8 mM Glucose	2.8 mM Glucose	2.8 mM Glucose	2.8 mM Glucose	2.8 mM Glucose
0.33 mM Sodium pyruvate	0.33 mM Sodium pyruvate		0.33 mM Sodium pyruvate	0.33 mM Sodium pyruvate
21.4 mM lactic acid	21.4 mM lactic acid	21.4 mM lactic acid	21.4 mM lactic acid	21.4 mM lactic acid
21 mM HEPES	21 mM HEPES	21 mM HEPES	21 mM HEPES	21 mM HEPES
pH 7.4	pH 7.4	pH 7.4	pH 7.4	pH 7.4

2.13.4 Sperm membrane protein preparation

To isolate membrane proteins from sperm, 1 x 10^7 cells were sonified two times for 30 s in 50 µl sonification buffer (25 mM Hepes, 100 mM NaCl, mPIC 1:100, pH 7.5). 0.3 % SDS was added and the sample was incubated for 10 min in the cold room on a rotating wheel. To remove insoluble cell components, the sample was centrifuged (55000 rpm, 15 min, 4°C) and the supernatant was transferred to a fresh tube. After quantifying the protein concentration by BCA test, the sample was analyzed by Western blotting.

2.13.5 Acrosome reaction assay

To analyze if ZP proteins evoke the acrosome reaction, 1 x 10^6 non-capacitated or capacitated sperm were incubated with buffer, ZPs or heterologous ZP proteins, or 2 µM ionomycin as positive control for 10 min at 37°C. Samples were washed by centrifugation at 700 x g for 7 min and resuspended in 50 to 100 µl PBS. From each sample, a smear was prepared on a glass slide and dried on a 37°C heat plates. Subsequently, cells were fixed in 100 % EtOH for 30 min at RT. After washing with PBS, sperm were surrounded with a Liquid Blocker Pen (Vector Laboratories, Burlingame, USA) and incubated for 30 min in the dark with 5 µg/ml lectin coupled to FITC in PBS. Peanut lectin coupled to FITC (PNA-FITC) was used for mouse sperm, pea lectin coupled to FITC (PSA-FITC) was used for human sperm. Additionally, sperm were counterstained with 2 µg/ml DAPI. Subsequent to washing with PBS, cells were covered with cover glasses using

Aqua Poly/Mount (Polyscience, Eppelheim) as mounting medium and analyzed with an Olympus FV10 microscope; images were captured with an Olympus DP71 camera using the FV10-ASW 3.0 Viewer software (Olympus, Japan). For each condition, at least three times 200 cells were counted using ImageJ version 1.47. The fraction of acrosome-reacted sperm in each sample was normalized to the fraction of acrosome-reacted sperm in the buffer-treated control group.

2.13.6 Antigen retrieval for ICC on sperm

To improve ICC on mouse sperm, antigen retrieval with citrate buffer was performed. 2 x 10^5 cells were smeared on positively charged microscope slides and dried at RT. A steamer was preheated to 99°C, staining cuvettes were filled with citrate buffer (10 mM sodium citrate, 0.05 % Tween-20, pH 6) and preheated in the steamer for 10 min. Sperm slides were placed into the staining cuvettes and incubated in the steamer for 20 min. After the antigen retrieval, slides were transferred into staining cuvettes with PBS, cooled down for 10 min and subsequently dried in ICC chambers. With a Liquid Blocker Pen (Vector Laboratories, Burlingame, USA), a border was drawn around the sperm and ICC was performed as described in 2.8.1.

2.13.7 STORM analysis of sperm flagellar proteins

All STORM imaging experiments were performed in an imaging buffer (50 mM Tris, pH 8, 10 mM NaCl) with an oxygen scavenging system (0.5 mg/mL glucose oxidase, 40 µg/mL catalase, 10 % glucose, and 10 mM 2-aminoethanethiol. 10.000 – 60.000 frames were acquired per data set using 647 nm excitation at 100 mW at the sample plane unless mentioned otherwise. A 405 nm laser was used to maintain an adequate number of localizations per frame. A cylindrical lens was introduced in the detection path for 3D STORM acquisition. Perfect focus system from Nikon was used to minimize axial drifting and a vibration isolation table was used to minimize lateral drifting. STORM movies were analyzed as described previously using either the Nikon software package based on a technology developed by Dr. Xiaowei Zhuang (Huang et al. 2008). Briefly, fluorescence peaks corresponding to individual molecules were identified in each frame and fit using least-squares fitting or maximum-likelihood estimator fitting with a two-dimensional Gaussian to determine the (x,y) position of each molecule. For 3D imaging, the ellipticity of the Gaussian was used to assign a z coordinate. Drift correction was applied using cross-correlation.

STORM images were rendered with each localization plotted as a Gaussian whose width is weighted by the inverse square root of the number of detected photons for that switching event. Images were filtered to reject molecules with low photon number (below 500 photons). Molecules with aspect ratio higher than 1.5 for 2D and 2.5 for 3D datasets were rejected. Moreover, molecules that appear for >10 consecutive frames were rejected. Non-specifically bound antibodies can give background in the STORM images, which appears as scattered localizations at low local densities. This background noise was removed by a local density filter.

Low-density localizations were filtered out by removing a localization if it was surrounded by fewer than 10 localizations in the 80 nm × 80 nm region surrounding the localization.

2.13.8 Flagellar beat analysis

Freely beating sperm were observed in shallow perfusion chambers with 200 µm depth. Sperm were tethered to the glass surface by lowering the BSA concentration to 0.3 mg/ml allowing to exchange the imaging buffer during recordings. An inverted dark-field video microscope (IX71; Olympus) with a 10 x objective (UPlanFL, NA 0.4; Olympus) and an additional 1.6 x magnification lens (16 x final amplification) was combined with a high-speed camera (Dimax; PCO). Dark-field videos were recorded with a frame rate of 200 Hz. During the recordings, the temperature was set to 37°C (Incubator; Life Imaging Services). The flagellar beat was quantified with an in-house developed software package SpermQ (Jan Niklas Hansen, research center ceasar).

2.13.9 Electrophysiological recordings from human sperm

In preparation of electrophysiological recordings of human sperm, 5 mm glass plates were coated with PLL. Subsequently, sperm were added and incubated for 30 min at 37 °C to enable sedimentation of sperm. The glass plates were transferred to the measurement chamber of the patch-clamp setup. The patch-clamp setup was placed on a vibration-cushioned table and was surrounded by a Faraday cage. An inverse microscope (IX 73, Olympus) was supplemented by two micromanipulators (PatchStar, Scientifica), enabling a precise positioning of the patch pipette and the object table. The object table was equipped with the measurement chamber and a perfusion system. Patch pipettes were pulled from borosilicate glass (Hilgenberg, Malsfeld) using a micropipette puller (DMZ universal puller, Zeitz-Instrumens, Martinsried) and extensively fire polished. The reference electrode consisted of a silver chloride wire, which was connected to the bath solution via an agar bridge (3M KCl). The pipette solution was connected to the pre-amplifier by a silver chloride electrode. Measurements were carried out using a patch-clamp amplifier (Axopatch 200B, Axon), coupled to a PC via a data acquisition system (Digidata 1550A, Axon).

Only motile sperm, with their head tethered to the glass surface but with a freely moving flagellum, were chosen for recordings. Slight overpressure was applied to the pipette before immersion into the bath solution to prevent cell debris from entering the pipette. As the sperm membrane is tightly attached to the rigid intracellular structures, it is not possible to generate a giga-ohm seal between the pipette and the sperm membrane. Only recently it was identified that at the cytoplasmic droplet (Fig. 2.4a, yellow arrows), the membrane is only loosely attached to the intracellular structures, enabling the attachment of a patch pipette with a high electrical resistance in between pipette and membrane (Lishko *et al.*, 2010). The droplet could be sucked into the pipette by application of a slight suction (Fig. 2.4b). If the connection was strong enough, the sperm cell was lifted off the glass slide. To reach the whole-cell configuration, a

short voltage pulse of 500 – 750 mV was applied for 0.5 ms, rupturing the membrane within the pipette. In this whole-cell configuration, the whole intracellular space is accessible through the pipette, as demonstrated by injection of Lucifer yellow into the pipette (Fig. 2.4c). Hence, currents flowing over the entire cell membrane are measured in this configuration. Seals between pipette and sperm were formed in standard extracellular solution (HS) (in mM, 135 NaCl, 5 KCl, 1 $MgSO_4$, 2 $CaCl_2$, 5 glucose, 1 Na-pyruvate, 10 Lactic acid, and 20 HEPES, adjusted to pH 7.4 with NaOH). CatSper currents were recorded in divalent-free (DVF) solutions containing (in mM) 140 CsCl, 40 HEPES, 1 EGTA, adjusted to pH 7.4 with CsOH with a pipette solution containing (in mM) 130 Cs-aspartate, 50 HEPES, 5 EGTA, 5 CsCl, adjusted to pH 7.3 with CsOH.

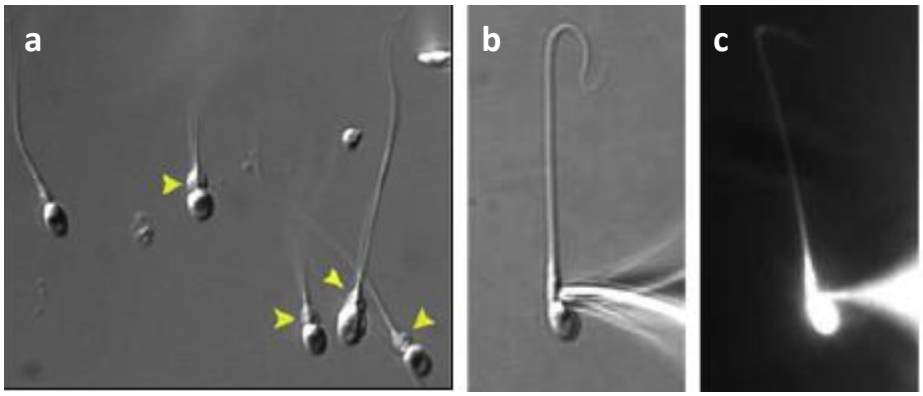

Fig. 2.4: Patch-clamp technique on human sperm.

(a) DIC-picture of human sperm. Yellow arrows depict the cytoplasmic droplet. **(b)** Human sperm attached to a patch pipette (left). Diffusion of the dye Lucifer yellow (2 mM) inside the sperm, after transition into the whole-cell configuration (right) (Lishko *et al.*, 2010).

2.14 Fluorometric measurements in sperm

Fluorometric measurements were used to monitor alterations in $[Ca^{2+}]_i$ and pH_i of mouse and human sperm. Measurements of sperm populations were performed either in multi-well plates in a fluorescence plate reader (FLUOstar Omega; BMG Labtech, Ortenburg, DE) (2.14.3) or in cuvettes using the stopped-flow instrument SFM400 (Biologic, Cliax, France) (2.14.4).

2.14.1 Fluorescent Ca^{2+} indicator CAL520

The high affinity, non-ratiometric fluorescent Ca^{2+} indicator CAL520 is based on the xanthene fluorophore fluorescein (green), which is attached to the Ca^{2+} chelator 1,2-bis(o-

aminophenoxy)ethane-N,N,N',N'-tetraacetic acid (BAPTA) (blue) (Grynkiewicz *et al.*, 1985; Minta *et al.*, 1989) (Fig. 2.5a). Binding of Ca^{2+} ions to the BAPTA moiety changes the fluorescent properties of CAL520, hence the intensity of the fluorescence emission spectrum is dependent on the free $[Ca^{2+}]_i$ (Fig. 2.5b). If no Ca^{2+} is bound, the dye exhibits nearly no fluorescence, while upon Ca^{2+} binding, fluorescence increases up to 100 fold. With a dissociation constant (K_D) of 625 nM, CAL520 is compatible with the sperm $[Ca^{2+}]_i$ and is thereby suitable to monitor changes in sperm $[Ca^{2+}]_i$. In the FLUOstar, the fluorophore was excited at 480 nm; the fluorescence emission was recorded at 520 nm with bottom optics. In the stopped flow, the excitation wavelength was adjusted using a 494/20 BrightLine single-band bandpass filter (Semrock, USA). The emitted light was sent through a 536/40 nm BrightLine single-band bandpass filter (Semrock, USA).

To load sperm with CAL520, the membrane permeable CAL520 acetoxymethyl ester (CAL520-AM) was used *(Tsien, 1981)*. CAL520-AM does not bind Ca^{2+} as the charged Ca^{2+}-chelating carbonic acid residues of the BAPTA moiety are esterified. CAL520-AM is of neutral charge and thereby membrane permeable. Inside the cell, the acetoxymethyl ester groups are hydrolyzed by unspecific esterases, converting CAL520-AM into the charged, Ca^{2+}-sensitive fluorescent dye CAL520. Sperm were loaded for 45 min with 5 µM CAL520-AM (AAT Bioquest) in the presence of Pluronic F-127 (0.02% v/v) (Fig. 2.5c,d). For Ca^{2+} fluorimetry with capacitated mouse sperm, subsequent to dye loading, the cells were incubated for 90 min with TYH containing 25 mM $NaHCO_3$ and 3 mg/ml BSA. For Ca^{2+} fluorimetry with capacitated human sperm, CAL520-AM was added during the last 45 min of capacitation. After incubation with the fluorophore, human sperm were washed once by centrifugation (700 x g, 7 min) with 2 ml buffer while mouse sperm were washed three times.

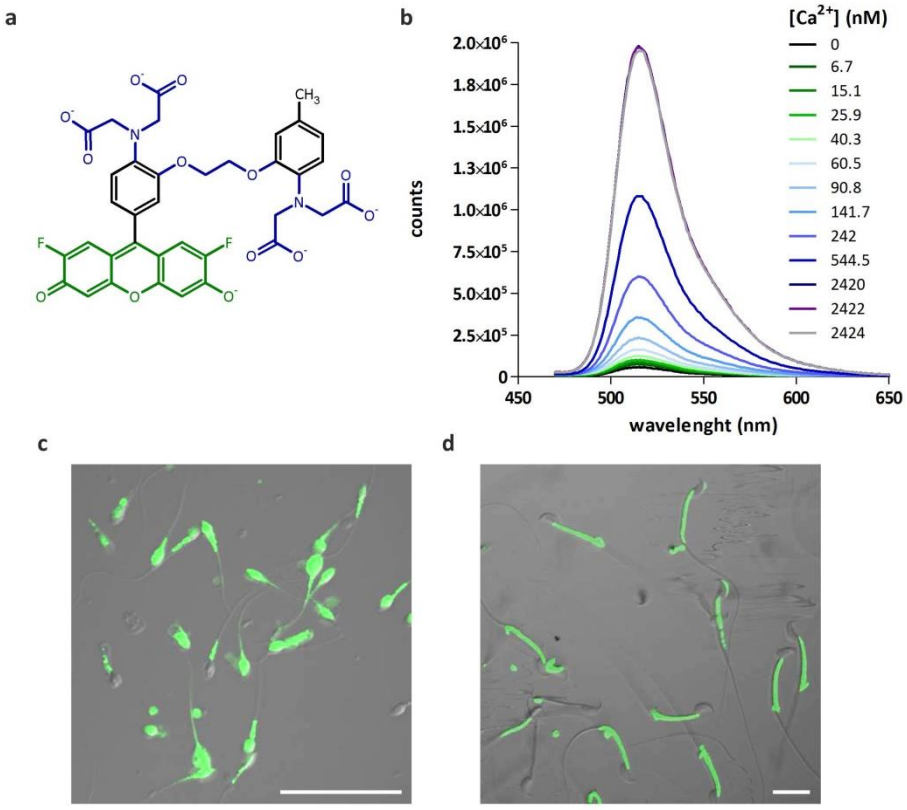

Fig. 2.5: Properties of the fluorescent Ca^{2+} indicator CAL520

(a) Chemical structure of a non-ratiometric Ca^{2+} indicatior. The fluorescein moiety is labelled in green, the Ca^{2+} chelator highlighted in blue. **(b)** Fluorescence emission spectra of the Ca^{2+} indicator CAL520 in pH 7.4 buffer with free Ca^{2+} values ranging from 0 to 2.4 µM, CAL520 was excited at 450 nm. **(c,d)** Non-capacitated **(c)** mouse and **(d)** human sperm loaded with CAL520-AM visualized using fluorescence microscopy; scale bar: 20 µm.

2.14.2 Fluorescent pH_i indicator BCECF

For pH_i fluorimetry, sperm were loaded with the fluorescent pH_i indicator BCECF (2',7'-Bis-(2-carboxyethyl)-5(und-6)carboxyfluorescein), a fluorescein derivative that changes its fluorescence spectrum with pH (Fig. 2.6a). With a pK_s value of 7.0, BCECF is well suited to detect changes in sperm pH_i. Upon excitation at 490 nm, the fluorescence intensity detected at 510 nm increases with alkalization (Fig. 2.6b, blue). In parallel, the fluorescence intensity of the fluorophore is pH-independent upon excitation at 440 nm (isosbestic point) (Fig. 2.6b, green). This allows a ratiometric measurement in the fluorescent plate reader by alternatively exciting the fluorophore at 440 nm and 490 nm while detecting the emission at 510 nm. An increase in the ratio $\frac{440\ ex;\ 510\ em}{490\ ex;\ 510\ em}$ resembles alkalization while a decrease resembles acidification, independent of both the amount of cells and effectiveness of BCECF loading. Further, the ratiometric measurement reduces injection artifacts and bleaching effects. Since in the stopped

flow, it is not possible to monitor two excitation wavelengths simultaneously, I took advantage of the fact that the emission spectrum of BCECF is also dependent on pH. Alkalisation and acidification shifts the emission spectrum to shorter or longer wavelength, respectively (Fig. 2.6c). Therefore, for pH measurements in the stopped flow, BCECF was excited using a 452/45 nm BrightLine single-band bandpass while two emission wavelengths were recorded in parallel.

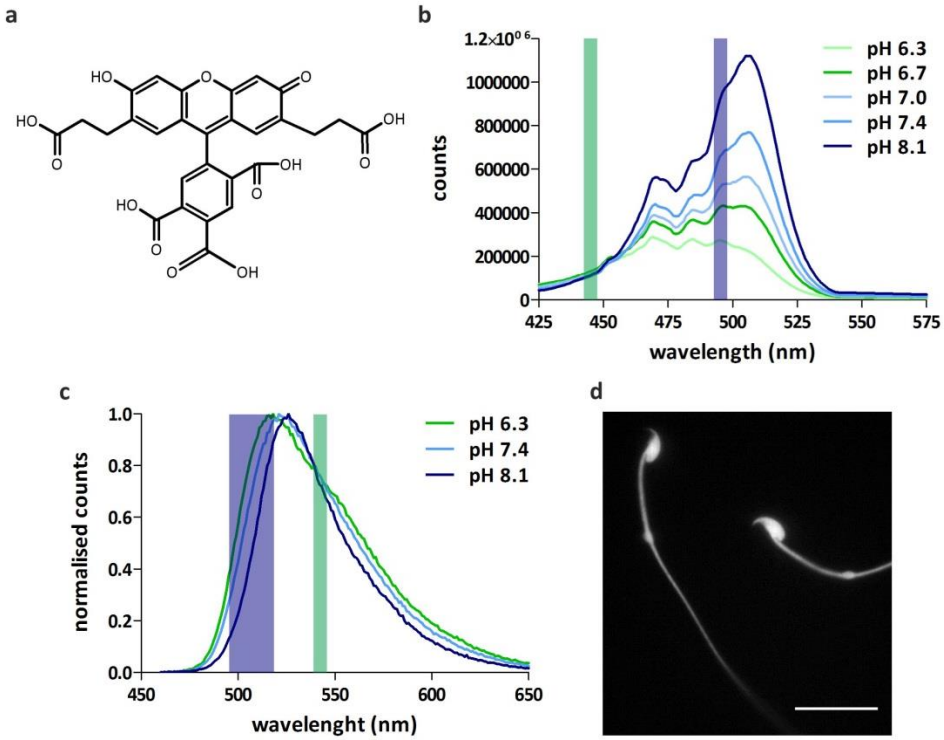

Fig. 2.6: Properties of the fluorescent pH_i indicator BCECF

(a) Chemical structure of BCECF. **(b)** Relative fluorescence intensity of BCECF in dependence of pH (6.2 – 9.5). During FLUOstar experiment, BCECF was excited at 440 nm (green) and 490 nm (blue), emission was detected at 510 nm. **(c)** Fluorescence emission spectra of the fluorescent pH_i indicator BCECF in sperm buffer with varying pH_i. During stopped flow experiment, BCECF was excited at 452 nm, emission was detected at 494 nm (blue) and 540 nm (green). **(d)** Non-capacitated mouse sperm loaded with BCECF. BCECF was exited with 488 nm; scale bar: 20 µm.

A 494/20 nm BrightLine single-band bandpass filter (Semrock) was used for the left part of the spectrum (blue), which is highly dependent on the pH. The second emission was detected with a 540/10 nm BrightLine single-band bandpass filter (Semrock) at the isosbestic point of the spectrum (green), where the spectrum is pH independent. An increase of the ratio $\frac{452\text{ ex; }494\text{ em}}{452\text{ ex; }540\text{ em}}$ represents alkalization; a decrease represents acidification. To measure changes in pH_i in sperm, cells were loaded for 10 min with 10 µM BCECF-AM and subsequently washed with 2 ml buffer to remove residual extracellular fluorophore (Fig. 2.6d). For pH_i fluorimetry in capacitated sperm, BCECF-AM was added during the last 10 min of capacitation.

2.14.3 Ca^{2+} and pH_i fluorimetry in multi-well plates

Fluorescence measurements of sperm populations in multiwell plates were carried out using the fluorescence plate-reader Fluostar Omega (BMG Labtech, Ortenberg). For the measurements, 384 well plates (Greiner Bio-One) were used, enabling to analyze several conditions and stimuli in parallel over long time intervals. In the Fluostar, the multi-well plate is moved past a detector head, which records the fluorescence individually from the bottom of each well. Fluorescence is excited by a flash tube and the resulting fluorescence value is averaged from individually measured values. The time resolution of each measurement is dependent on the number of wells that are recorded, determining the time needed for a full measurement cycle. Each well contained 50 µl of a fluorophore-loaded sperm suspension set to a concentration between 0.5 and 5 x 10^6 sperm/ml. After 10 cycles, the experiment was interrupted, and 10 to 50 µl stimuli, inhibitor or buffer as control were added to the sperm suspension. The solutions were injected manually into the wells with an electronic multichannel pipette. For data analysis and evaluation the software Prism 5.1 (GraphPad software, USA) was used.

2.14.4 Stopped-flow device

The kinetic stopped-flow technique allows to detect reactions in the millisecond to second time scale (Johnson, 1986) after rapidly mixing a single or multiple solutions with a reacting agent. Mixing takes place in a special mixing chamber; afterwards, the reactants are transferred into a detection chamber, e.g. a cuvette. The reaction can be monitored with optical, calorimetric, or electrical methods. The time resolution (T) of the stopped flow depends on the volume of the system (V) and on the flow rate (F) and can be calculated with T = V/F. The central part of the stopped flow is the SFM-400 module, which consists of four 10 ml syringes (a simplified representation with two syringes is shown in Fig. 2.7). The syringes can be filled with solutions using a filling valve. The plungers of the syringes can be moved with stepping motors. Using the Biokine Software (version 4.45, Biologic), the stepping motors are navigated with the control unit (MPS-60, BioLogic). The solutions in the syringes are mixed in a mixing chamber. For pH_i and Ca^{2+} fluorimetry the sperm suspension was filled in syringe 3 (S3), the test solution in syringe 4 (S4), and the washing solution for rinsing the cuvette between measurements in syringe 1. For detection, a quartz cuvette (FC-15) installed behind the mixing chamber with a reaction volume of 31 µl was used. The dead time between mixing of sperm with the test solution and the start of the detection was 87.7 ms at a flow rate of 0.5 ml/s. Alterations of the liquid column in the cuvette can result in considerable noise. To avoid these fluctuations, a hard-stop valve is installed, which closes the detection chamber after the injection and prevents a post-pulse oscillation of the liquid column. The hard-stop valve is operated by the control software of the stopped-flow device.

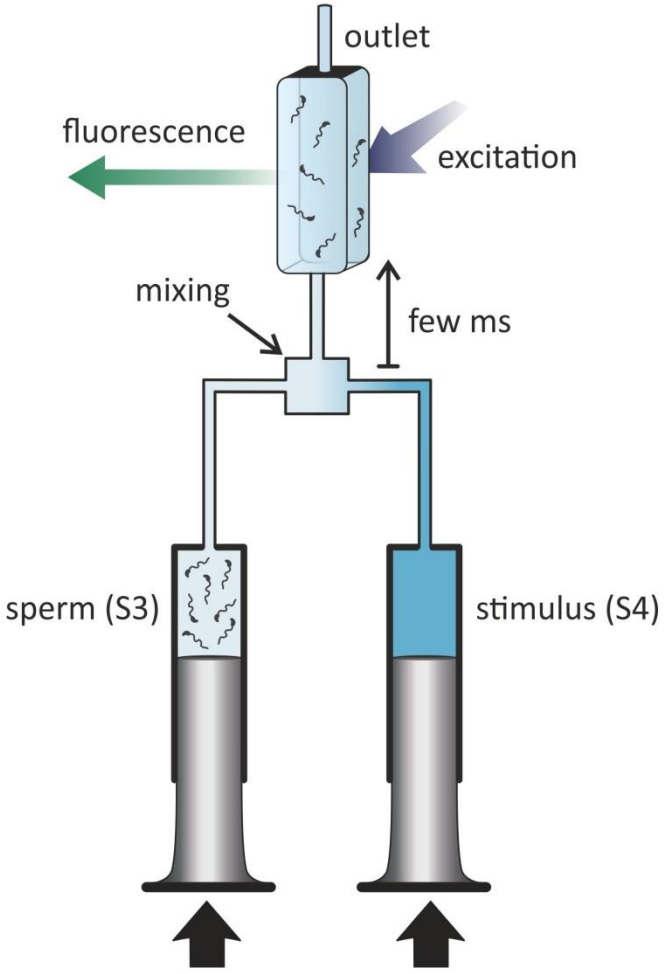

Fig. 2.7: Measuring principle of the SFM-400 stopped-flow device

For Ca^{2+} and pH_i fluorimetry the sperm suspension was filled in S3, the test solution in S4. The dead time between starting the reaction by mixing the sperm with the test solution and detecting the reaction in the cuvette was 87.7 ms at a flow rate 0f 0.5 ml/s. See text for details. S = syringe.

2.14.5 Ca^{2+} and pH_i fluorimetry in the stopped-flow device

Kinetic Ca^{2+} and pH_i fluorimetry were performed in the stopped-flow device (SFM400, Bio-Logic, Grenoble, F) at 37°C. In the stopped-flow device, the sperm suspension (5 x 10^6 sperm/ml) was rapidly mixed (1:1 v/v; flow rate 0.5 ml/s) with different stimuli. At this flow rate, no physical damage of sperm was detected, and their swimming behavior appeared normal. Fluorescence was evoked by a LED light source (Spectra X; Lumencor, Beaverton, USA) and recorded by a photomultiplier (H9656-20; Hamamatsu Photonics, Hamamatsu City, Japan) with connected amplifier (C7169; Hamamatsu). At the beginning of a measurement, the stepper motors were synchronized (50 ms) and the system was rinsed with 400 µl sperm buffer within 200 ms. After a subsequent pause of 200 ms, 100 µl sperm suspension were mixed with 100 µl test solution. After 200 ms, the hard stop valve was closed, resulting in a dead time between the mixer and

the cuvette of 87.7 ms. Changes in pH_i or $[Ca^{2+}]_i$ were fluorometrically recorded in the cuvette. Data were analyzed using Prism 5.1 (GraphPad software, USA). For each experiment, sperm were first mixed with buffer and a baseline was recorded (Fig. 2.8a). Then, sperm were subsequently mixed with the stimuli. For each stimulus, two or three traces were recorded and directly averaged. Using the Prism 5.1 software, after the measurement each trace was normalized to the mean value of the first three data points of the recording (Fig. 2.8b). Then the baseline was subtracted from each trace (Fig. 2.8c). To improve the resolution, the signal was smoothed with four neighbors on each side (Fig. 2.8d).

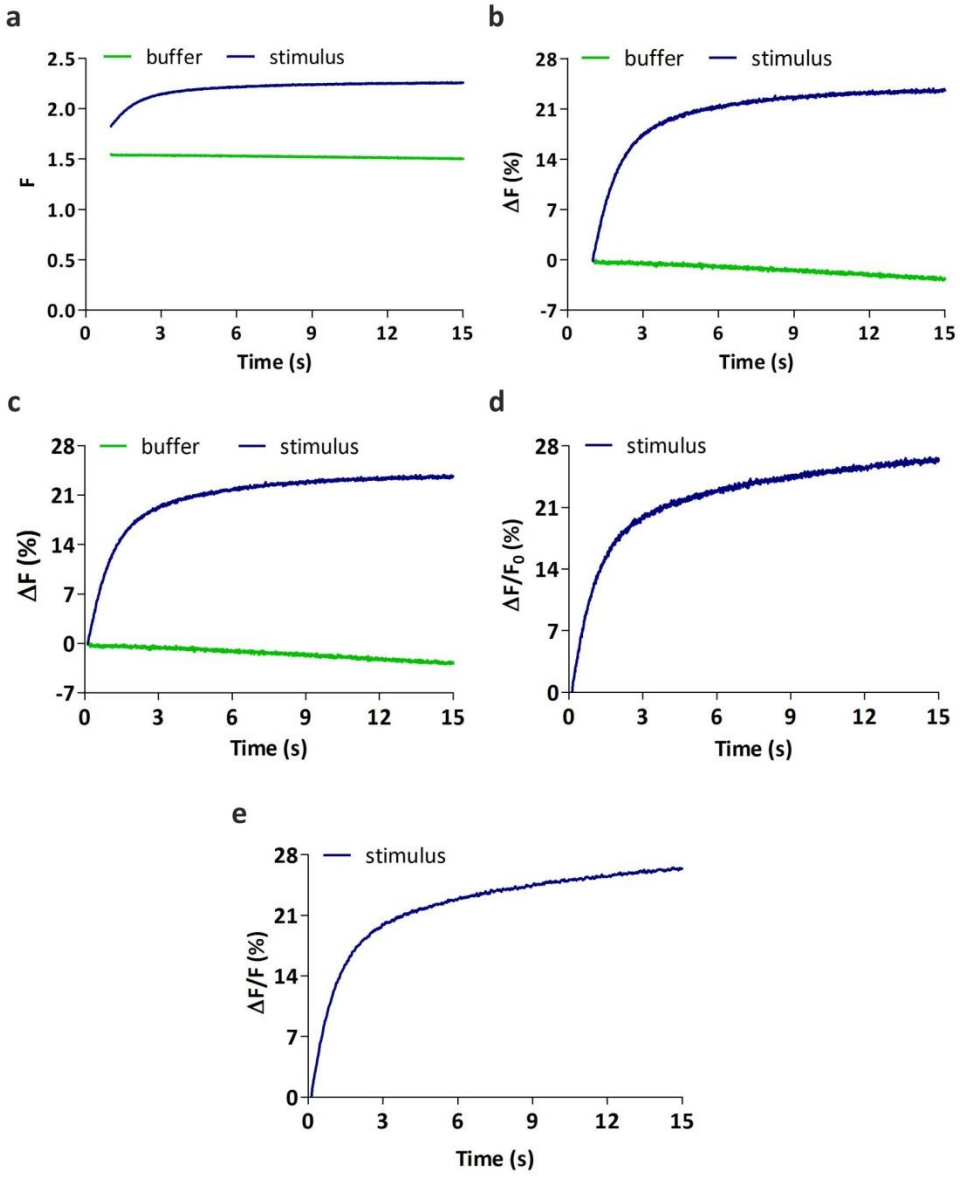

Fig. 2.8: Analysis of stopped flow raw data with the GraphPad Prism software

(a) Stopped-flow raw data. **(b)** Normalization to the mean value of the first three data points. **(c)** Subtraction of dead time from each y data point. **(d)** Subtraction of baseline from stimulus trace. **(e)** Smoothing of the stimulus trace with four neighbors on each side. F = fluorescence.

2.14.6 Calculation of EC_{50} values from dose-response curves

The half maximal effective concentration (EC_{50}) describes the potency of a substance to induce an effect. To determine EC_{50} values, sperm were stimulated with different concentrations of the substance. The maximal relative change in CAL520 fluorescence ($\Delta F/F_0$) was determined and plotted against the logarithmic substance concentration. The resulting data set was fitted to a modified Hill equation (F = fluorescence, [P] = concentration of substance, n = Hill coefficient).

$$\Delta F/F_0 = \frac{\Delta F/F_{min} - \Delta F/F_{max}}{1 + ([P]/EC_{50})^n} + \Delta F/F_{max}$$

Data analysis was carried out using Prism 5.1 (GraphPad software, USA).

3 Results

3.1 The action of zona pellucida glycoproteins in mouse sperm

3.1.1 Isolation and functional characterization of native mouse zona pellucida glycoproteins

To study zone pellucida (ZP)-induced signaling events in mouse sperm, ZP glycoproteins were isolated from mouse oocytes. To this end, oviducts were prepared from the genital tract of superovulated female mice (Fig. 3.1a_i). Fig. 3.1a_{ii} illustrates the swollen oviductal ampulla, containing a high number of ovulated oocytes. The ampulla was ruptured to release the oocytes (Fig. 3.1a_{iii}). In mice, the ZP is made up of three different ZP glycoproteins, ZP1, ZP2, and ZP3, which form a mesh-like structure (Fig. 3.1b). Staining of the isolated oocytes with antibodies against ZP1, ZP2, and ZP3 labeled the ring-shaped ZP surrounding the oocyte (Fig. 3.1c). The zona pellucidae (ZPs) were mechanically peeled off the oocytes by trituration using a Pasteur pipette (Ø 50 nm) (Fig. 3.1$_{iv}$). Overall, about 400 to 600 ZPs were isolated from 30 superovulated mice. ZPs were counted, homogenized by heat-solubilization, and the ZP homogenate was adjusted to a “concentration” of 1 ZP per µl. On Western blots of homogenized ZPs, anti-ZP1,

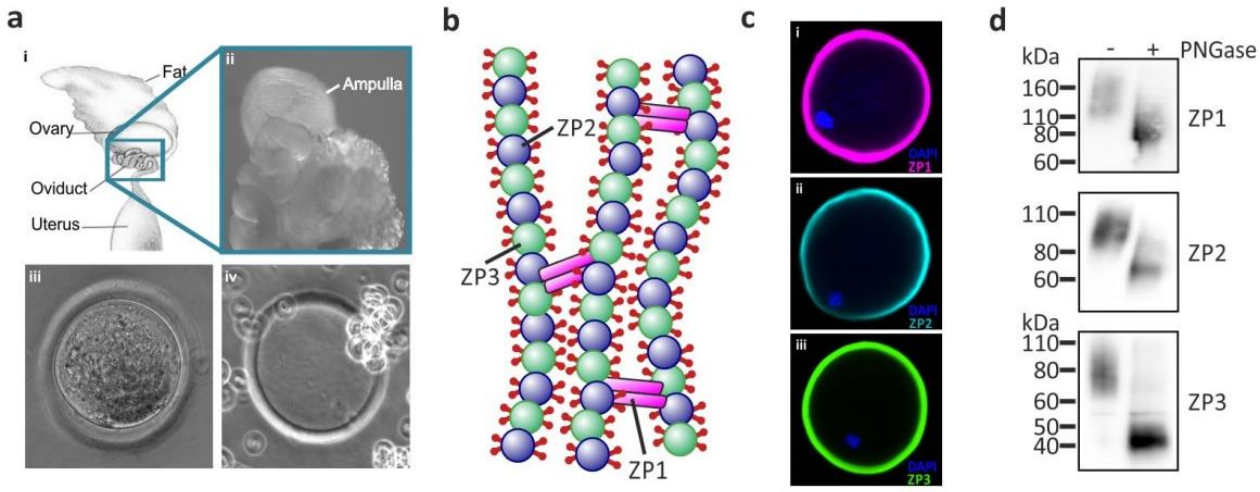

Fig. 3.1: Isolation of mouse zona pellucida glycoproteins

(a) Isolation of mouse zona pellucida (ZP) glycoproteins. (i) Mouse genital tract. (ii) Oviduct with swollen ampulla dissected from superovulated mice. (iii) Oocyte released from ampulla. (iv) Mouse ZP separated from oocytes. **(b)** ZP consists of three proteins: ZP2 and ZP3 heterodimers form long filaments that are interconnected by ZP1 dimers. Modified after Wasserman 1988. **(c)** Staining of mouse oocytes with antibodies directed against (i) ZP1 (purple), (ii) ZP2 (cyan), (iii) ZP3 (green); the DNA was labeled using DAPI (blue). **(d)** Immunoblots of isolated ZPs under control conditions (-) and after PNGase treatment (+) verified using specific ZP antibodies.

anti-ZP2, and anti-ZP3 antibody detected proteins of about 150, 100, and 80 kDa, respectively (Fig. 3.1d), which is in line with the molecular weight of the respective ZP glycoproteins reported before (Wassarman, 1988). Furthermore, the ZPs were treated with PNGase to test whether the isolation protocol preserved the glycosylation of the proteins. PNGase treatment decreased the apparent molecular weight of both ZP1 and ZP2 by around 20 kDa and of ZP3 by around 40 kDa, indicating that the isolation preserves the glycosylation of the individual ZP glycoproteins (Fig. 3.1d).

To test whether the homogenized ZPs are functional, I analyzed if they evoked the acrosome reaction in mouse sperm. Non-capacitated and capacitated sperm were incubated in buffer containing 0.5 ZP/µl or 1 ZP/µl or, as positive control, the Ca^{2+} ionophore ionomycin. The acrosome was labeled with peanut lectin coupled to a green fluorescent dye (PNA-FITC) (Lybaert *et al.*, 2009). The fraction of acrosome-reacted sperm was determined and to correct for spontaneous acrosome reaction, the results were normalized to acrosome reaction rates determined in sperm bathed in buffer (negative control). Fig. 3.2a shows a characteristic PNA-FITC and DAPI staining of acrosome-intact and acrosome-reacted mouse sperm heads. In acrosome-intact sperm, PNA-FITC labels the sickle-shaped acrosome that caps the nucleus (Fig. 3.2a, top), whereas in acrosome-reacted sperm, labeling of the sperm head is only sparse and punctuated or even completely absent (Fig. 3.2a, bottom). In capacitated sperm, incubation in 0.5 ZP/µl and 1 ZP/µl increased the fraction of acrosome-reacted sperm by 1.3- and 1.7-fold, respectively (Fig. 3.2b, teal bars). In non-capacitated sperm, the action of ZPs was strongly attenuated; incubation in 1 ZP/µl increased the fraction of acrosome-reacted sperm by only 1.2 fold and 0.5 ZP/µl did not evoke a response (Fig. 3.2b, gray bars), demonstrating that

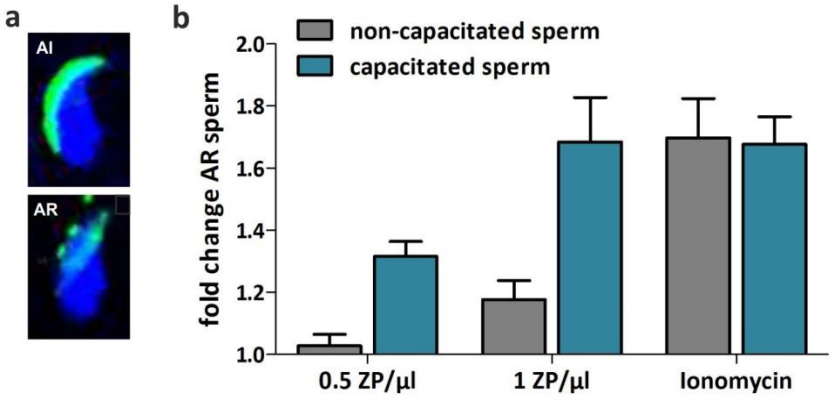

Fig. 3.2: Zona pellucida glycoproteins evoke the acrosome reaction in mouse sperm

(a) Sperm were immobilized on a glass slide and the acrosome was labelled with PNA-FITC (green), DNA was stained with DAPI (blue). Acrosome-intact sperm (AI), acrosome-reacted sperm (AR). **(b)** Acrosome reaction evoked by ZPs or 2 µM ionomycin in non-capacitated (grey) or capacitated (teal) mouse sperm. The data were normalized to spontaneous acrosome reaction rates of control sperm bathed in buffer. Data are shown as mean; error bars indicate + SD (n = 3).

capacitation primes sperm for ZP-induced acrosomal exocytosis. In both non-capacitated and capacitated sperm, ionomycin increased the fraction of acrosome- reacted sperm by 1.7 fold, indicating that the action of ionomycin is independent of capacitation. Altogether, these experiments demonstrate that the isolated ZPs are functional.

3.1.2 ZP-evoked $[Ca^{2+}]_i$ responses

Stimulation of mouse sperm with ZP glycoproteins evokes a Ca^{2+} influx (Arnoult *et al.*, 1996b; Jungnickel *et al.*, 2001; Publicover *et al.*, 2007) via CatSper (Xia & Ren, 2009). I set out to reproduce this result by monitoring changes in $[Ca^{2+}]_i$ in mouse sperm populations loaded with the fluorescent Ca^{2+} indicator CAL520-AM using the kinetic stopped-flow technique (Master thesis Melanie Balbach; Jansen *et al*., 2015; Schiffer *et al*., 2014; Schneider *et al*., 2016). First, I studied CatSper-mediated Ca^{2+} responses evoked by mixing of capacitated mouse sperm with alkaline-depolarizing medium (K8.6) or 8-Br-cAMP. As a positive control, I measured Ca^{2+} responses evoked by mixing with ionomycin. Fig. 3.3a-c show the individual Ca^{2+} responses in sperm from 18 different mice. All three stimuli evoked a rapid and sustained Ca^{2+} increase, demonstrating that the stopped-flow technique is suited to study Ca^{2+} signaling in mouse sperm. However, the overall signal amplitudes varied considerably among the different sperm samples. For the ease of illustration and to account for the variability, the individual traces were averaged and plotted along with the 95% confidence interval, as shown in Fig. 3.3d-f (dark blue). The light blue traces in Fig. 3.3d-f show the averaged Ca^{2+} responses evoked in non-capacitated sperm, which displayed a similar inter-experimental variation. The signal kinetics were overall similar in capacitated vs. non-capacitated sperm: irrespective of the stimulus and capacitation status, $[Ca^{2+}]_i$ rose without a measurable latency within the time resolution of the stopped-flow technique (∼90 ms) (Fig. 3.3d-f). Moreover, the time course of the K8.6-, 8-Br-cAMP-, and ionomycin-evoked responses were similar, i.e. the signal saturated at about 10 s, and stayed elevated throughout the recording time. The signal amplitudes evoked by K8.6 and 8-Br-cAMP were slightly enhanced in capacitated vs. non-capacitated sperm. However, the ionomycin-evoked amplitude, showing the upper response limit, was attenuated by capacitation. To correct for the different upper response limits in non-capacitated vs. capacitated sperm and for inter-experimental variations, the individual signal amplitudes evoked by K8.6 and 8-Br-cAMP were determined (Fig. 3.3a,b, gray bars) and normalized to the signal amplitude of the respective ionomycin control (Fig. 3.3c, gray bar). These individual normalized amplitudes were used to calculate the mean signal amplitudes. The normalized K8.6-induced signal amplitude was 0.11 ± 0.05 and 0.24 ± 0.12 in non-capacitated and capacitated sperm, respectively (Fig. 3.3h). The amplitude evoked by 8-Br-cAMP was 0.12 ± 0.04 and 0.33 ± 0.25 in non-capacitated and capacitated sperm, respectively (Fig. 3.3h). Altogether, this demonstrates that capacitation enhances CatSper-mediated Ca^{2+} influx.

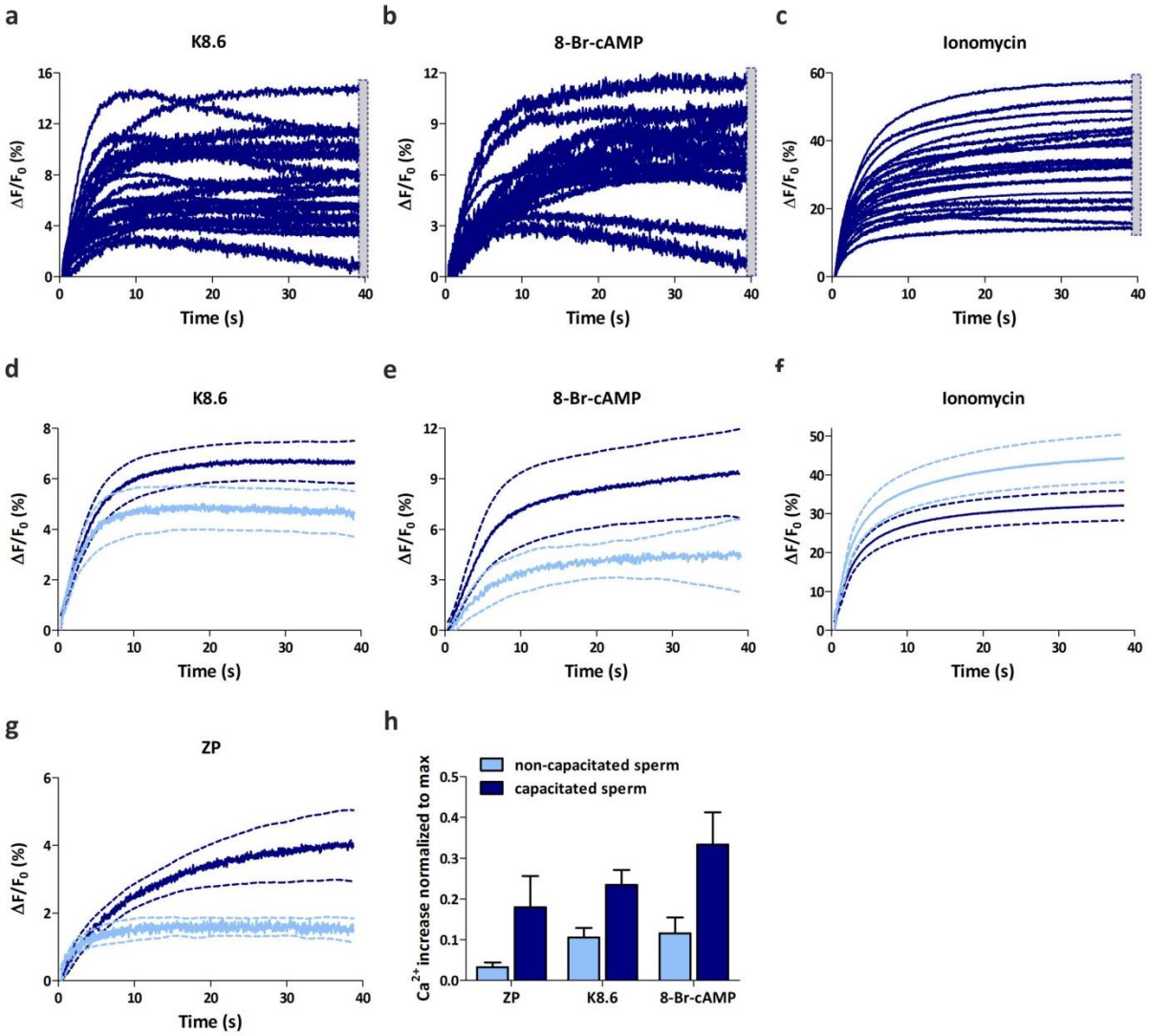

Fig. 3.3: Zona pellucida glycoproteins evoke Ca^{2+} responses in mouse sperm

(a-c) Individual responses in $[Ca^{2+}]_i$ in mouse sperm evoked by **(a)** alkaline depolarizing medium (K8.6), **(b)** 10 mM 8-Br-cAMP, **(c)** 2 µM ionomycin. Individual signal amplitudes used to calculate the mean amplitudes are highlighted with gray bars. **(d-g)** Changes in $[Ca^{2+}]_i$ evoked by **(d)** K8.6, **(e)** 10 mM 8-Br-cAMP, **(f)** 2 µM ionomycin, or **(g)** 0.5 ZP/µl in non-capacitated (light blue) and capacitated sperm (dark blue). Mean ± 95% CI (dashed traces) (n=7). Changes in $[Ca^{2+}]_i$ were recorded in a stopped-flow apparatus using sperm loaded with the Ca^{2+}-sensitive fluorophore CAL520-AM. $\Delta F/F_0$ (%) indicates the percentage change in fluorescence (ΔF) with respect to the mean basal fluorescence (F_0) of the first 3 data points recorded immediately after mixing (F). **(h)** Mean signal amplitudes normalized to the maximal response evoked by 2 µM ionomycin; error bars indicate + SD (n = 7).

Fig. 3.3g shows the Ca^{2+} response evoked by mixing of sperm with 0.5 ZP/µl. In both non-capacitated and capacitated sperm, the ZPs evoked a rapid and sustained Ca^{2+} increase; the signal saturated at about 10 to 20 s and settled at an elevated level throughout the recording

time. The amplitude of the ZP response was strongly enhanced in capacitated versus non-capacitated sperm; the normalized amplitudes were 0.18 ± 0.07 and 0.03 ± 0.01, respectively, demonstrating that capacitation primes sperm to respond to stimulation by ZPs.

Next, I scrutinized whether the ZP-induced Ca^{2+} response is mediated by CatSper by studying ZP responses in capacitated CatSper$^{-/-}$ sperm (Fig. 3.4). In CatSper$^{-/-}$ sperm, ionomycin, but not ZPs or K8.6 and 8-Br-cAMP evoked a Ca^{2+} response. To verify that this particular batch of ZPs was functional, I studied in parallel Ca^{2+} responses in wildtype as a control. In wildtype sperm, ZPs, K8.6, and 8-Br-cAMP evoked a Ca^{2+} response. Altogether, these experiments confirm that the ZP-, K8.6-, and 8-Br-cAMP-induced Ca^{2+} influx is mediated by CatSper.

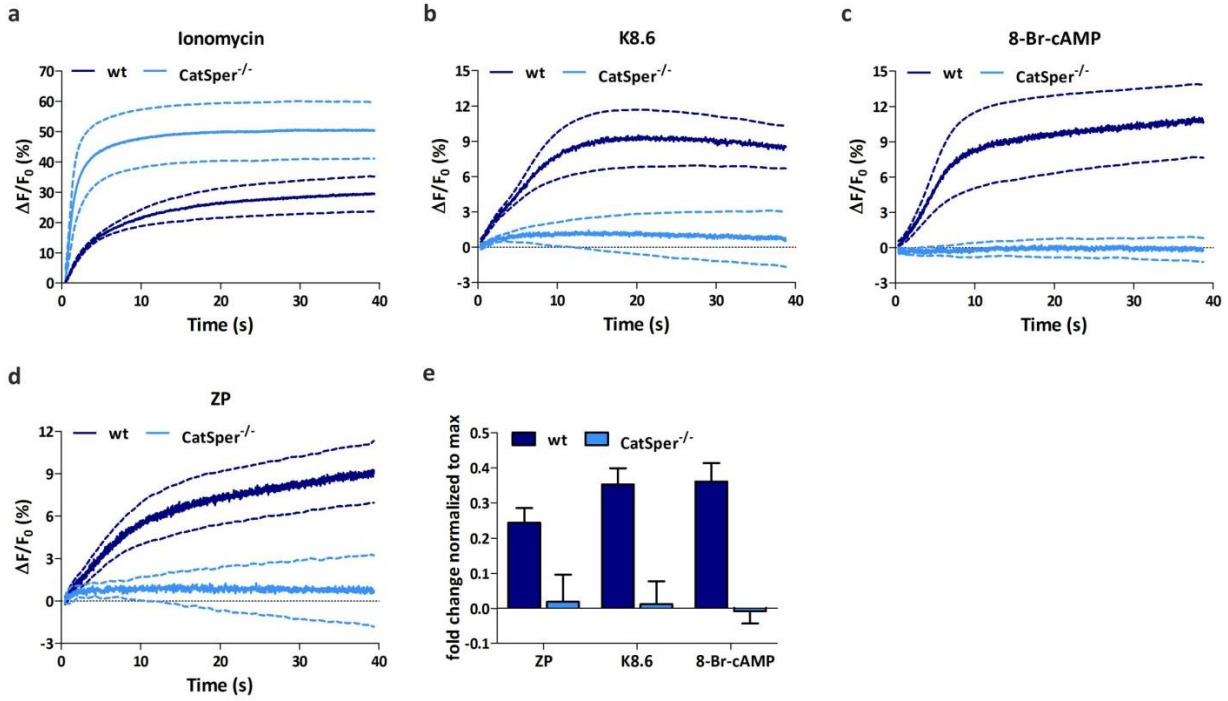

Fig. 3.4: CatSper mediates the ZP-induced Ca^{2+} increase in mouse sperm

(a-d) Changes in $[Ca^{2+}]_i$ evoked by **(a)** 2 µM ionomycin, **(b)** K8.6, **(c)** 8-Br-cAMP, and **(d)** 0.5 ZP/µl in capacitated wildtype (wt) (dark blue) or CatSper$^{-/-}$ (light blue) mouse sperm. Mean ± 95 % CI (dashed traces), n = 4. **(e)** Mean signal amplitudes, normalized to the maximal Ca^{2+} response evoked by 2 µM ionomycin; error bars indicate + SD (n = 4).

3.1.3 ZP-evoked pH_i responses

Stimulation of mouse sperm with isolated ZPs evokes a pH_i increase (Arnoult *et al.*, 1996b). I tried to reproduce this result using the kinetic stopped-flow technique. To this end, changes in pH_i were monitored in capacitated mouse sperm populations loaded with the fluorescent pH indicator BCECF-AM. First, I studied pH_i responses evoked by the weak base ammonium chloride (NH_4Cl), which is commonly used to alkalize the pH_i of cells. Mixing of sperm with NH_4Cl evoked

a rapid increase of the BCECF fluorescence ratio $\Delta R/R_0$ (Fig. 3.5a), indicating a pH_i increase. To account for the variability among different sperm samples, the individual pH_i responses were averaged and plotted along with the 95 % confidence interval. The pH_i signal rose within the time resolution of the stopped-flow technique (~90 ms), saturated at about 20 s, and remained elevated throughout the recording time (Fig. 3.5a). Thus, BCECF faithfully reports pH_i changes in mouse sperm. Next, I studied ZP-evoked pH_i responses. Mixing sperm with ZPs evoked a rapid and sustained pH_i increase (Fig. 3.5b), confirming the results by Arnault *et al.*. The pH_i rose without a measurable latency within the time resolution of the system, the signal saturated at around 20 s, and the pH_i stayed elevated throughout the recording time. I wondered whether the ZP-induced pH_i increase requires Ca^{2+} influx via CatSper. Mixing CatSper$^{-/-}$ sperm with either NH_4Cl or ZPs evoked a pH_i increase whose kinetics and time course was similar to that evoked in wildtype sperm (Fig. 3.5c-d). Moreover, also the amplitude of the pH_i response was similar in wildtype and CatSper$^{-/-}$ sperm (3.3 % ± 1.1 vs. 2.3 % ± 1.1, respectively) (Fig. 3.5e). These results indicate that the ZP-induced pH_i increase happens independent and most likely upstream of the Ca^{2+} influx via CatSper.

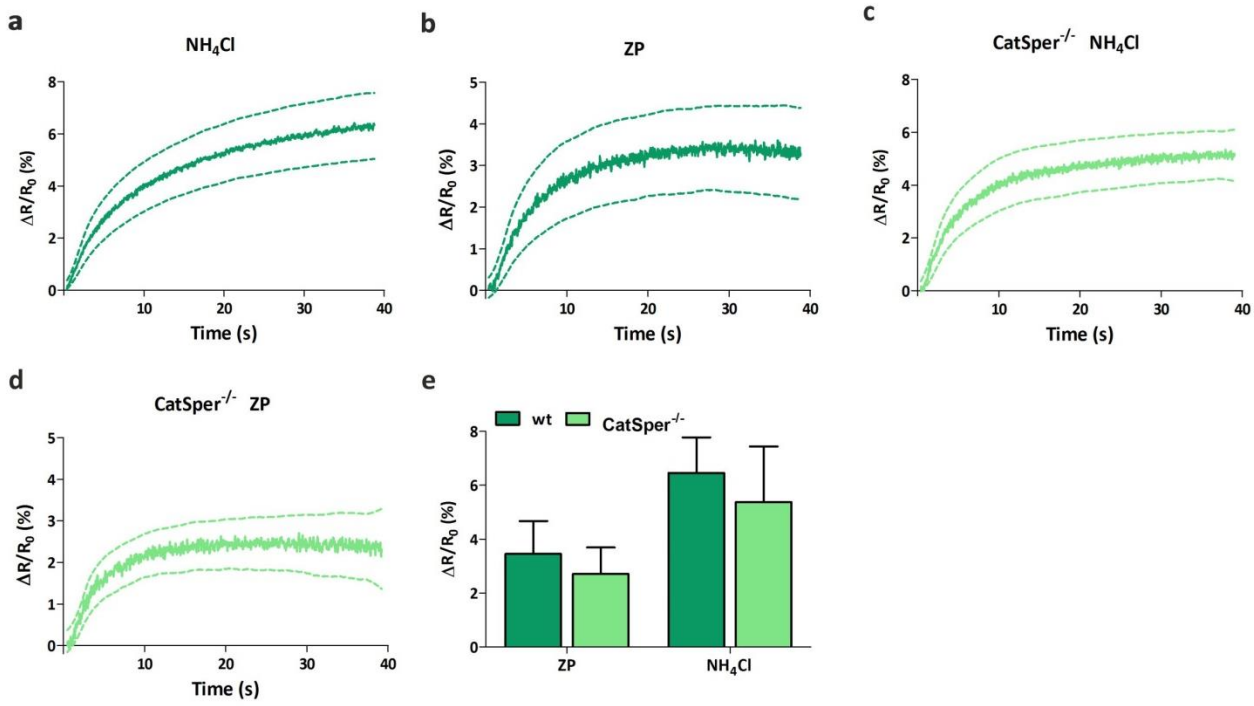

Fig. 3.5: ZP evokes a pH_i response in wildtype and CatSper $^{-/-}$ sperm

(a) Change in pH_i evoked by mixing of sperm with 10 mM NH_4Cl. **(b)** Change in pH_i evoked by 0.5 ZP/µl in capacitated mouse sperm. **(c,d)** Change in pH_i evoked by **(c)** 10 mM NH_4Cl or **(d)** 0.5 ZP/µl in capacitated CatSper$^{-/-}$ mouse sperm. Mean ± 95 % CI (dashed traces), n = 7. Changes in pH_i were recorded in a stopped-flow apparatus in sperm loaded with the pH indicator BCECF-AM. **(e)** Mean signal amplitudes; error bars indicate + SD (n = 7).

In fact, CatSper is activated by intracellular alkalization. Fig. 3.6a shows a NH_4Cl-induced Ca^{2+} increase in mouse sperm. Thus, the ZP-induced pH_i increase might underlie the activation of CatSper by ZPs. This implies that the alkalization precedes the Ca^{2+} influx via CatSper, i.e. the latency of the pH_i increase must be shorter than that of the Ca^{2+} increase. Fig. 3.6b shows a superposition of the ZP-evoked pH and Ca^{2+} signals. Analyzing the first 10 s of the signal revealed that both signals rise without a measurable latency within the time resolution of the system (Fig. 3.6c). This renders the delineation of the sequence of events impossible. Therefore, I used a different approach to gain a deeper insight into the mechanism underlying the ZP-induced alkalization.

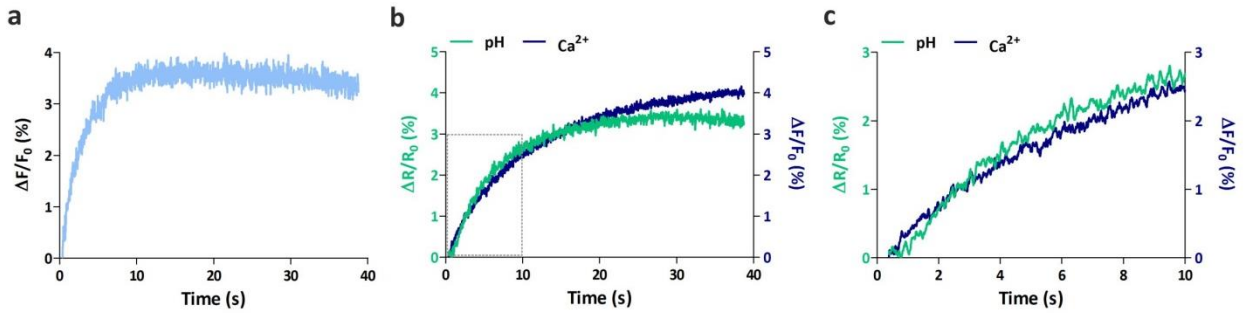

Fig. 3.6: Kinetic of the ZP-evoked pH_i and $[Ca^{2+}]_i$ increase

(a) Change in $[Ca^{2+}]_i$ evoked by 10 mM NH_4Cl in capacitated mouse sperm. **(b)** Superposition of ZP-evoked pH_i (green) and $[Ca^{2+}]_i$ (blue) responses. **(c)** First 10 s of ZP-evoked pH_i (green) and $[Ca^{2+}]_i$ (blue) increase, enlarged plot of boxed section from (b).

Fig. 3.7 shows ZP-induced pH_i signals in sperm bathed in 5 mM (control) or 138 mM extracellular K^+ ($[K^+]_o$) to depolarize V_M. Under control conditions, the ZPs induced the characteristic pH_i

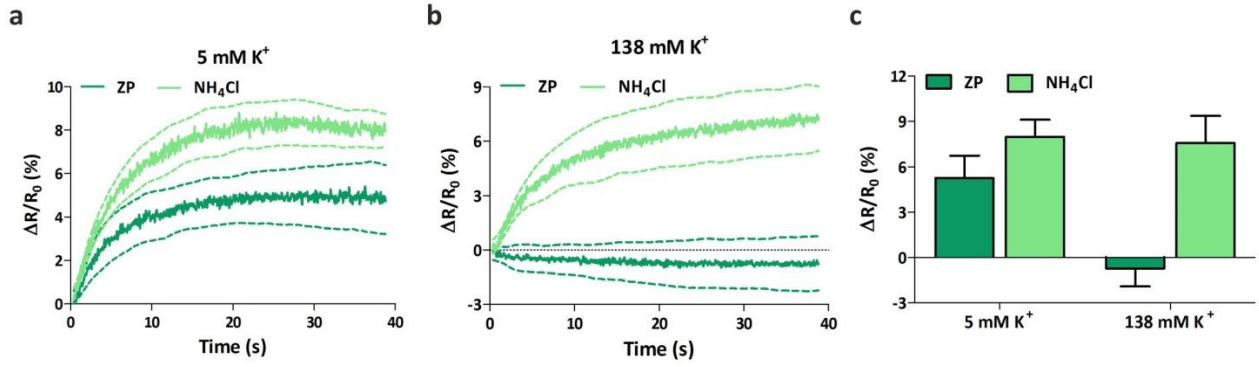

Fig. 3.7: ZP-induced pH_i responses at low and high extracellular K^+ concentrations

(a,b) Change in pH_i evoked by 0.5 ZP/µl (dark green) or 10 mM NH_4Cl (light green) in capacitated sperm bathed in **(a)** 5 mM (control) or **(b)** 138 mM K^+ buffer. Mean ± 95 % CI (dashed traces), n = 3. **(c)** Mean signal amplitudes; error bars indicate + SD (n = 3).

increase, whereas, at high $[K^+]_o$, the ZP-evoked alkalization was abolished ($\Delta R/R_0$ = 4.8 ± 1.6 % vs. -0.7 ± 1.44 %) (Fig. 3.7a,b). The NH_4Cl-evoked pH_i increase was, however, rather independent of $[K^+]_o$ (Fig. 3.7c). These results suggest that depolarization of V_M disables ZP-induced pH signaling.

To scrutinize this hypothesis, I studied ZP-induced pH_i responses in sperm deficient for the K^+ channel Slo3 or for its accessory subunit LRRC52. Both $Slo3^{-/-}$ and $LRRC52^{-/-}$ sperm suffer from

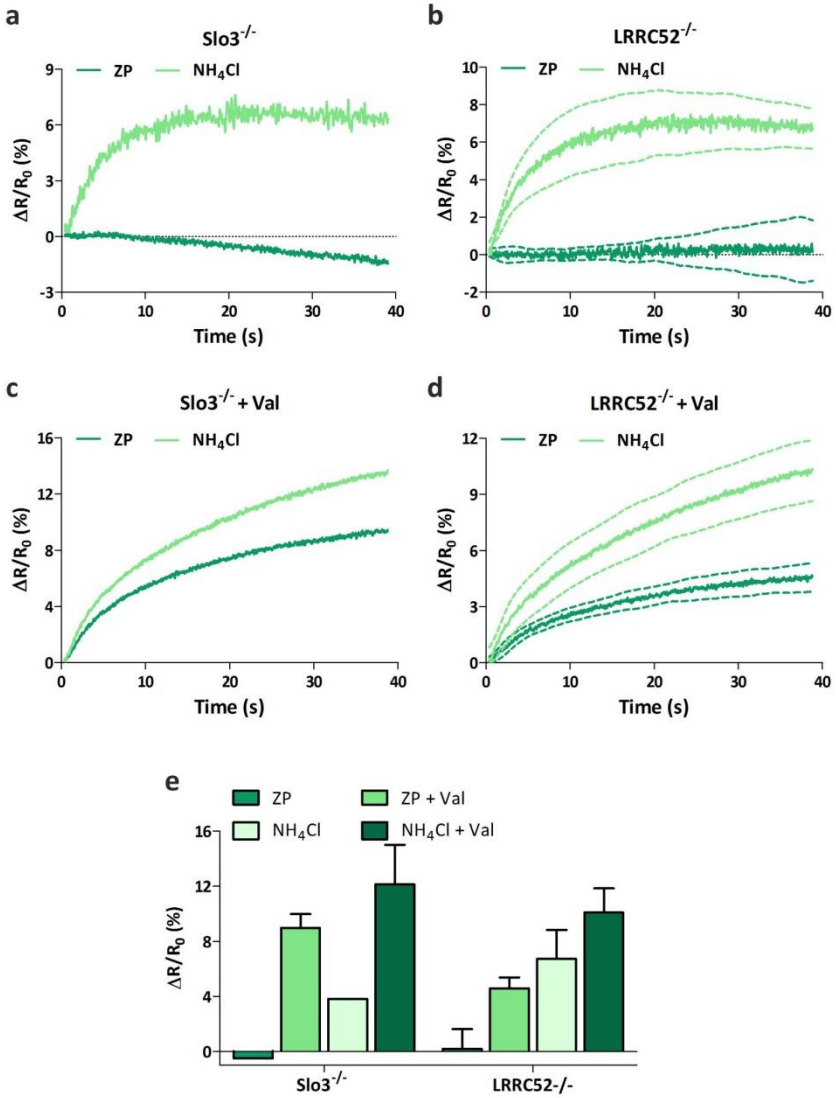

Fig. 3.8: ZP-induced pH_i responses in $Slo3^{-/-}$ and $LRRC52^{-/-}$ sperm

(a,b) Change in pH_i evoked by 0.5 ZP/µl (dark green) or 10 mM NH_4Cl (light green) in capacitated **(a)** $Slo3^{-/-}$ (n = 1) and **(b)** capacitated $LRRC52^{-/-}$ mouse sperm. **(c,d)** Change in pH_i evoked by 0.5 ZP/µl (dark green) or 10 mM NH_4Cl (light green) in capacitated **(c)** $Slo3^{-/-}$ (n = 2) and **(d)** $LRRC52^{-/-}$ mouse sperm after preincubation with 2 µM valinomycin (Val). Mean ± 95 % CI (dashed traces), n = 4. **(e)** Mean signal amplitudes; error bars indicate + SD (n ≥ 1).

a depolarized V_M (Zeng *et al.*, 2011; Zeng *et al.*, 2015). Whereas mixing of $Slo3^{-/-}$ and $LRRC52^{-/-}$ sperm with NH_4Cl evoked an alkalization, ZPs did not change pH_i (Fig. 3.8a,b). Furthermore, in $Slo3^{-/-}$ and $LRRC52^{-/-}$ sperm bathed in the K^+ ionophore valinomycin, which hyperpolarizes V_M, the ZP-induced alkalization was restored (Fig. 3.8c,d). Taken together, these experiments support the notion that a polarized membrane potential is required for ZP-induced pH_i signaling.

Next, I studied ZP-evoked Ca^{2+} responses in $LRRC52^{-/-}$ and wildtype sperm bathed in 5 mM and 138 mM $[K^+]_o$. In wildtype sperm, the ZP-evoked Ca^{2+} response was strongly attenuated at high $[K^+]_o$; the relative signal amplitudes were 0.12 ± 0.09 and 0.02 ± 0.05 at 5 mM and 138 mM $[K^+]_o$, respectively (Fig. 3.9a,b), confirming previous results (Chávez *et al.*, 2014; De La Vega-Beltran *et al.*, 2012). Moreover, in $LRRC52^{-/-}$ sperm, the ZP-evoked Ca^{2+} response was abolished (Fig. 3.9c,d). This suggests that the ZP-induced alkalization is crucial for the Ca^{2+} response.

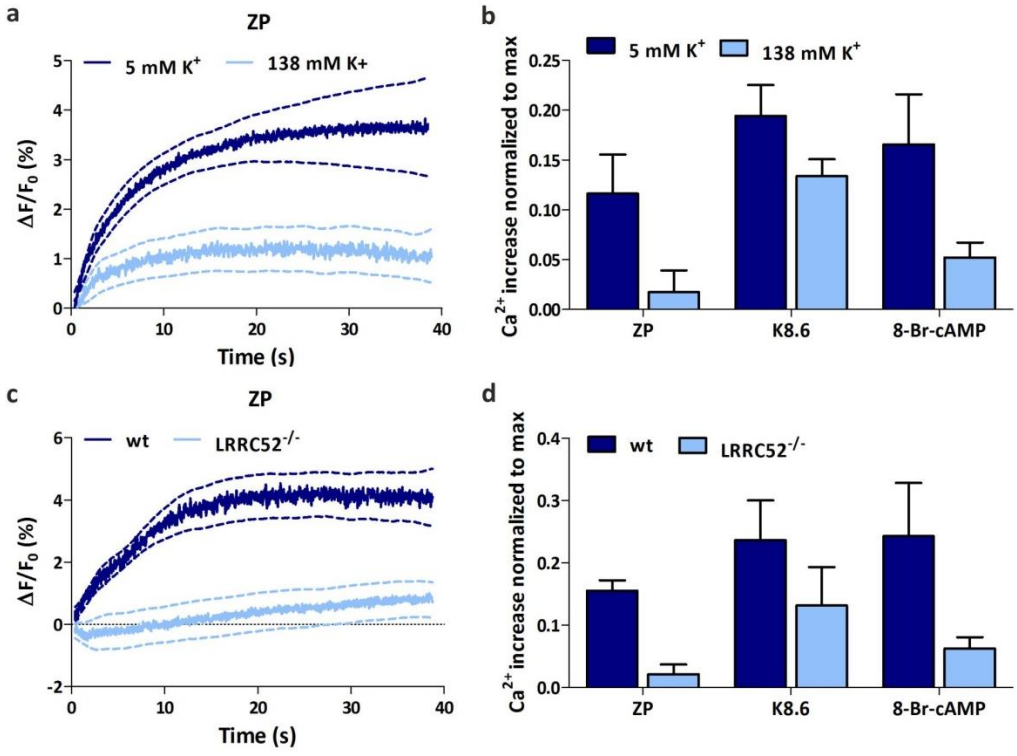

Fig. 3.9: ZP-, K8.6, and 8-Br-cAMP-evoked Ca^{2+} responses in $LRRC52^{-/-}$ sperm and in sperm bathed in high extracellular K^+

(a) Change in $[Ca^{2+}]_i$ evoked by 0.5 ZP/µl in capacitated sperm bathed in 5 mM (dark blue) or 138 mM K^+ buffer (light blue). Mean ± 95 % CI (dashed traces), n = 4. **(b)** Mean signal amplitudes, normalized to the maximal Ca^{2+} response evoked by 2 µM ionomycin; error bars indicate + SD (n = 4). **(c)** Change in $[Ca^{2+}]_i$ evoked by 0.5 ZP/µl in capacitated wildtype (dark blue) or $LRRC52^{-/-}$ (light blue) sperm. Mean ± 95 % CI (dashed traces), n = 4. **(d)** Mean signal amplitudes, normalized to the maximal Ca^{2+} response evoked by 2 µM ionomycin; error bars indicate + SD (n = 4).

However, independent of the stimulus, CatSper-mediated Ca^{2+} signals were in general smaller at depolarized V_M: in LRRC52$^{-/-}$ sperm and in wildtype sperm at high $[K^+]_o$, the relative amplitudes of K8.6- and 8-Br-cAMP-evoked Ca^{2+} signals were attenuated (Fig. 3.9b,d); of note, in LRRC52$^{-/-}$ sperm and in wildtype sperm at high $[K^+]_o$, mixing with K8.6 increased pH_i, but did not further depolarize V_M. I did, however, not test whether at depolarized V_M, ZP concentration > 0.5 ZP/µl are required to evoke a Ca^{2+} response. Therefore, it remains unclear whether the ZP-evoked alkalization is indeed required for activation of CatSper by ZPs.

3.1.4 Molecular mechanism underlying the ZP-evoked pH_i response

The mechanism underlying the ZP-induced pH_i increase is unknown. To investigate the contribution of a protein of the Na^+/H^+ exchanger family to the ZP pH_i signaling, I studied ZP-induced pH_i signals in sperm bathed in 138 mM (control) and 0 mM extracellular Na^+. Under control conditions, ZPs evoked the characteristic pH_i increase, whereas at low $[Na^+]_o$, the ZP-evoked alkalization was abolished ($\Delta R/R_0$ = 3.7 ± 1.9 % vs. -0.2 ± 1.3 %) (Fig. 3.10a,b). The pH_i increase evoked by NH_4Cl was, however, similar at high and low $[Na^+]_o$ (Fig. 3.10c). These results support the notion that the ZP-induced alkalization is mediated by Na^+/H^+ exchangers. A promising candidate is the sperm-specific sodium proton exchanger (sNHE) (Wang *et al.*, 2003), which is potentially regulated by changes in V_M because it contains a putative voltage-sensor domain.

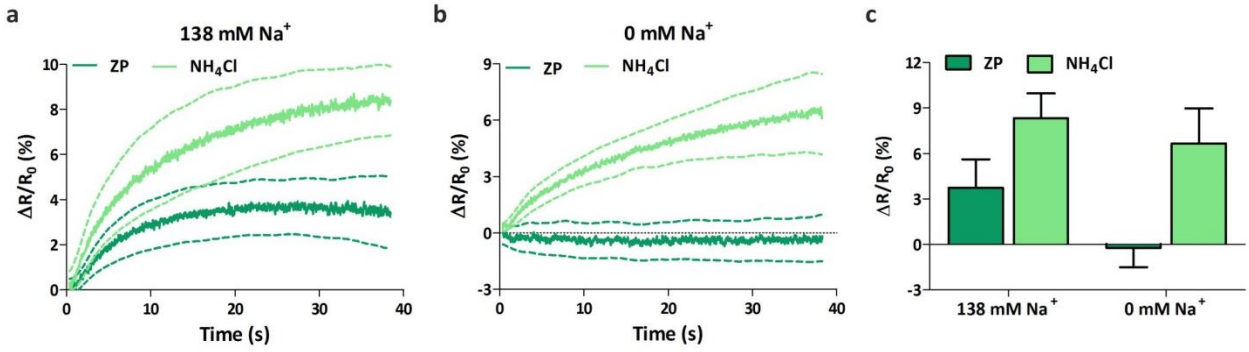

Fig. 3.10: ZP-evoked pH_i responses at high and low extracellular Na^+

(a,b) Change in pH_i evoked by 0.5 ZP/µl (dark green) or 10 mM NH_4Cl (light green) in capacitated sperm bathed in **(a)** 138 mM or **(b)** 0 mM Na^+ buffer. Mean ± 95 % CI (dashed traces), n = 3. **(c)** Mean signal amplitudes; error bars indicate + SD (n = 4).

To reveal the role of sNHE in ZP signaling, I analyzed ZP-evoked pH_i and Ca^{2+} responses in sNHE-deficient sperm. Mixing of sNHE$^{-/-}$ sperm with NH_4Cl evoked an alkalization, whereas ZPs did not change pH_i (Fig. 3.11a). This finding supports the notion that the sNHE mediates the ZP-induced alkalization. Moreover, in sNHE$^{-/-}$ sperm, also the ZP-evoked Ca^{2+} response (1.1 ± 2.5 %), but not the Ca^{2+} response evoked by K8.6 or ionomycin, was abolished (Fig. 3.11b,c). Taken together,

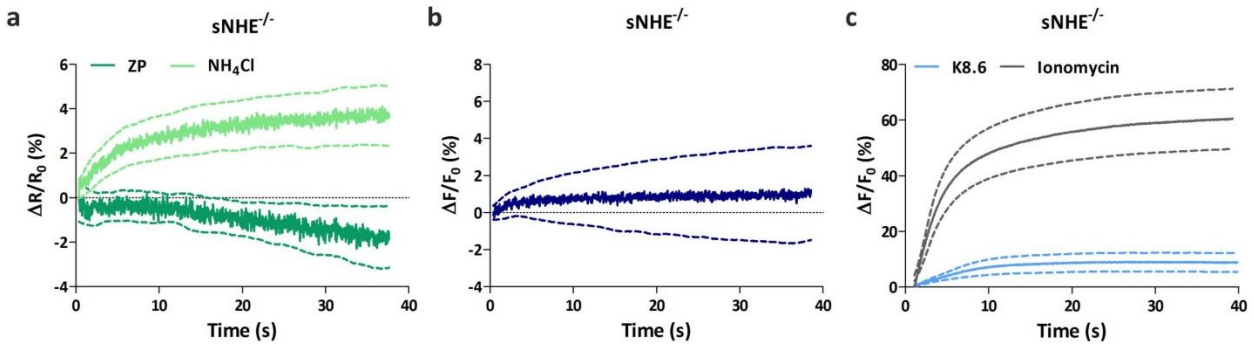

Fig. 3.11: ZP-induced pH_i and Ca^{2+}_i response in $sNHE^{-/-}$ sperm

(a) Change in pH_i evoked by 0.5 ZP/µl (dark green) or 10 mM NH_4Cl (light green) in capacitated $sNHE^{-/-}$ sperm. Mean ± 95 % CI (dashed traces), n = 4. **(b)** Change in $[Ca^{2+}]_i$ evoked by 0.5 ZP/µl in capacitated $sNHE^{-/-}$ mouse. Mean ± 95 % CI (dashed traces), n = 4. **(c)** Change in $[Ca^{2+}]_i$ evoked by K8.6 (light blue) or 2 µM ionomycin (grey) in capacitated $sNHE^{-/-}$ sperm. Mean ± 95 % CI (dashed traces), n = 7.

these experiments suggest that alkalization mediated by the sNHE is crucial for the ZP-evoked Ca^{2+} response.

However, sNHE forms a signaling complex with SACY, and deletion of the *Slc9c1* gene also disrupts SACY expression. Therefore, $sNHE^{-/-}$ sperm not only lack the sNHE, but also SACY function. To disentangle whether the lack of ZP signaling in $sNHE^{-/-}$ sperm is due to a lack of

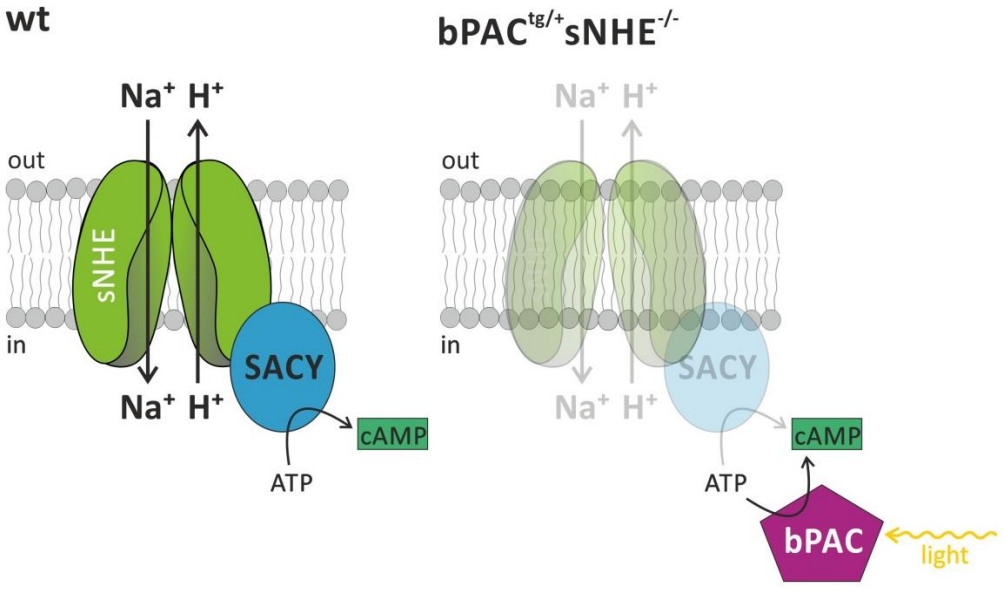

Fig. 3.12: Light-induced activation of bPAC stimulates cAMP synthesis in $bPAC^{tg/+}sNHE^{-/-}$ sperm

Left panel: In wildtype sperm, SACY converts ATP into the second messenger cAMP. Right penal: SACY is lost in $sNHE^{-/-}$ sperm. To rescue cAMP synthesis, a light-activateable adenylate cyclase from bacteria (bPAC) is crossed into $sNHE^{-/-}$ sperm.

sNHE, SACY, or a combination of both, I used the following approach: It has been reported that incubation of sNHE$^{-/-}$ sperm with membrane-permeable cAMP derivates restores the loss of SACY, and, thereby, sperm motility (Wang *et al*., 2007). Therefore, I tested whether restoring cAMP levels in sNHE$^{-/-}$ sperm rescues the ZP responses. We have generated transgenic mice expressing a bacterial, photoactivatable adenylate cyclase (bPAC) exclusively in sperm (Jansen *et al.*, 2015). Stimulating of bPAC-expressing sperm with blue light increased cAMP levels (Jansen *et al.*, 2015). We crossed these mice with sNHE$^{-/-}$ mice to generate bPAC$^{tg/+}$sNHE$^{-/-}$ mice. First, we tested whether cAMP production in sNHE$^{-/-}$ sperm, and thereby sperm motility, can be rescued by light- induced stimulation of cAMP synthesis (Fig. 3.12). To this end, the motility of sNHE$^{-/-}$ sperm was studied via dark-field microscopy. Fig. 3.13a shows the waveform of the flagellar beat before and after activation of bPAC (experiment was performed by Vera Jansen). In the

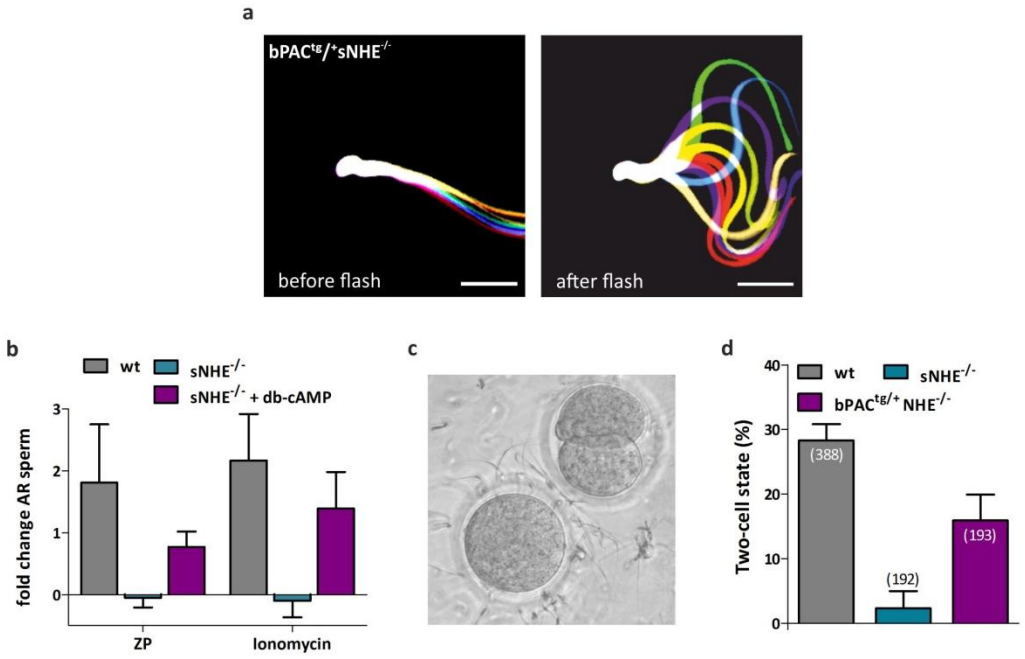

Fig. 3.13: Infertility of sNHE$^{-/-}$ mice can be rescued by an artificial increase of intracellular cAMP levels

(a) Light stimulation restores flagellar beating of sNHE$^{-/-}$bPAC$^{tg/+}$ sperm. Flagellar waveform of sNHE$^{-/-}$ bPAC$^{tg/+}$ sperm before (left) and after light stimulation (right). Color-coded frames are superimposed creating a 'stop-motion' image, illustrating one flagellar beating cycle; scale bar: 30 µm. **(b)** Acrosome reaction evoked by 1 ZP/µl or 2 µM ionomycin in capacitated wildtype and sNHE$^{-/-}$ sperm before and after preincubation with 5 mM db-cAMP. Data are shown as mean + SD percentage of acrosome-reacted (AR) sperm normalized to the buffer-treated control, n = 4. **(c)** Non-fertilized and fertilized oocyte in one- and two-cell state, respectively. **(d)** Rate of two-cell state oocytes after incubation of oocytes with sperm from wildtype, sNHE$^{-/-}$, and bPAC$^{tg/+}$sNHE$^{-/-}$ sperm. The bPAC$^{tg/+}$sNHE$^{-/-}$ sperm were illuminated for 90 min with blue light prior to the *in vitro* fertilization experiment (mean + SD, n = total number of oocytes from three independent experiments).

dark, bPAC$^{tg/+}$sNHE$^{-/-}$ sperm were immotile. However, after activating bPAC by light, sperm regained a symmetric flagellar beat, resulting in a regular, progressive movement. These results confirm that the immotility of sNHE$^{-/-}$ sperm is due to the lack of cAMP synthesis via SACY.

Next, I studied acrosome reaction in sNHE$^{-/-}$ sperm in the absence and presence of db-cAMP (Fig. 3.13b). In the absence of cAMP, both ZPs and ionomycin failed to evoke the acrosome reaction in sNHE$^{-/-}$ sperm. Similar results have been reported for SACY$^{-/-}$ sperm (Xie *et al.*, 2006). Bathing sNHE$^{-/-}$ sperm in db-cAMP restored the ZP- and ionomycin-evoked acrosome reaction, demonstrating that SACY-dependent cAMP synthesis, but no the sNHE function, is required for the acrosome reaction.

Moreover, I tested whether light-induced cAMP synthesis rescues the infertility phenotype of sNHE$^{-/-}$ sperm. In an *in vitro* fertilization assay, capacitated wildtype or bPAC$^{tg/+}$sNHE$^{-/-}$ sperm were incubated with wildtype oocytes. After 24 hours, the number of two-cell-stage oocytes was quantified as a measure for fertilization (Fig. 3.13c). Wildtype sperm fertilized about 30 % of

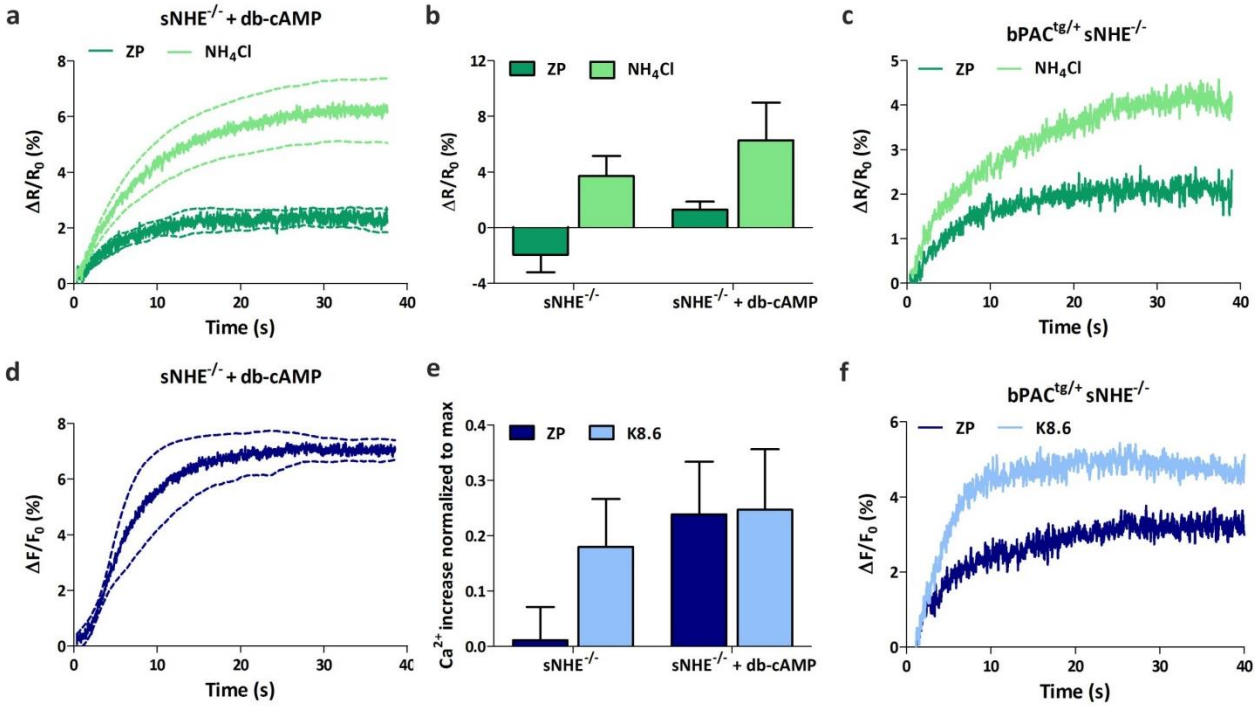

Fig. 3.14: Increase in cAMP rescues ZP-induced pH$_i$ and [Ca^{2+}]$_i$ increase in sNHE$^{-/-}$ sperm

(a) Change in pH$_i$ evoked by 0.5 ZP/µl (dark green) or 10 mM NH_4Cl (light green) in capacitated sNHE$^{-/-}$ sperm after preincubation with 5 mM db-cAMP. Mean ± 95 % CI (dashed traces), n = 4. **(b)** Mean signal amplitudes; error bars indicate + SD (n = 4). **(c)** Change in pH$_i$ evoked by 0.5 ZP/µl (dark green) or 10 mM NH_4Cl (light green) in bPAC$^{tg/+}$sNHE$^{-/-}$ sperm after light stimulation. **(d)** Change in [Ca^{2+}]$_i$ evoked by 0.5 ZP/µl in capacitated sNHE$^{-/-}$ sperm after preincubation with 5 mM db-cAMP. Mean ± 95 % CI (dashed traces), n = 4. **(e)** Mean signal amplitudes normalized to the maximal response evoked by 2 µM ionomycin; error bars indicate + SD (n = 4). **(f)** Change in [Ca^{2+}]$_i$ evoked by 0.5 ZP/µl (dark blue) or K8.6 (light blue) in bPAC$^{tg/+}$sNHE$^{-/-}$ sperm after light stimulation.

the oocytes, whereas in bPAC$^{tg/+}$sNHE$^{-/-}$ sperm the fertilization rate was 2 % (Fig. 3.13c). This residual fertilization rate reflected the spontaneous first mitotic division that occurs in some oocytes due to *in vitro* maturation (Bałakier & Casper, 1991; Cheng *et al.*, 2012). However, after light stimulation, bPAC$^{tg/+}$sNHE$^{-/-}$ sperm were able to fertilize the oocyte, resulting in a fertilization rate of 16 % (Fig. 3.13d). These results demonstrate that light-induced cAMP synthesis restores the fertility of sNHE$^{-/-}$ sperm.

Finally, I studied ZP-induced pH_i and Ca^{2+} responses in sNHE$^{-/-}$ sperm that were bathed in db-cAMP and in bPAC$^{tg/+}$sNHE$^{-/-}$ sperm stimulated with blue light to activate bPAC (Fig. 3.14). Both, db-cAMP and light-stimulated cAMP synthesis via bPAC restored the pH_i and Ca^{2+} response in sNHE$^{-/-}$ sperm, demonstrating that the sNHE does not underlie the ZP-induced alkalization-signaling in mouse sperm.

3.1.5 The ZP-evoked pH_i response in mouse involves the NHA1 Na^+/H^+ exchanger

To further analyze, which protein underlies the ZP-evoked alkalization, we investigated other members of the NHE family. Members of the Na^+/H^+ antiporter (NHA) subfamily, NHA1 and NHA2 (encoded by *Slc9b1* and *Slc9b2*, respectively), are possible candidates (Chen *et al.*, 2016; Liu *et al.*, 2010). Using mass spectrometry, ten peptides proteotypic for NHA1 were identified

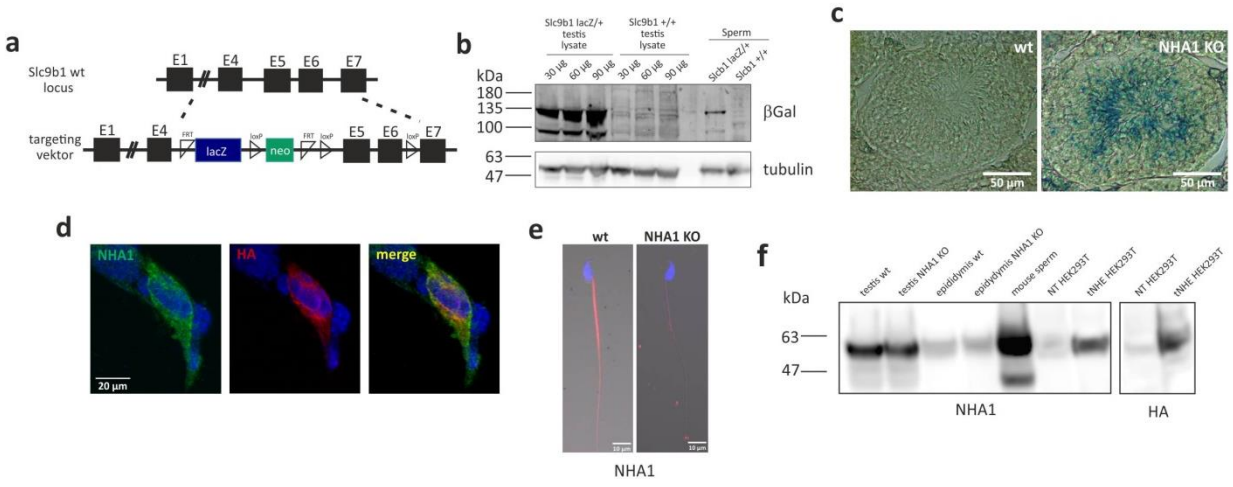

Fig. 3.15: Generation and characterization of NHA1$^{-/-}$ mouse

(a) Targeting strategy to generate NHA1$^{-/-}$ mice. **(b)** Western blot analysis using testis and sperm lysates from wildtype (+/+)- and heterozygous NHA1 knockout-mice (lacZ/+). **(c)** XGal staining of wildtype and NHA1$^{-/-}$ testis section; scale bar: 50 µm. **(d)** Staining of wildtype and NHA1$^{-/-}$ sperm with an anti-NHA1 antibody; scale bar: 10 µm. **(e)** Immunoblot of wildtype and NHA1$^{/-}$ testis, epididymis, and wildtype sperm lysates. Heterologously expressed NHA1 serves as positive control. **(f)** Staining of HEK 293 cells expressing NHA1-HA with an anti-NHA1 and anti-HA antibody; scale bar: 20 µm.

in lysates from mouse sperm (Fig. 6.1), confirming the presence of NHA1 in sperm. To investigate whether NHA1 is involved in ZP signaling, a knockout mouse was generated using genetically modified embryonic stem cells available from EUCOMM. NHA1 knockout mice contained a floxed lacZ/NEO cassette in the *Slc9b1* locus (Fig. 3.15a), which abolishes *Slc9b1* gene expression and conveys expression of the *lacZ* gene, encoding a beta-galactosidase, under the control of the Slc9b1 promotor. This allows to indirectly visualize the transcription of the *Slc9b1* gene. Western blot analysis using an anti-beta-galactosidase antibody demonstrated *Slc9b1* expression in testis and sperm in heterozygous NHA$^{lacZ/+}$, but not in wildtype mice (Fig. 3.15b). In testis sections, XGal staining revealed the beta-galactosidase expression in developing sperm of NHA1$^{lacZ/lacZ}$ mice, but not in wildtype mice (Fig. 3.15c). To verify the expression pattern, I applied a commercially-available NHA1 antibody. To scrutinize the specificity of the antibody, I used HEK293 cells transiently transfected with NHA1. Both in immunocytochemistry and Western blot analysis, the antibody detected NHA1 in transfected, but not in non-transfected cells (Fig. 3.15d,f). In wildtype sperm, the anti-NHA1 antibody stained the midpiece; in NHA1$^{-/-}$ sperm, the staining was gone (Fig. 3.15e). These results question findings from of Liu *et al*., demonstrating that NHA1 is located in the principal piece (Liu *et al.*, 2010). In lysates from testis, epididymis, and sperm, a band was detected at the height of the predicted molecular weight of around 61 kDa. However, the band was detected in both wildtype and NHA1$^{-/-}$ mice.

NHA1$^{-/-}$ mice were viable without any gross phenotype and were born in Mendelian ratios from heterozygous matings. Testis and epididymis weight of male NHA1$^{-/-}$ and wildtype littermates were similar (Fig. 3.16a). Furthermore, the average count of sperm isolated from the cauda was identical (1.6 x 10^7) in both wildtype and NHA1$^{-/-}$ males, demonstrating that sperm development

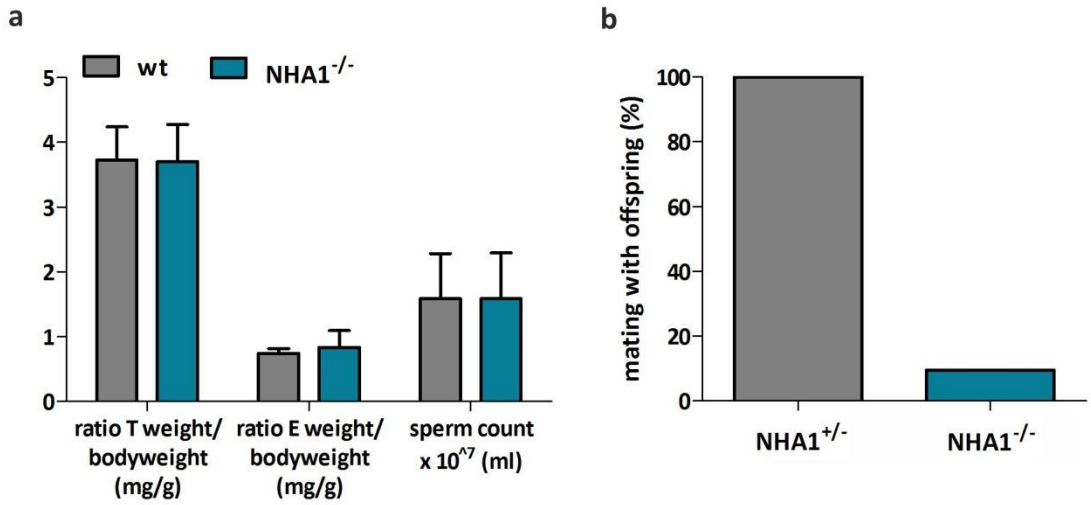

Fig. 3.16: NHA1$^{-/-}$ mice are strongly impaired in their fertilization capacity

(a) Testis (T) weight, epididymis (E) weight, and cauda epididymal sperm counts between wildtype (n = 6) and NHA1$^{-/-}$ (n = 8) animals. **(b)** Mating with offspring (%) following mating of eight NHA1$^{+/-}$ and NHA1$^{-/-}$ males with twenty-one females.

is not impaired. However, the fertility of NHA1$^{-/-}$ males was strongly reduced (Fig. 3.16b). Only two out of twenty-one matings of NHA1$^{-/-}$ males produced offspring, whereas heterozygous littermates reproduced normally. These results demonstrate that NHA1 is crucial for sperm function and fertilization, confirming the results by Chen *et al*. (Chen *et al.*, 2016). The study by Chen and colleagues (Chen *et al.*, 2016) suggested that deletion of the *Slc9b1* gene also disrupts the expression of SACY and, thereby, renders the majority of sperm immotile. However, my results are not in line with these findings. The percentage of motile sperm with symmetric flagellar beat and progressive movement was similar between wildtype and NHA$^{-/-}$ sperm (Fig. 3.17a,b). Furthermore, a detailed characterization of the flagellar beat using the SpermQ software developed by Jan Niklas Hansen revealed that the basal beat frequency was also similar between wildtype and NHA1$^{-/-}$ sperm (8.5 Hz and 6.4 Hz, respectively) (Fig. 3.17c). Stimulation of NHA1$^{-/-}$ sperm with 25 mM HCO_3^- to activate SACY increased the flagellar beat frequency by 1.9 fold to 12.3 Hz, similar to what was observed for wildtype sperm (15.6 Hz) (Fig. 3.17c). These results demonstrate that the ablation of NHA1 does not affect SACY function. However, NHA1$^{-/-}$ sperm displayed a restricted motility of the midpiece (Fig. 3.17b), resembling a phenotype that has been described for sperm deficient for calcineurin or CatSper ζ (Chung *et al.*, 2017; Miyata *et al.*, 2015).

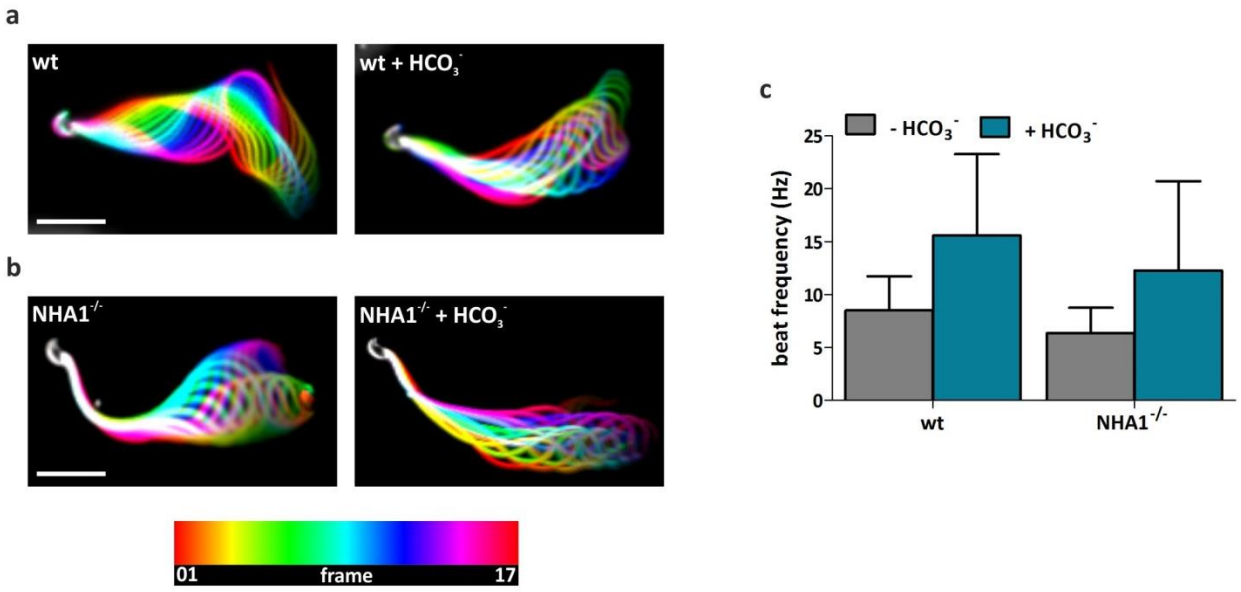

Fig. 3.17: Motility analysis of NHA1$^{-/-}$ sperm

(a,b) Flagellar waveform of **(a)** wildtype and **(b)** NHA1$^{-/-}$ sperm before (left) and after (right) stimulation with 25 mM HCO_3^-. Color-coded frames 1 to 17 are superimposed creating a 'stop-motion' image, illustrating one flagellar beating cycle; scale bar: 30 µm. **(c)** Flagellar beat frequency in wildtype and NHA1$^{-/-}$ sperm before (grey) and after (teal) stimulation with 25 mM HCO_3^-. Data are shown as mean, error bars indicate + SD (n = 5, 13 sperm analyzed in total).

To investigate the motility defect in the midpiece in more detail, I performed an ultra-structural analysis. Along the flagellum, Ca^{2+} signaling domains organized by CatSper display a quadrilateral arrangement; this supramolecular structure is crucial for sperm motility (Chung *et al.*, 2014). We applied super-resolution microscopy to scrutinize whether the stiffness of the $NHA1^{-/-}$ sperm midpiece is caused by defects in the ultrastructure of the Ca^{2+} signalosome. The experiments were performed by Hussein Hamzeh. Mouse sperm were labeled with an antibody against the CatSper1 subunit, demonstrating localization of the CatSper channel in the principal piece (Fig. 3.18a). When subjecting these samples to stochastic optical reconstruction microscopy (STORM), clustering of CatSper in four distinct Ca^{2+} signaling domains aligned longitudinally to the sperm flagellum was observed in both wildtype and $NHA1^{-/-}$ sperm (Fig. 3.18b,c). Thus, the stiff midpiece in $NHA1^{-/-}$ sperm does not seem to relate to defects in the ultra-structure of the Ca^{2+} signalosome.

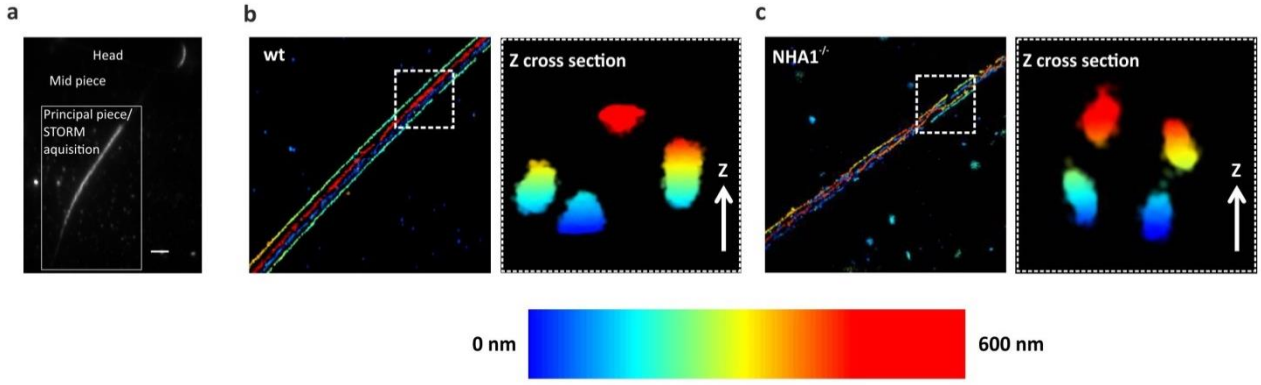

Fig. 3.18: Ultrastructure of CatSper channel complex is intact in NHA1-deficient sperm

(a) Epifluorescence image of a CatSper immunostained mouse sperm showing nonspecific labeling in the acrosome and specific labeling exclusively in the principal piece; scale bar: 5 µm. **(b,c)** 3D STORM image of CatSper in **(b)** wildtype and **(c)** $NHA1^{-/-}$ sperm in x-y projection color coded for z (scale bar on right), image shows the four CatSper domains that runs along each side of the longitudinal columns of the sperm principal piece; scale bar: 5 µm. Enlarged image of boxed section from (d,e): Z cross-section of principal piece showing the four CatSper domains across the flagella in wildtype and $NHA1^{-/-}$ sperm; scale bar: 5 µm. Experiments performed by Hussein Hamzeh.

Next, I studied ZP-induced pH_i signaling in NHA1-deficient sperm. Compared to wildtype sperm, the amplitude of the ZP-evoked alkalization was strongly attenuated in $NHA1^{-/-}$ sperm ($\Delta R/R_0$ = 4.0 ± 0.9 % vs. 1.2 ± 1.1 %) (Fig. 3.19a,b), whereas the pH_i increase evoked by NH_4Cl was similar (Fig. 3.19a,b). Preincubation of $NHA1^{-/-}$ sperm with db-cAMP did not restore the ZP-induced alkalization (Fig. 3.19e), arguing against that defective cAMP signaling accounted for the attenuation of the pH_i response. Altogether, these results indicate that ZP-induced alkalization-signaling involves Na^+/H^+ exchange via NHA1.

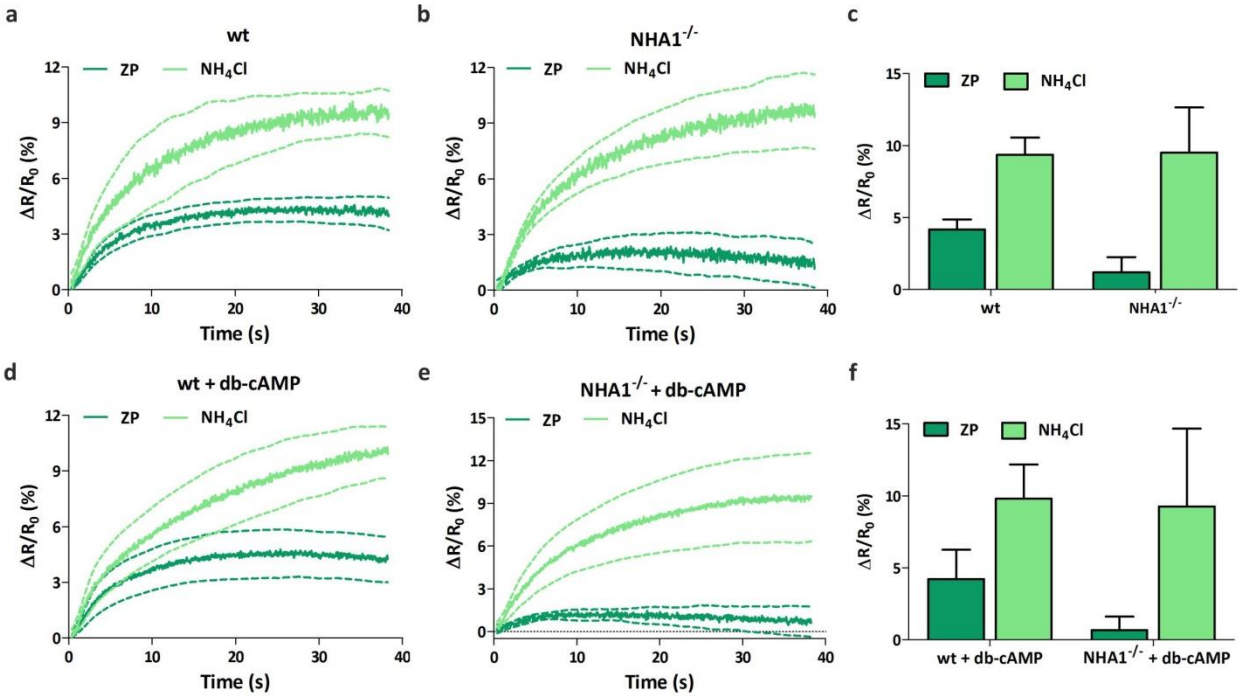

Fig. 3.19: The ZP-induced alkalization involves NHA1

(a,b) Change in pH_i evoked by 0.5 µg/ml ZP (dark green) or 10 mM NH_4Cl (light green) in capacitated **(a)** wildtype and **(b)** $NHA1^{-/-}$ sperm. Mean ± 95 % CI (dashed traces), n =3. **(c)** Mean signal amplitudes; error bars indicate + SD (n = 3) **(d,e)** Change in pH_i evoked by 0.5 µg/ml ZP (dark green) or 10 mM NH_4Cl (light green) in capacitated **(d)** wildtype and **(e)** $NHA1^{-/-}$ mouse sperm preincubated with 5 mM db-cAMP. Mean ± 95 % CI (dashed traces), n = 3. **(f)** Mean signal amplitudes; error bars indicate + SD (n = 3).

Moreover, I studied whether the ZP-induced alkalization via NHA1 is involved in the ZP-induced Ca^{2+} influx via CatSper. To this end, I studied ZP-induced Ca^{2+} responses in $NHA1^{-/-}$ sperm. Compared to wildtype sperm, the amplitude of the ZP-evoked Ca^{2+} signal was strongly attenuated in $NHA1^{-/-}$ sperm ($\Delta F/F_0$ = 3.5 ± 1.1 % vs. 1.1 ± 0.6 %) (Fig. 3.20a,b), whereas K8.6-evoked Ca^{2+} responses were similar (Fig. 3.20b). This finding supports the notion that the ZP-evoked alkalization stimulates the ZP-evoked Ca^{2+} influx via CatSper.

However, the ZP-evoked pH_i and Ca^{2+} response was not abolished in NHA1-deficient sperm, suggesting that additional proteins contribute to the ZP-evoked alkalization. Considering that the ZP-induced pH_i increase requires extracellular Na^+, NHA2 is a promising candidate. To test this hypothesis, a knockout for NHA2 is required, which was, however, not available.

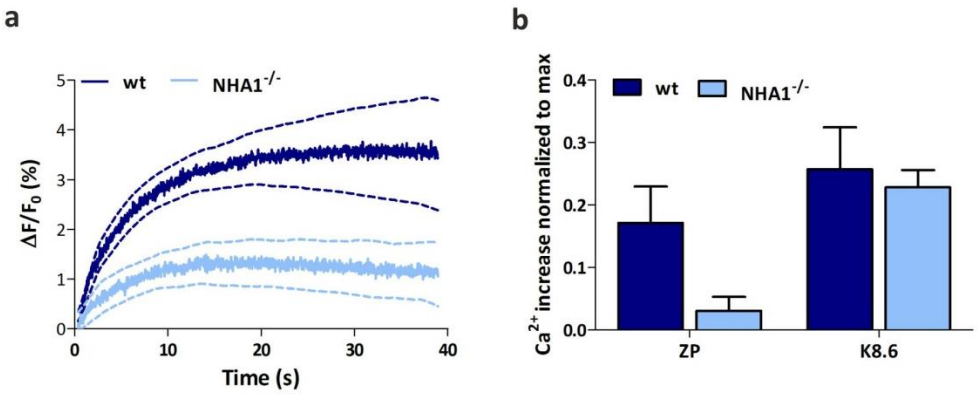

Fig. 3.20: Alkalization via NHA1 controls the ZP-induced $[Ca^{2+}]_i$ increase

(a) Change in $[Ca^{2+}]_i$ evoked by 0.5 ZP/µl in capacitated wildtype or NHA1$^{-/-}$ sperm. Mean ± 95 % CI, n = 4. **(b)** Mean signal amplitudes; error bars indicate + SD (n = 4).

3.1.6 The ZP-induced acrosome reaction in mouse sperm requires a polarized membrane potential and alkalization

To reveal how ZP signaling regulates the behavioral responses facilitating ZP penetration, I studied the molecular mechanism(s) underlying the ZP-evoked acrosome reaction. The Ca^{2+} influx via CatSper is reportedly dispensable for the ZP-induced acrosome reaction (Xia & Ren, 2009). I tried to reproduce this result in wildtype and CatSper$^{-/-}$ sperm (Fig. 3.21a.b): ZPs increased the fraction of acrosome-reacted sperm by about 2.8 and 1.4 fold, respectively (Fig. 3.21c), suggesting that the ZP-evoked acrosome reaction is strongly attenuated in CatSper$^{-/-}$

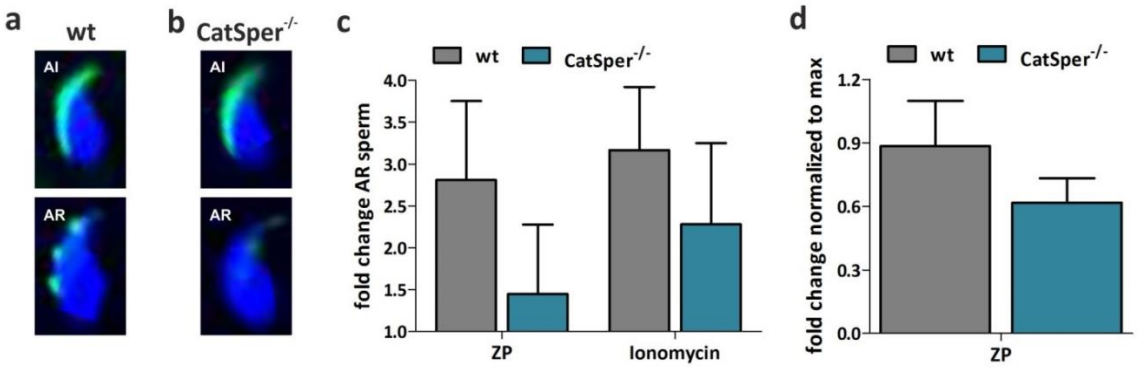

Fig. 3.21: ZP-evoked acrosome reaction in CatSper$^{-/-}$ sperm

(a,b) Acrosome reaction assay of **(a)** wildtype and **(b)** CatSper$^{-/-}$ sperm, the acrosome was labelled with PNA-FITC (green), DNA in the nucleus was stained with DAPI (blue). Acrosome-intact sperm (AI), acrosome-reacted sperm (AR). **(b)** Acrosome reaction evoked by 1 ZP/µl or 2 µM ionomycin in wildtype (grey) or CatSper$^{-/-}$ (teal) sperm. Data are shown as mean + SD percentage of acrosome-reacted (AR) sperm normalized to the buffer-treated control; (n = 3). **(c)** ZP-evoked acrosome reaction in wildtype and CatSper$^{-/-}$ sperm normalized to the maximal response evoked by ionomycin.

sperm. However, in CatSper$^{-/-}$ sperm also the action of ionomycin was diminished. The reason for this is unclear. Normalization of the ZP-evoked acrosome reaction to the ionomycin control revealed, that ZP action was only slightly attenuated in CatSper$^{-/-}$ sperm (Fig. 3.21d). This result confirmed that the ZP-evoked acrosome reaction does not require Ca^{2+} influx via CatSper.

To test whether the ZP-evoked acrosome reaction requires a polarized V_M, sperm were bathed in low (control) or high $[K^+]_o$ (Fig. 3.22a). Under control conditions, ZPs increased the fraction of acrosome-reacted sperm by 1.6 fold, whereas at high $[K^+]_o$, the response was strongly attenuated (1.1 fold increase). The action of ionomycin was, however, similar at low and high $[K^+]_o$, confirming that a depolarized membrane potential impairs the action of ZPs (Escoffier *et al.*, 2015).
In sperm bathed in low $[Na^+]_o$, ZPs failed to evoke the acrosome reaction, whereas ionomycin evoked the acrosome reaction even at low $[Na^+]_o$ (Fig. 3.22b). These results suggest that the ZP-evoked alkalization is required for the ZP-induced acrosome reaction. To test this hypothesis, an acrosome reaction assay should be performed with NHA1-deficient sperm, which was, so far, not possible due to limited numbers of NHA1-deficient males.

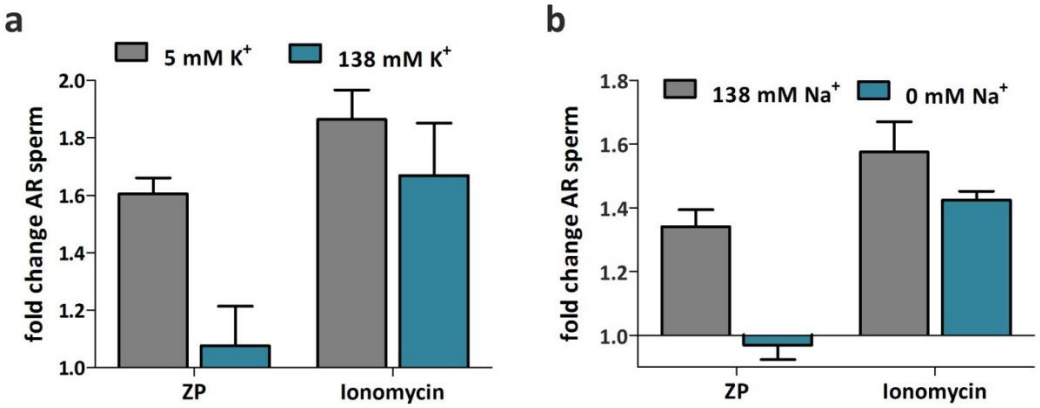

Fig. 3.22: ZP-evoked acrosome reaction in sperm bathed in high $[K^+]_o$ and low $[Na^+]_o$

(a) Acrosome reaction evoked by 1 µg/ml ZP or 2 µM ionomycin in capacitated sperm bathed in 5 mM (grey) or 138 mM extracellular K^+ (teal) buffer. **(b)** Acrosome reaction evoked by 1 µg/ml ZP or 2 µM ionomycin in 138 mM (grey) (control) or 0 mM Na^+ buffer (teal). Data are shown as mean + SD percentage of acrosome-reacted (AR) sperm normalized to the buffer-treated control (n =4).

3.1.7 Summary

The data presented in this first part of my thesis provide new insights into the molecular mechanism underlying ZP-evoked $[Ca^{2+}]_i$ and pH_i signaling in mouse sperm: the ZP-evoked alkalization requires extracellular Na^+ and involves Na^+/H^+ exchange carried by NHA1, but not

sNHE. The mechanism underlying NHA1 activation remains, however, elusive. Furthermore, the ZP-evoked Ca^{2+} influx via CatSper is abolished at conditions preventing ZP-evoked alkalization, which suggests that the alkalization is crucial for activation of CatSper. The ZP-evoked acrosomal exocytosis does, however, not require Ca^{2+} influx via CatSper but seems to be initiated by the ZP-evoked alkalization. Finally, my data indicate that a polarized V_M mediated by Slo3 and LRRC52 and the second messenger cAMP are required for the ZP-induced increase in pH_i and $[Ca^{2+}]_i$ and acrosomal exocytosis.

3.1.8 Heterologous expression and characterization of mouse zona pellucida glycoproteins

So far, it is not known, which of the ZP glycoproteins initiates ZP signaling in mouse sperm. To answer this question, I used heterologously expressed ZP glycoproteins. First, I established an eukaryotic expression system using HEK293T cells for ZP glycoproteins (Fig. 3.23a). The cDNA sequences encoding for mouse ZP1, ZP2, or ZP3 were cloned into the expression vector pHLsec. Thereby, a signal peptide was added to the N-terminus of the proteins, promoting their secretion into the medium. Additionally, a polyhistidine tag was introduced upstream of the conserved furin cleavage site (CFCS) that serves as a processing site for C-terminal cleavage. In the secreted, cleaved proteins, the polyhistidine tag is located at the C-terminus, allowing for purification of the proteins from the medium. The expression of ZP1, ZP2, and ZP3 was scrutinized by immunocytochemistry and Western Blot using an anti-His (red) and anti-ZP antibodies (green) (Fig. 3.23b,c). The apparent molecular weight of the heterologous proteins was slightly lower than that of the native proteins (compare Fig. 3.23 and Fig. 3.1), but PNGase digestion confirmed that the heterologous proteins were glycosylated.

To determine the time course of secretion, the supernatant was collected over six consecutive days after transfection and analyzed by Western blot. All three proteins were detected already one day after transfection (Fig. 3.23d). The time point where secretion was maximal varied between the different proteins: for ZP1, protein secretion was maximal at day six, whereas for ZP2 and ZP3, four or three days seemed to be optimal. The proteins were subjected to batch purification using a Ni-NTA resin. The polyhistidine tag of ZP3 forms a chelating complex with the nickel ions of the resin. Fig. 3.23e shows the Western blot analysis of a representative purification of ZP3. After subsequent washing steps to remove unbound proteins, ZP3 was eluted with imidazole (Fig. 3.23e), demonstrating that the proteins can be purified from the supernatant. Subsequently, the purification was scaled up using the ÄKTA protein purification system and a Co^{2+}-charged HiTrap column. Fig. 3.23f shows the Western blot analysis of a representative purification of ZP3. ZP3 was bound to the column and after washing, proteins were eluted with a linear gradient of 10 to 500 mM imidazole and collected in multiple fractions. Fractions containing the respective purified proteins were subjected to buffer exchange to remove the imidazole and then used for further experiments. In total, from 70 ml medium, 3 ml of protein with a maximal concentration of 40 µg/ml was purified. However, even

after buffer exchange, samples might still contain ≤ 5 mM imidazole. Imidazole, like NH_4Cl, is a weak base that alkalizes the pH_i of cells and thereby evokes a CatSper-mediated Ca^{2+} increase (Fig. 6.2). Thus, as a control, an "empty" fraction was generated, which was eluted from a Co^{2+}-charged HiTrap column and then buffer-exchanged similar as described above, yet, in the absence of proteins.

To test whether the heterologous ZP glycoproteins are functional, I performed acrosome reaction assays (Fig. 3.24). Bathing of sperm in the empty fraction did not evoke acrosome reaction, whereas ionomycin increased the fraction of acrosome-reacted sperm by about 1.5

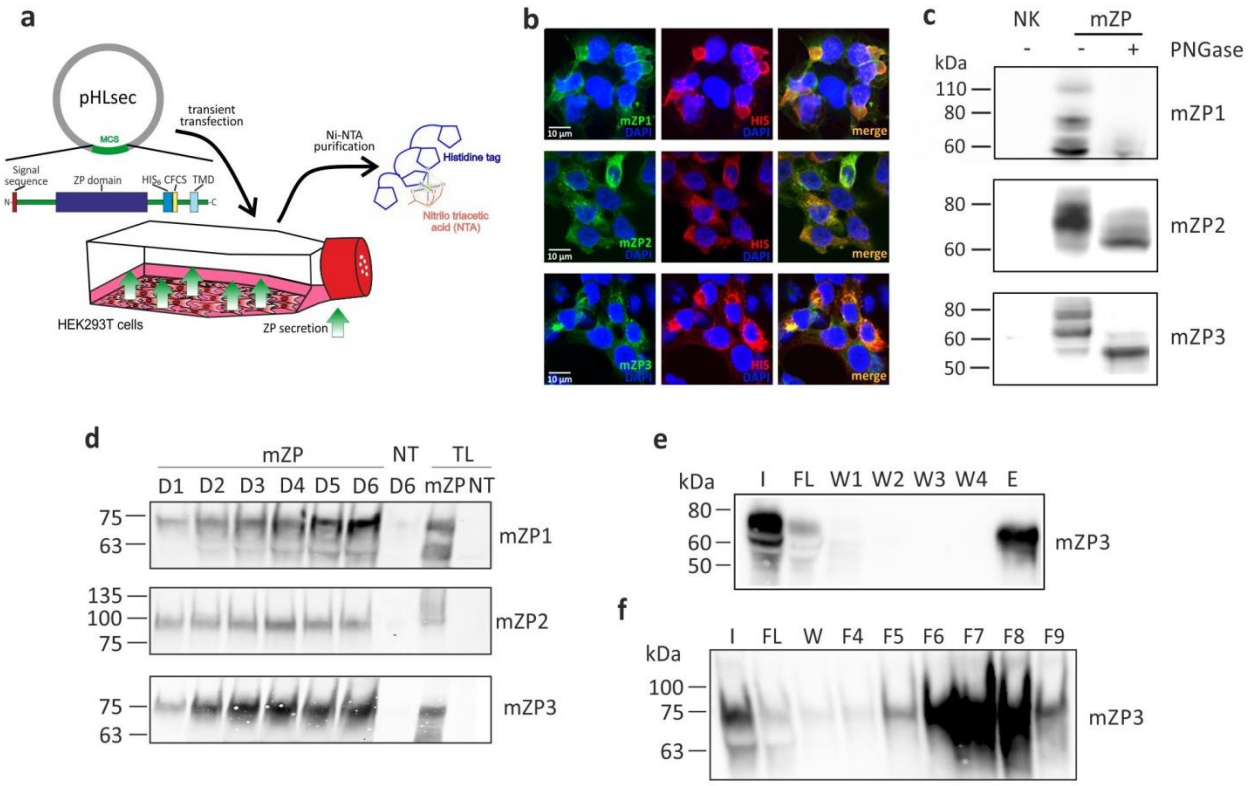

Fig. 3.23: Heterologous expression and purification of mouse ZP glycoproteins

(a) cDNA of mouse ZP glycoproteins were cloned into a pHLsec vector for expression in HEK293T cells. Heterologous ZPs secreted into the supernatant were purified via their polyhistidine tag. **(b)** Staining of HEK293T cells expressing mouse ZP glycoproteins with an anti-His and anti-ZP antibodies; scale bar: 10 µm. **(c)** Western blots of cell lysates from mock (negative control, NK) and ZP-transfected cells with and without PNGase treatment. **(d)** Secretion of mouse ZP peaks after three to six days. **(e)** Batch purification of secreted mZP3 using Ni-NTA agarose. I = input, FL = flow through, W = washing step, e = Elute. **(f)** Purification of secreted mZP3 using a Co^{2+}-HiTrap column via the ÄKTA protein purification system. Bound protein was eluted using a linear imidazol gradient and collected in multiple fractions. I = input, FL = flow through, W = wash, F = fraction.

fold in non-capacitated and capacitated sperm. Bathing sperm in 22.5 µg/ml ZP3 increased the fraction of acrosome-reacted sperm by 1.2 fold and 1.5 fold in non-capacitated and capacitated sperm, respectively (Fig. 3.24). This result demonstrates that heterologous ZP3 is functional and confirms that capacitation primes the sperm for ZP-induced acrosomal exocytosis. Acrosome reaction rates were also increased by ZP2. However, ZP2 was less efficacious than ZP3 and its action was rather similar in non-capacitated and capacitated sperm (Fig. 3.24). Finally, ZP1 did not evoke the acrosome reaction.

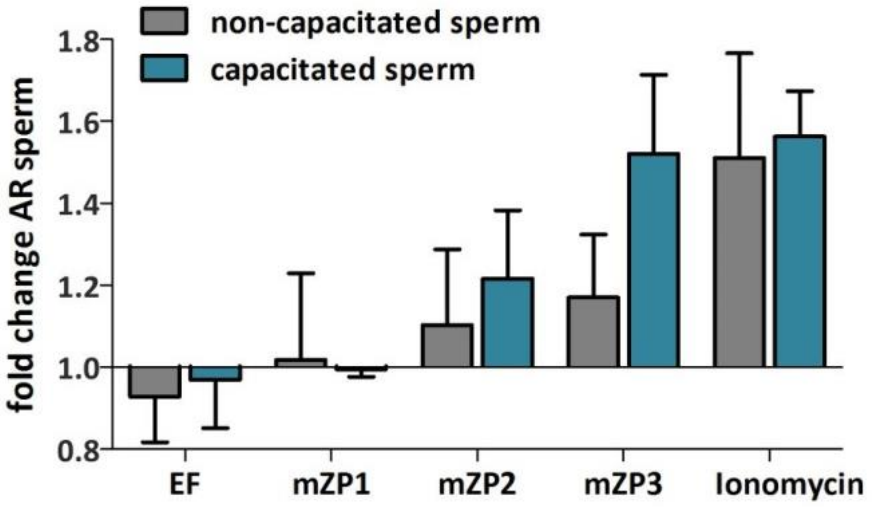

Fig. 3.24: Heterologous ZP2 and ZP3 evoke an acrosome reaction in mouse sperm

Acrosome reaction evoked by empty fraction (EF), 22.5 µg/ml mZP1, 22.5 µg/ml mZP2, 22.5 µg/ml mZP3, or 2 µM ionomycin in non-capacitated (grey) and capacitated (teal) mouse sperm. Data are shown as mean + SD percentage of acrosome-reacted (AR) sperm normalized to the buffer-treated control, error bars indicate + SD; (n = 4).

Next, I studied the action of the heterologous ZP glycoproteins on $[Ca^{2+}]_i$ in capacitated mouse sperm. Mixing of sperm with ZP1 evoked only a small Ca^{2+} increase (Fig. 3.25a), whereas ZP3 and ZP2 evoked a sizeable Ca^{2+} response (Fig. 3.25b,c). The relative potency of the individual ZP isoforms to evoke a Ca^{2+} response was ZP3 > ZP2 >> ZP1 (Fig. 3.25d). ZP3 evoked Ca^{2+} responses in a dose-dependent fashion: both the kinetics and amplitude of the Ca^{2+} response became faster and larger, respectively, with increasing ZP3 concentrations (Fig. 3.25e); the signal amplitude did not saturate up to 20 µg/ml. However, due to the experimental design, higher ZP3 concentrations could not be achieved. Of note, the empty fraction did not evoke a Ca^{2+} response and the ZP3 response was abolished in CatSper$^{-/-}$ sperm (Fig. 3.25f).

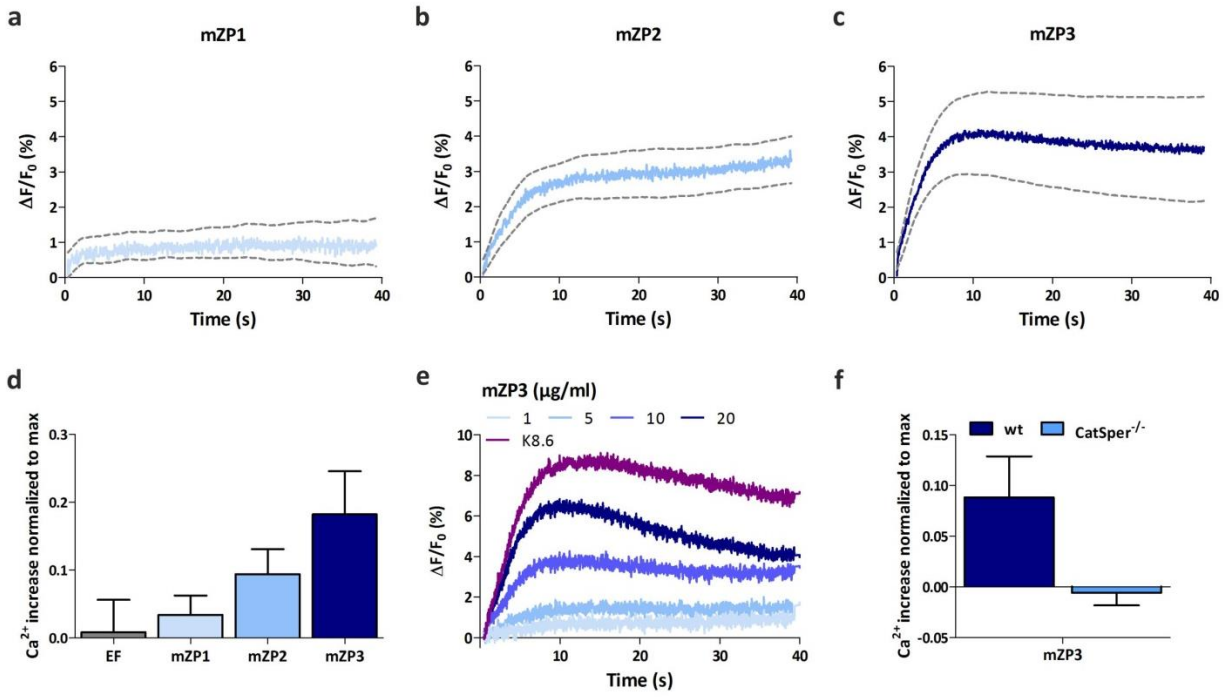

Fig. 3.25: Heterologous ZP glycoproteins evoke Ca^{2+} responses in mouse sperm

(a,b,c) Changes in $[Ca^{2+}]_i$ evoked by **(a)** 20 µg/ml mZP1, **(b)** mZP2, or **(c)** mZP3 in capacitated mouse sperm. Mean ± 95 % CI (dashed traces), n =4. **(d)** Mean signal amplitudes; error bars indicate + SD (n = 4). **(e)** Change in $[Ca^{2+}]_i$ evoked by increasing concentrations of mZP3 or by K8.6. **(f)** Change in $[Ca^{2+}]_i$ evoked by 20 µg/ml mZP3 in wildtype (dark blue) and $CatSper^{-/-}$ sperm normalized to the maximal response evoked by 2 µM ionomycin. Data are shown as mean; error bars indicate + SD (n = 4).

Next, I studied whether the heterologous ZP glycoproteins also evoke a pH_i response. Mixing of sperm with ZP1 and ZP2 evoked only a small pH_i increase compared to ZP3, which evoked a prominent alkalization (Fig. 3.26a-c). The kinetics and amplitude of the ZP3-evoked alkalization became faster and increased, respectively, with increasing ZP concentrations (Fig. 3.26e). The empty fraction did not change pH_i (Fig. 3.26d). Similar to native ZPs, ZP3 did not evoke an alkalization in $sNHE^{-/-}$ sperm, whereas preincubation of sperm in db-cAMP restored the alkalization (Fig. 3.26f).

Taken together, heterologously expressed and native ZP glycoproteins display a similar action in mouse sperm. Moreover, among the three recombinant ZP glycoproteins, ZP3 seems to be the most potent in evoking Ca^{2+} and pH_i responses; ZP2 is less potent, while ZP1 evokes only minuscule responses. This indicates that ZP signaling *in vivo* can be ascribed to a combined action of ZP2 and ZP3. Furthermore, these experiments demonstrate that functional recombinant ZP glycoproteins can serve as a surrogate for native ZP. This paves the way for analyzing ZP signaling in human sperm.

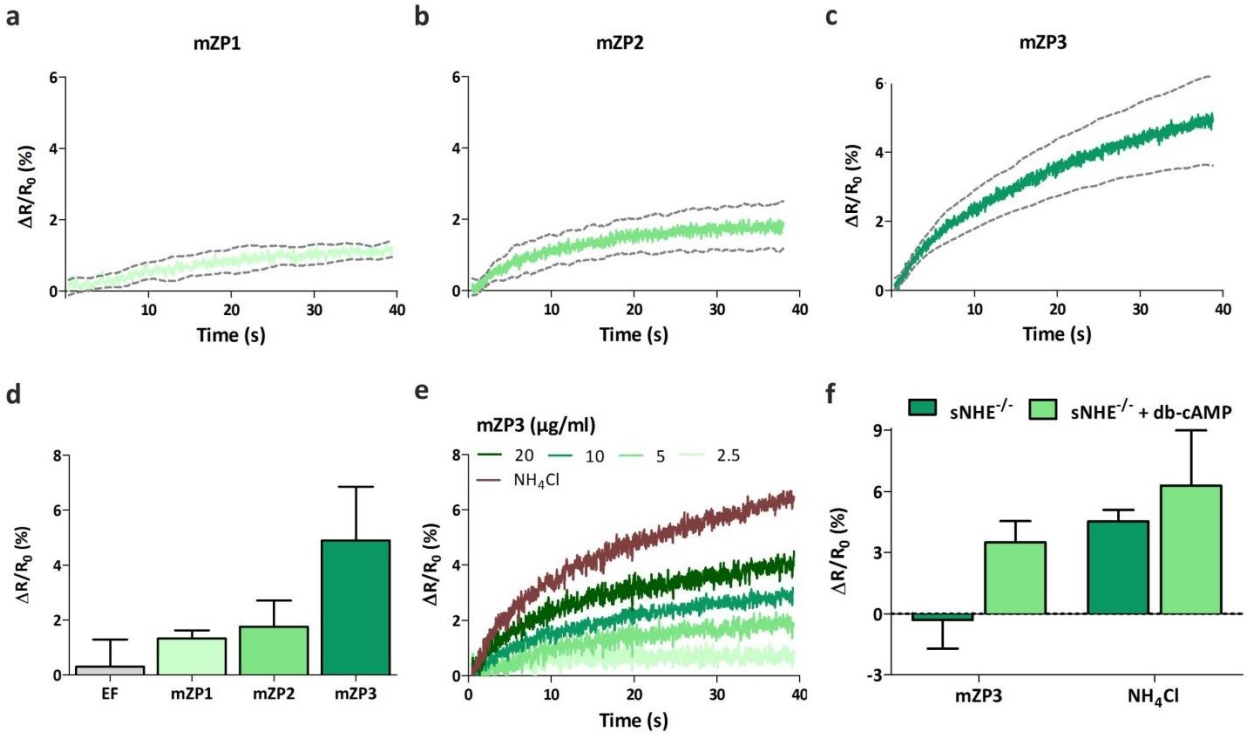

Fig. 3.26: Heterologous ZP glycoproteins evoke a pH_i increase in mouse sperm

(a,b,c) Changes in pH_i evoked by **(a)** 20 µg/ml mZP1, **(b)** 20 µg/ml mZP2, or **(c)** 20 µg/ml mZP3 in capacitated mouse sperm. Mean ± 95 % CI (dashed traces), n = 4. **(d)** Mean signal amplitudes; error bars indicate + SD (n = 4). **(e)** Change in pH_i evoked by increasing concentrations of mZP3 or 10 mM NH_4Cl. **(f)** Change in pH_i evoked by 20 µg/ml mZP3 or 10 mM NH_4Cl in $sNHE^{-/-}$ sperm before (dark green) and after (light green) preincubation with 5 mM db-cAMP. Data are shown as mean; error bars indicate + SD (n = 4).

3.2 The action of human zona pellucida glycoproteins in human sperm

3.2.1 Heterologous expression and characterization of human zona pellucida glycoproteins

To study the action of ZP glycoproteins in human sperm, human ZP2 and ZP3 were expressed in HEK293T cells. To this end, the cDNA sequence of ZP2 and ZP3 were cloned into the pHLsec vector. Protein expression of ZP2 and ZP3 was verified by immunocytochemistry and Western blot using an anti-His (red) and anti-ZP2 and -ZP3 antibodies (green) (Fig. 3.27a,b). For ZP2 and ZP3, bands at 100 and 60 kD were detected, respectively, which is in line with the apparent molecular weight of the native proteins (Bauskin *et al.*, 1999). PNGase treatment decreased the apparent molecular weight of the proteins by about 10 kDa, confirming that the proteins were glycosylated. Analyzing the supernatant of ZP2- and ZP3-expressing cells at six consecutive days after transfection revealed that the secretion peaked at day three and four for ZP2 and ZP3, respectively (Fig. 3.27c). For the following experiments, the ZP glycoproteins were purified in large scale, using the same purification protocol established for the murine proteins. After purification, a maximal protein concentration of 40 µg/ml was achieved. To reach higher protein concentrations, ZP glycoproteins were concentrated using a centrifugal evaporator. This allowed to stimulate human sperm with ZP2 and ZP3 concentrations up to 200 µg/ml. Similar to the protocol described for mouse proteins, an empty fraction was generated in parallel.

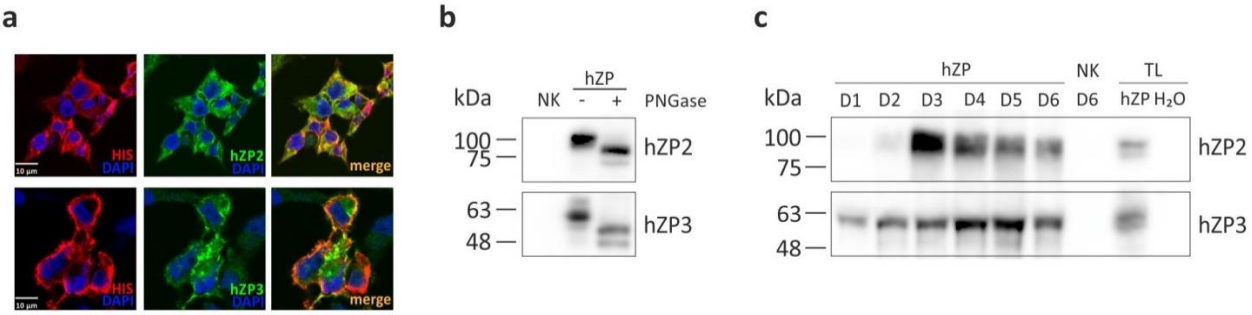

Fig. 3.27: Heterologous expression of human ZP glycoproteins

(a) Staining of heterologous ZPs in HEK293T cells using anti-His and specific anti-ZP antibodies; scale bar: 10 µm. **(b)** Immunoblots of cell lysates from mock (negative control, NK) and heterologous ZP-transfected cells with and without PNGase treatment. **(c)** Secretion of heterologous ZP peaks after three to four days.

To test whether the heterologous human ZP glycoproteins are functional, I studied acrosome reaction in human sperm (Fig. 3.28). Non-capacitated and capacitated human sperm were incubated with 22.5 µg/ml ZP2 and ZP3 or, as a positive control, with ionomycin. The acrosome was labeled with a pea lectin coupled to a green fluorescent molecule (PSA-FITC) (Lybaert *et al.*, 2009). Similar to the experiments performed in mouse sperm, the fraction of acrosome-reacted

sperm was determined and normalized to acrosome reaction rates determined of sperm bathed in buffer (negative control). Fig. 3.28a shows a characteristic PSA-FITC and DAPI staining of acrosome-intact and acrosome-reacted human sperm. In acrosome-intact sperm, the acrosomal cap was stained (Fig. 3.28a, top), whereas, in acrosome-reacted sperm, only the equatorial region of the head was labeled (Fig. 3.28a, bottom).

In non-capacitated and capacitated sperm, neither the empty fraction nor ZP2 evoked a sizeable change in in the fraction of acrosome-reacted sperm (Fig. 3.28b). In non-capacitated sperm, also ZP3 had rather no effect, whereas, in capacitated sperm, ZP3 evoked a pronounced, 3-fold increase in the fraction of acrosome-reacted sperm. These results support the notation that in human sperm, ZP3 but not ZP2 stimulates the acrosome reaction and that capacitation primes human sperm for the ZP-induced acrosomal exocytosis. Finally, these results demonstrate that heterologous human ZP glycoproteins are functional.

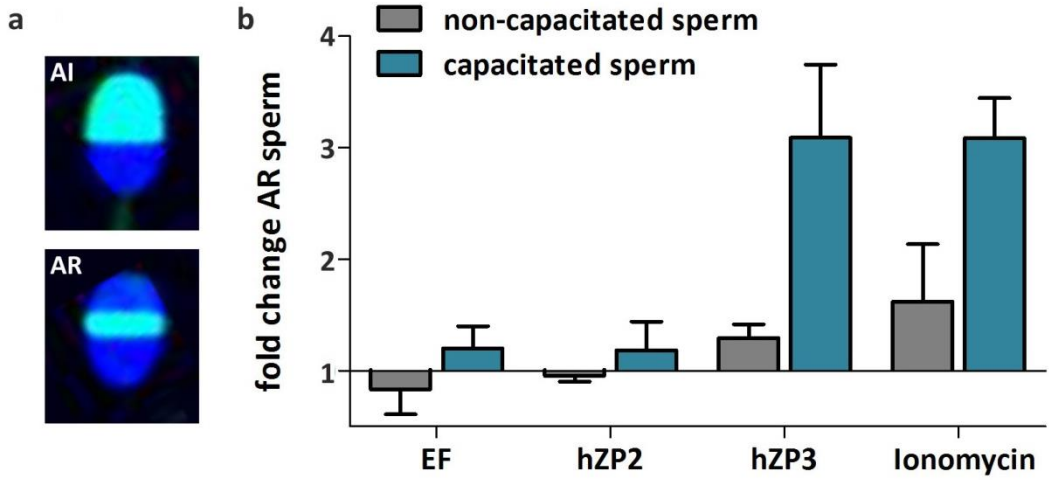

Fig. 3.28: Heterologous ZP3 evokes acrosome reaction in capacitated human sperm

(a) Acrosome reaction assay in human sperm. Sperm were immobilized on a glass slide and the acrosome was labelled with PSA-FITC (green), DNA in the nucleus was stained with DAPI (blue). Acrosome-intact sperm (AI), acrosome-reacted sperm (AR). **(b)** Acrosome reaction in non-capacitated (grey) and capacitated (teal) human sperm induced by empty fraction (EF), 22.5 µg/ml hZP2, 22.5 µg/ml hZP3, or 2 µM ionomycin. Data are shown as mean + SD percentage of acrosome-reacted (AR) sperm normalized to the buffer-treated control, error bars indicate + SD; (n = 4).

3.2.2 ZP-evoked $[Ca^{2+}]_i$ responses

Similar to mouse sperm, stimulation of human sperm with ZP glycoproteins evokes a Ca^{2+} increase (Bray *et al.*, 2002; Brewis *et al.*, 1996a; Patrat *et al.*, 2006). I monitored changes in $[Ca^{2+}]_i$ in human sperm loaded with the fluorescent Ca^{2+} indicator CAL520, using a fluorescent plate reader (FLUOstar). First, as a positive control, I studied CatSper-mediated Ca^{2+} responses evoked by stimulation of capacitated sperm with progesterone. The hormone evoked a rapid,

transient Ca^{2+} increase; the mean signal amplitude ($\Delta F/F_0$) was 188.7 ± 57.7 % (Fig. 3.29a,b). Stimulation of capacitated sperm with ZP2 and ZP3 (100 µg/ml) evoked a transient Ca^{2+} increase (Fig. 3.29a) with a mean amplitude of 145.1 ± 44.2 % and 69.4 ± 26.4 %, respectively (Fig. 3.29b). The empty fraction did not change $[Ca^{2+}]_i$ (Fig. 3.29a). Moreover, heat denaturation of ZP2 and ZP3 by incubation at 100 °C for 10 min abolished the Ca^{2+} increase, whereas similar heat treatment of progesterone did not affect the Ca^{2+} response (Fig. 3.29b). Taken together, these experiments confirm that ZP glycoproteins evoke a rapid Ca^{2+} increase in human sperm and, moreover, indicate that ZP3 acts more potently than ZP2.
Next, I studied the dose dependence of ZP3 action in capacitated and non-capacitated sperm. In capacitated sperm, ≥ 5 µg/ml ZP3 evoked a sizeable transient Ca^{2+} increase. The response amplitude rose with increasing ZP3 concentrations and saturated a protein concentration of 150 µg/ml (Fig. 3.29c). Of note, at ≥ 25 µg/ml ZP3, $[Ca^{2+}]_i$ did not recover to basal levels, but rather settled at an elevated level. Analysis of the dose-response relationship (Fig. 3.29d) yielded a half maximal effective concentration (EC_{50}) of 47.3 ± 7.5 µg/ml, i.e. 790 nM, (mean of n=4), indicating that ZP3 acts at nanomolar concentrations. In non-capacitated sperm, ZP3 concentrations of ≥ 25 µg/ml were required to induce a Ca^{2+} influx and the response did not saturate at up to 200 µg/ml ZP3 (Fig. 3.29f). Because the ZP3-evoked Ca^{2+} signals in non-capacitated sperm did not saturate, the EC_{50} could not be determined (Fig. 3.29f). These results indicate that capacitation renders the sperm more sensitive to ZP3.

To investigate the kinetics of the ZP3-evoked Ca^{2+} signal, I studied the ZP glycoprotein-evoked Ca^{2+} responses at higher time resolutions using the stopped-flow technique. For the stopped-flow experiments, larger volumes of buffer containing human ZP glycoproteins were required. Therefore, it was only feasible to mix sperm with ZP3 at concentrations ≤ 20 µg/ml. First, I studied Ca^{2+} responses evoked by mixing of capacitated sperm with progesterone. As control, to determine the upper response limit, I studied Ca^{2+} signals evoked by mixing with ionomycin. For the ease of illustration and to account for the variability between different samples, the individual traces were averaged and plotted along with the 95 % confidence interval. After mixing with either progesterone or ionomycin, $[Ca^{2+}]_i$ rose without a measurable latency within the time resolution of the stopped-flow apparatus (~40 ms) (Fig. 3.30a,b). The ionomycin-evoked signal saturated at about 5 s and $[Ca^{2+}]_i$ settled at a constant, elevated level throughout the recording time. Progesterone induced a transient Ca^{2+} increase; the signal reached its maximum after about 7 s and $[Ca^{2+}]_i$ almost recovered to basal levels within the recording time.
Next, I studied the action of ZP3. Fig. 3.3c illustrates that ZP3 evoked a rapid Ca^{2+} response; the signal kinetics and amplitude became faster and larger, respectively, with increasing ZP3 concentrations (Fig. 3.30c); the signal amplitude did not saturate at concentrations up to 20 µg/ml. The signal reached its maximum at about 5 to 10 s and $[Ca^{2+}]_i$ almost recovered to basal levels within the recording time. Zooming into the first three seconds of the ZP3-induced Ca^{2+} signals shows that $[Ca^{2+}]_i$ rose without a measurable latency within the time resolution

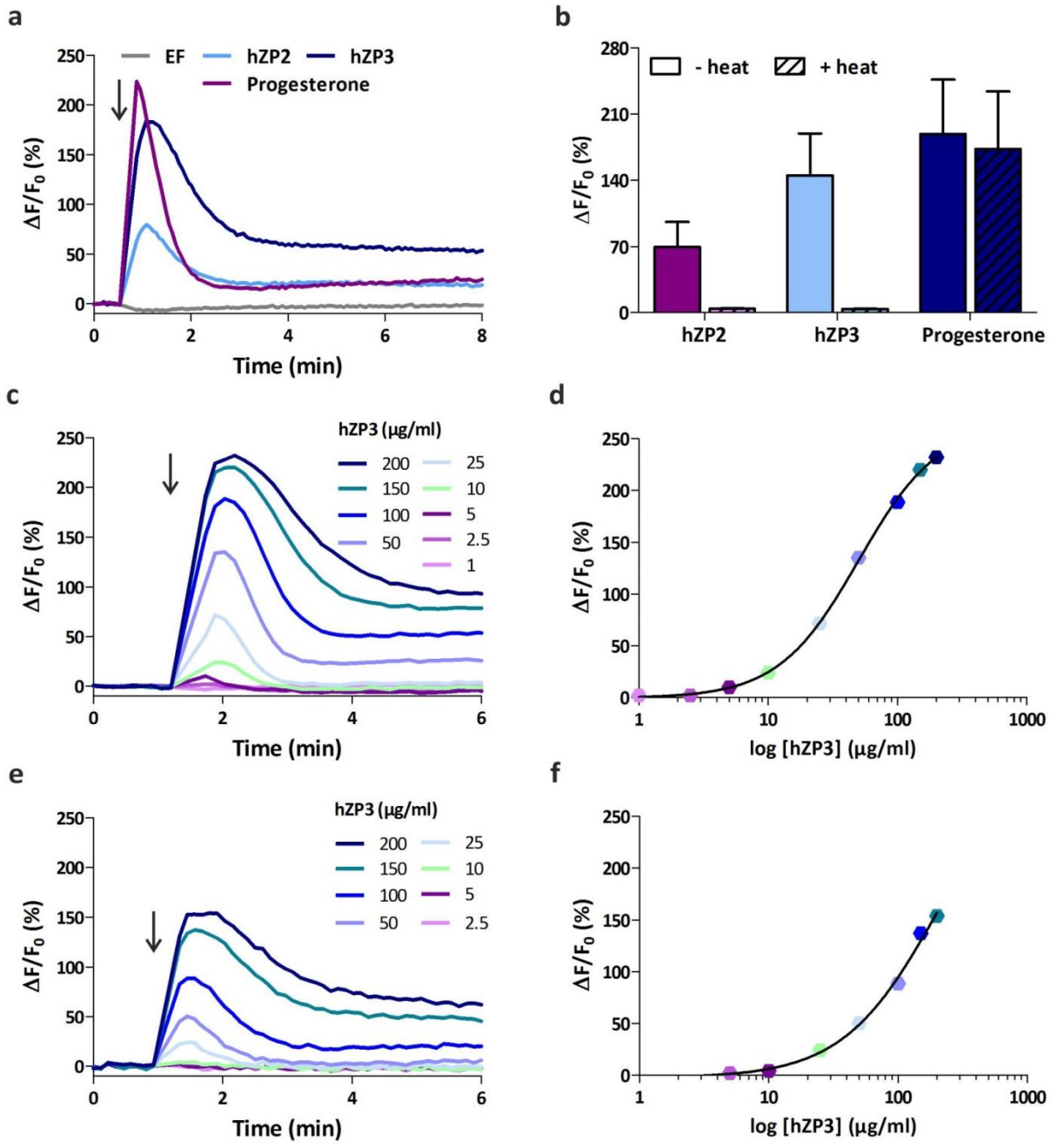

Fig. 3.29: Heterologous human ZP glycoproteins evokes a Ca^{2+} response in human sperm

(a) Change in $[Ca^{2+}]_i$ evoked by the empty fraction (EF) (light purple), 100 µg/ml hZP2 (light blue), 100 µg/ml hZP3 (dark blue), or 2 µM progesterone (dark purple) in capacitated human sperm; representative measurement. **(b)** Change in $[Ca^{2+}]_i$ evoked by EF, hZP2, hZP3 or progesterone before and after incubation at 100 °C for 10 min. Data are shown as mean, error bars indicate + SD (n = 6). **(c,e)** Dose-dependent $[Ca^{2+}]_i$ increase evoked by hZP3 in **(c)** capacitated and **(e)** non-capacitated human sperm; representative measurement. **(d,f)** Representative dose-response relationship of hZP3-induced Ca^{2+} increase in **(d)** capacitated (EC_{50} = 50 µg/ml) and **(f)** non-capacitated human sperm. The arrow indicates the time point of stimulus stimulation.

of the stopped-flow apparatus (~40 ms) (Fig. 3.30d).

To scrutinize whether the ZP3-induced Ca^{2+} response is mediated by CatSper, I used a pharmacological approach. To this end, I utilized the CatSper inhibitor RU1968F1 that was provided to me by Andreas Rennhack (caesar). Bathing sperm with RU1968F1 abolished the progesterone-induced Ca^{2+} response (Fig. 3.30f), confirming that the blocker suppresses CatSper-mediated Ca^{2+} signals. In sperm bathed in RU1968F1, the ZP3-evoked Ca^{2+} signal was abolished (Fig. 3.30e,f), demonstrating that also in human sperm, CatSper mediates the human ZP-induced Ca^{2+} influx.

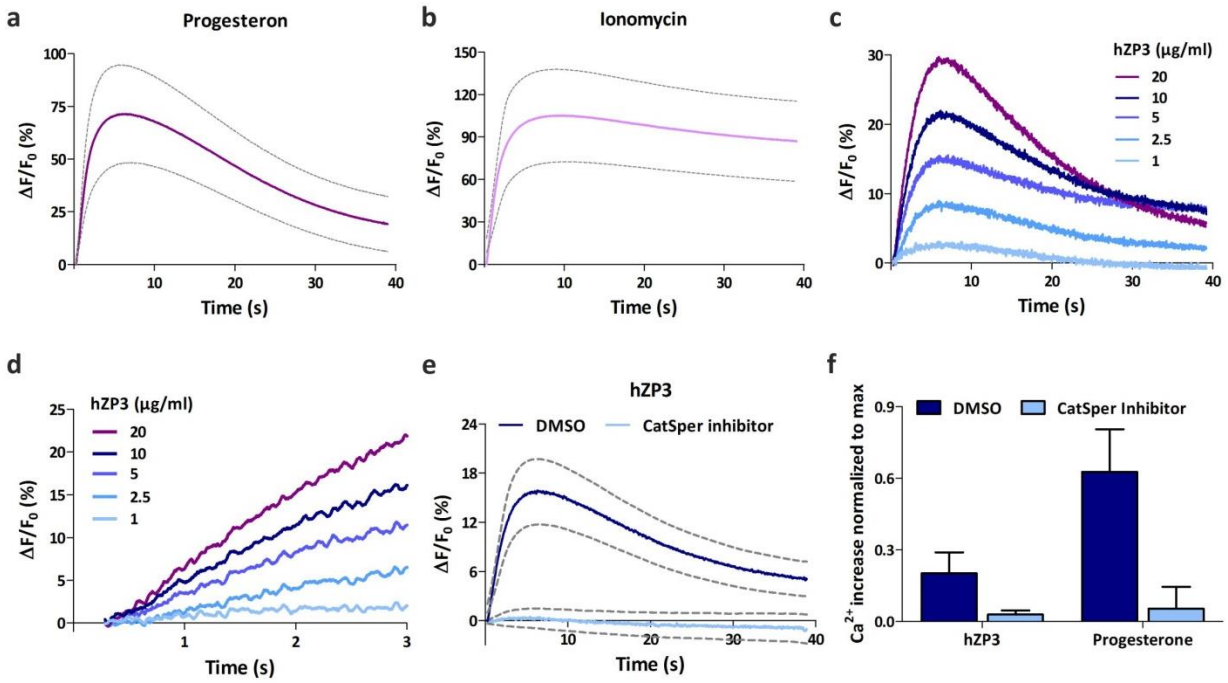

Fig. 3.30: CatSper mediates the human ZP glycoprotein-induced Ca^{2+} increase in human sperm

(a,b) Change in $[Ca^{2+}]_i$ evoked by **(a)** 2 µM ionomycin and **(b)** 2 µM progesterone in capacitated human sperm. Mean ± 95 % CI (dashed traces), n = 10. **(c)** Representative measurement of Ca^{2+} responses evoked by increasing concentrations of hZP3. **(d)** First three seconds of hZP3-evoked Ca^{2+} increase. **(e)** Change in $[Ca^{2+}]_i$ evoked by 20 µg/ml hZP3 in capacitated human sperm before (dark blue) and after (light blue) preincubation with 30 µM RU1968F1. Mean ± 95 % CI (dashed traces), n = 4. **(f)** Mean signal amplitudes before (dark blue) and after (light blue) preincubation with 30 µM RU1968F1, normalized to the maximal response evoked by 2 µM ionomycin. All values are given as mean + SD, error bars indicate + SD (n = 4).

3.2.3 Species-specificity of heterologous mouse and human ZP glycoproteins

The ZP ensures species specificity during fertilization. To test for the species specificity of the heterologous ZP glycoproteins, acrosome reaction assays were performed with mouse and human ZP3 glycoproteins in both mouse and human sperm. Mouse and human ZP3 increased the fraction of acrosome-reacted in mouse and human sperm by 1.6 and 3 fold, respectively. However, mouse ZP3 did not evoke the acrosome reaction in human sperm and *vice versa* (Fig. 3.31), demonstrating that heterologous ZP3 evokes the acrosome reaction in a species-specific fashion.

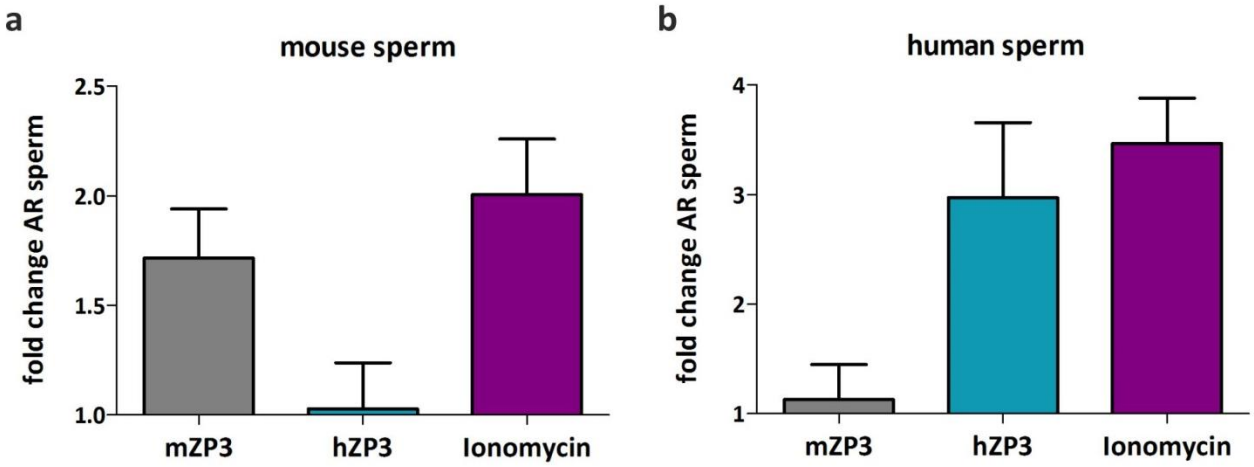

Fig. 3.31: Species-specificity of ZP3-evoked acrosome reaction

(a) Acrosome reaction evoked by 22.5 µg/ml mZP3 (grey), 22.5 µg/ml hZP3 (teal), or 2 µM ionomycin (purple) in capacitated **(a)** mouse and **(b)** human sperm. Data are shown as mean + SD percentage of acrosome-reacted (AR) sperm normalized to the buffer-treated control, error bars indicate + SD; (n = 4).

Moreover, I studied Ca^{2+} responses evoked by mixing of mouse sperm with human ZP2 and ZP3 (100 µg/ml). The human ZP glycoproteins did not induce a Ca^{2+} increase in mouse sperm (Fig. 3.32a,b). In contrast, at 100 µg/ml, mouse ZP3 evoked a sizeable Ca^{2+} increase in human sperm, indicating that mZP3 activates human CatSper (Fig. 3.32c,d); heat denaturation abolished the mZP3-evoked Ca^{2+} response in human sperm (Fig. 3.32d). Of note, mouse ZP3 was less potent to evoke a Ca^{2+} response than human ZP3 and human ZP2 (signal amplitudes: 39.1 ± 22.9 % vs. 145.1 ± 44.2 % vs. 69.3 ± 26.4 %). Human CatSper is promiscuously activated by a variety of ligands (Brenker *et al.*, 2012; Schiffer *et al.*, 2014), which might explain the cross-species action of mouse ZP3 in human sperm

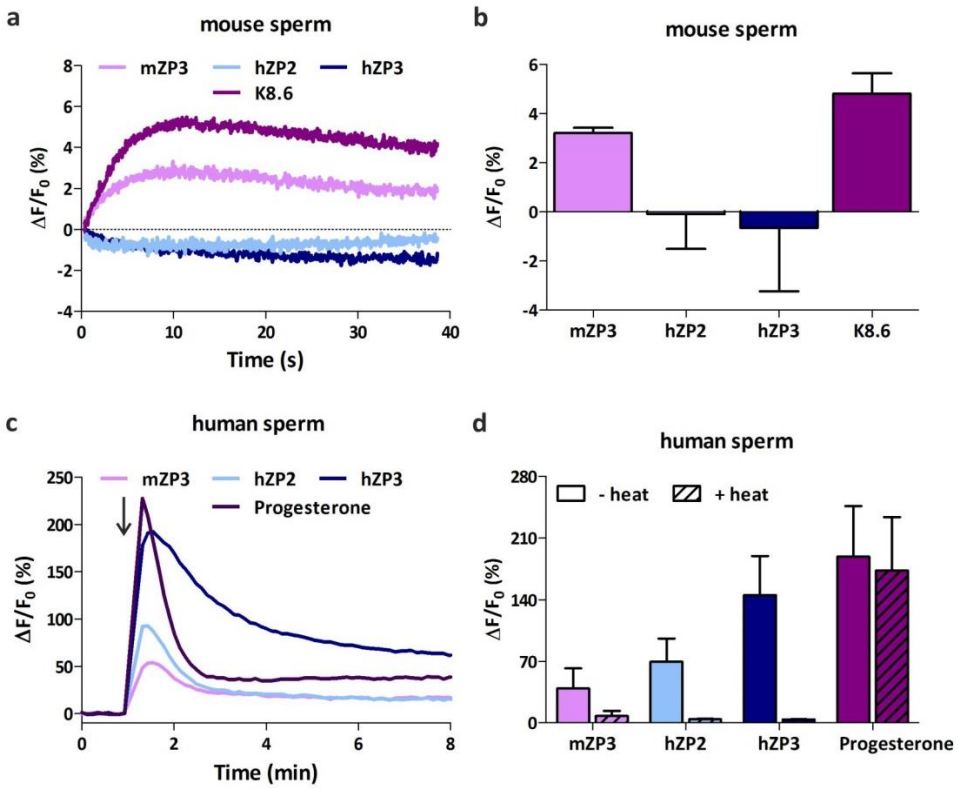

Fig. 3.32: Species-specificity of the ZP-evoked Ca^{2+} response

(a) Change in $[Ca^{2+}]_i$ evoked by 100 µg/ml mZP3 (light purple), 100 µg/ml hZP2 (light blue), 100 µg/ml hZP3 (dark blue), or K8.6 (dark purple) in capacitated mouse sperm, representative measurement. **(b)** Mean signal amplitudes, error bars indicate + SD (n = 4). **(c)** Change in $[Ca^{2+}]_i$ evoked by 100 µg/ml mZP3 (light purple), 100 µg/ml hZP2 (light blue), 100 µg/ml hZP3 (dark blue), or 2 µM progesterone (dark purple) in capacitated human sperm; representative measurement. The arrow indicates the time point of stimulus stimulation. **(d)** Change in $[Ca^{2+}]_i$ evoked by mZP3, hZP2, hZP3, or progesterone before and after heat denaturation in capacitated human sperm. Data are shown as mean, error bars indicate + SD (n = 4).

3.2.4 ZP-evoked pH_i responses

Next, I studied whether human ZP glycoproteins evoke a pH_i response human sperm. To this end, I monitored changes in pH_i in human sperm loaded with the fluorescent pH indicator BCECF, using the FLUOstar. In capacitated human sperm, NH_4Cl evoked a rapid pH_i increase; the mean signal amplitude ($\Delta R/R_0$) was 26.6 ± 3.9 % (Fig. 3.33a,b). Similar to NH_4Cl, ZP2 and ZP3 (100 µg/ml) evoked a pH_i increase (Fig. 3.33a) with a mean amplitude of 7.6 ± 1.8 % and 18.3 ± 3.2 %, respectively (Fig. 3.33b). The empty fraction did not change pH_i (Fig. 3.33a,b). Taken together, these experiments demonstrate that ZP glycoproteins evoke a rapid alkalization in human sperm and suggests that ZP3 acts more potently than ZP2.

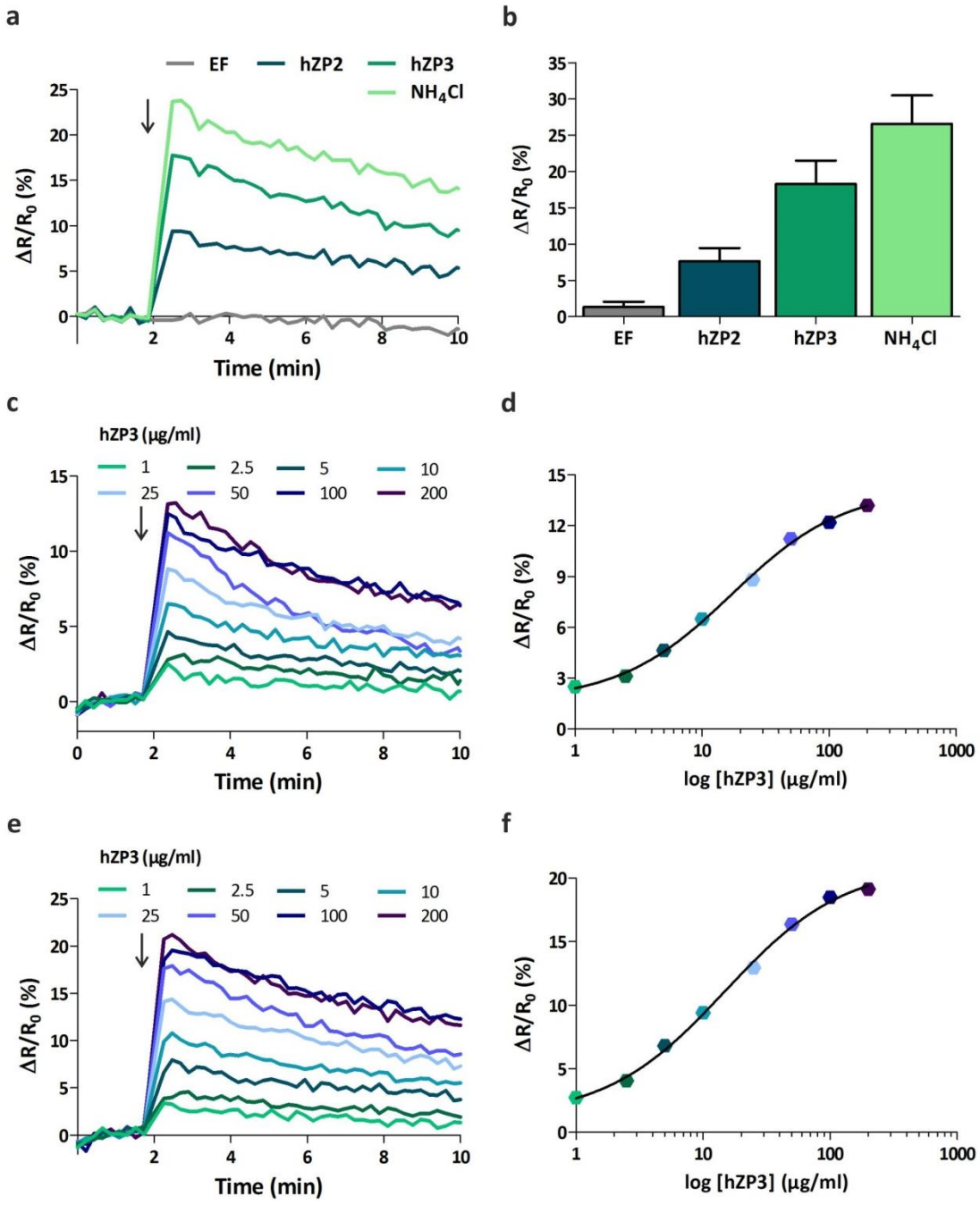

Fig. 3.33: ZP glycoprotein-evoked pH_i responses in human sperm

(a) Change in pH_i evoked by the empty fraction (EF) (grey), 100 µg/ml hZP2 (moss green), 100 µg/ml hZP3 (dark green), or 20 mM NH_4Cl (light green) in capacitated human sperm. **(b)** Change in pH_i evoked by EF, hZP2, hZP3 or NH_4Cl. Data are shown as mean + SD, (n = 6). **(c,e)** Dose-dependence of the pH_i increase evoked by hZP3 in **(c)** capacitated and **(e)** non-capacitated human sperm; representative measurement. **(d,f)** Representative dose-response relationship of hZP3-induced pH_i increase in **(d)** capacitated (EC_{50} = 20.3 µg/ml) and **(f)** non-capacitated human sperm (EC_{50} = 14.9 µg/ml). The arrow indicates the time point of stimulus stimulation.

Moreover, I investigated the dose dependence of the ZP3 action (Fig. 3.33c,e). In non-capacitated and capacitated sperm, ≥ 1 µg/ml ZP3 evoked a sizeable pH_i increase. The response amplitude rose with increasing ZP3 concentrations and commenced to saturate at protein concentrations of about 100 µg/ml. Analysis of the dose-response relation (Fig. 3.33d,f) yielded an EC_{50} of 20.5 ± 10.4 µg/ml (i.e. 390 nM, n=4) and 23.1 ± 4.6 µg/ml (i.e. 340 nM, n=4) for non-capacitated and capacitated sperm, respectively. Thus, capacitation does not potentiate the ZP3-evoked pH_i increase.

The kinetics of the ZP3-evoked pH_i signal was studied using the stopped-flow technique. As control, I studied pH signals evoked by mixing with NH_4Cl. Mixing of capacitated sperm with ZP3 (20 µg/ml) and NH_4Cl evoked a rapid pH_i increase with a mean signal amplitude of 11.4 ± 1 % (Fig. 3.34b) and 17.2 ± 1.5 % (Fig. 3.34a), respectively. The pH_i signals evoked by both ZP3 and NH_4Cl rose without a measurable latency within the time resolution of the stopped-flow apparatus (~40 ms). The superposition of ZP3-evoked pH_i and Ca^{2+} responses (Fig. 3.34c) demonstrates that the time resolution of the system does not allow to deliniate the sequence of events.

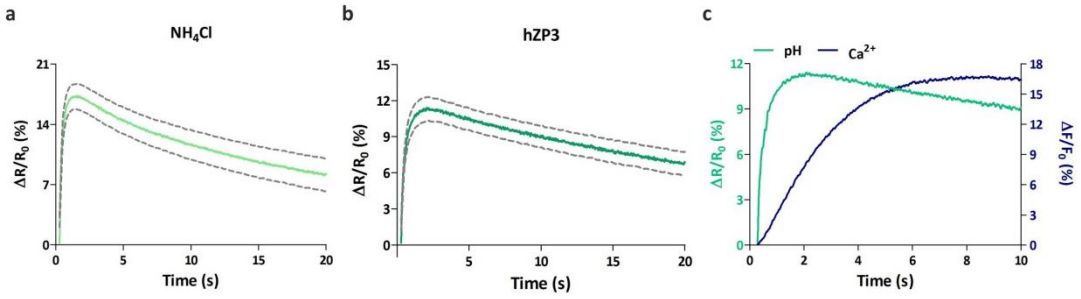

Fig. 3.34: Kinetics of the hZP3-evoked pH_i response

(a,b) Change in pH_i evoked by **(a)** 20 mM NH_4Cl or **(b)** 20 µg/ml hZP3 in capacitated human sperm. Mean ± 95 % CI (dashed traces), n = 3. **(c)** Superposition of hZP3-evoked pH_i (green) and $[Ca^{2+}]_i$ (blue) increase.

3.2.5 Molecular mechanism underlying the ZP glycoprotein-evoked pH_i response

To learn about the mechanism underlying the ZP-evoked alkalization, I studied ZP3-induced pH_i responses in sperm bathed in 5 mM (control) or 138 mM extracellular K^+ (Fig. 3.35). Under control conditions, 100 µg/ml ZP3 induced the characteristic pH_i increase, whereas at high $[K^+]_o$, the pH_i response was abolished ($\Delta R/R_0$ = 12.3 ± 2.7 % vs. 0.8 ± 0.2 %) (Fig. 3.35a,b). The NH_4Cl-evoked pH_i increase was only slightly attenuated at high $[K^+]_o$ (Fig. 3.35c). These results indicate that ZP-induced pH_i signaling in human sperm requires, similar to mouse sperm, a polarized membrane potential.

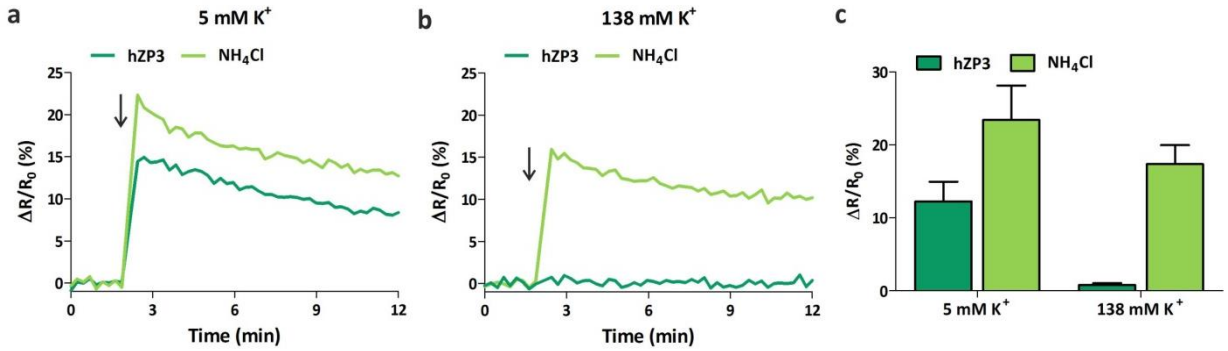

Fig. 3.35: ZP3-evoked pH_i responses at low and high extracellular K^+ concentrations

(a,b) Change in pH_i evoked by 100 µg/ml ZP3 (dark green) or 10 mMNH_4Cl (light green) in capacitated sperm bathed in **(a)** 5 mM $[K^+]_o$ (control) or **(b)** 138 mM $[K^+]_o$ buffer. The arrow indicates the time point of stimulus stimulation. **(c)** Mean signal amplitudes; error bars indicate + SD (n = 3).

Next, it was studied whether the ZP-evoked alkalization involves Na^+/H^+ exchange. Fig. 3.36 shows ZP3-induced pH_i responses in sperm bathed in 138 mM (control) or 0 mM extracellular Na^+. The pH_i response was similar in the presence and absence of Na^+, excluding that the ZP-evoked pH_i response in human sperm, in contrast to mouse sperm, involves Na^+/H^+ exchanger or proteins that require extracellular Na^+.

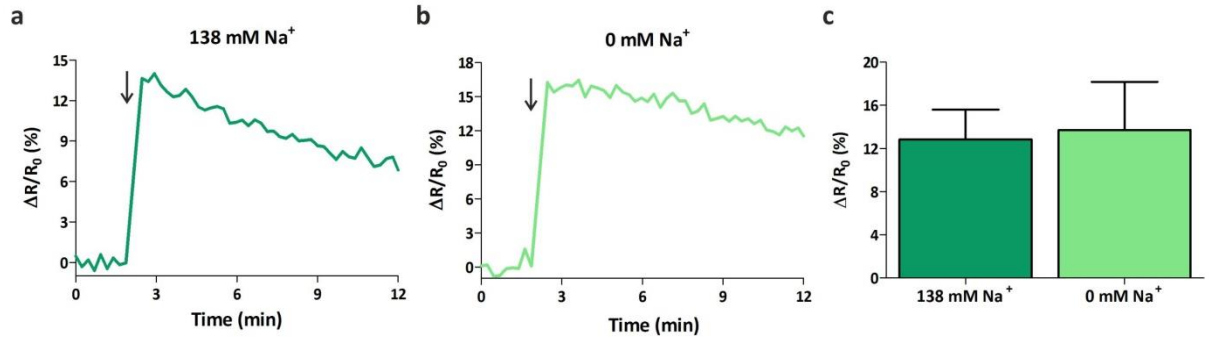

Fig. 3.36: ZP3-evoked pH_i responses at high and low extracellular Na^+

(a,b) Change in pH_i evoked by 100 µg/ml hZP3 in capacitated sperm bathed in **(a)** 138 mM $[Na^+]_o$ or **(b)** 0 mM $[Na^+]_o$ buffer, representative measurement. The arrow indicates the time point of stimulus stimulation. **(c)** Mean signal amplitudes; error bars indicate + SD (n = 3).

In human sperm, the flux of protons across the membrane is controlled by the voltage-gated H^+ channels Hv1 (Lishko 2010, Berger 2016). The role of Hv1 in human sperm is still enigmatic. To test whether Hv1 mediates the ZP-evoked alkalization, I studied the pH_i response in the presence of the HV1 inhibitors Zn^{2+} (Lishko *et al.*, 2010; Mahaut-Smith, 1989; Qui *et al.*, 2015) and 5-chloro-2-guanidinobenzimidazole (Ch-GBI) (Chiu *et al.*, 2010; Hong *et al.*, 2013). The pH_i

response was similar in the absence and presence of the inhibitors, demonstrating that the ZP3-evoked alkalization is not mediated by Hv1 (Fig. 3.37).

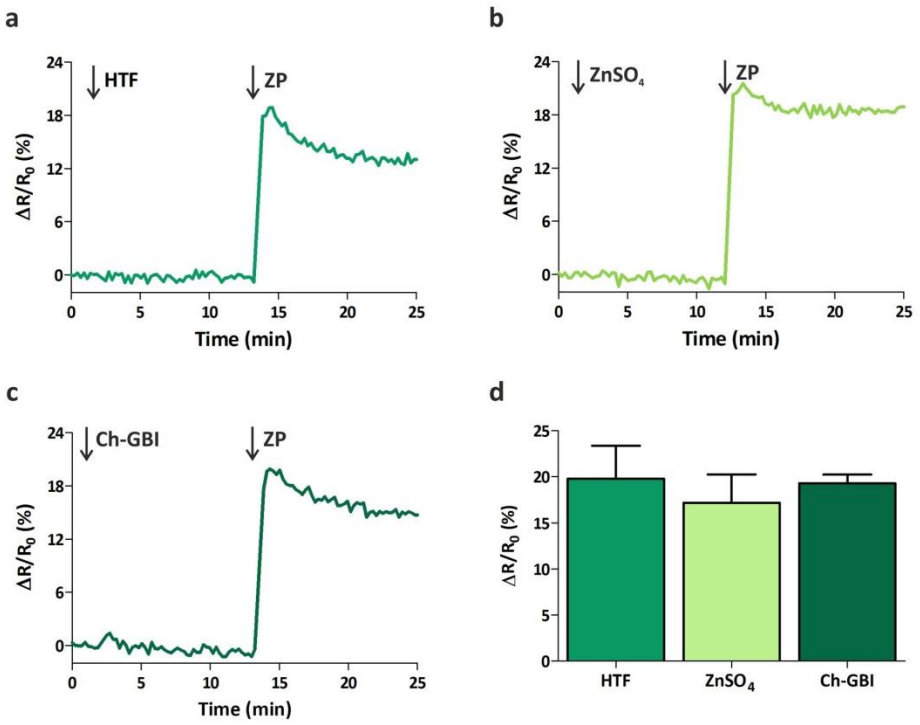

Fig. 3.37: ZP3-evoked pH_i response is not mediated by H_v1

(a,b,c) Change in pH_i evoked by 100 µg/ml hZP3 in capacitiated sperm bathed in **(a)** HTF (control), **(b)** 100 µM $ZnSO_4$, or **(c)** 200 µM Ch-GBI, representative mesurement. **(d)** Mean signal amplitudes; error bars indicate + SD (n = 5). The arrow indicates the time point of stimulus stimulation.

After excluding a Na^+/H^+ exchanger and Hv1 as proteins controlling the ZP glycoprotein-evoked pH_i response, I tried several other conditions to get further insights into the molecular mechanism underlying ZP-evoked pH_i signaling in human sperm. In sperm bathed in buffer lacking either Cl^- or Mg^{2+}, the ZP response was similar to that observed under control conditions (Fig. 3.38). Thus, transport mechanisms that require extracellular Cl^- or Mg^{2+} are not involved in the ZP-evoked pH_i response.

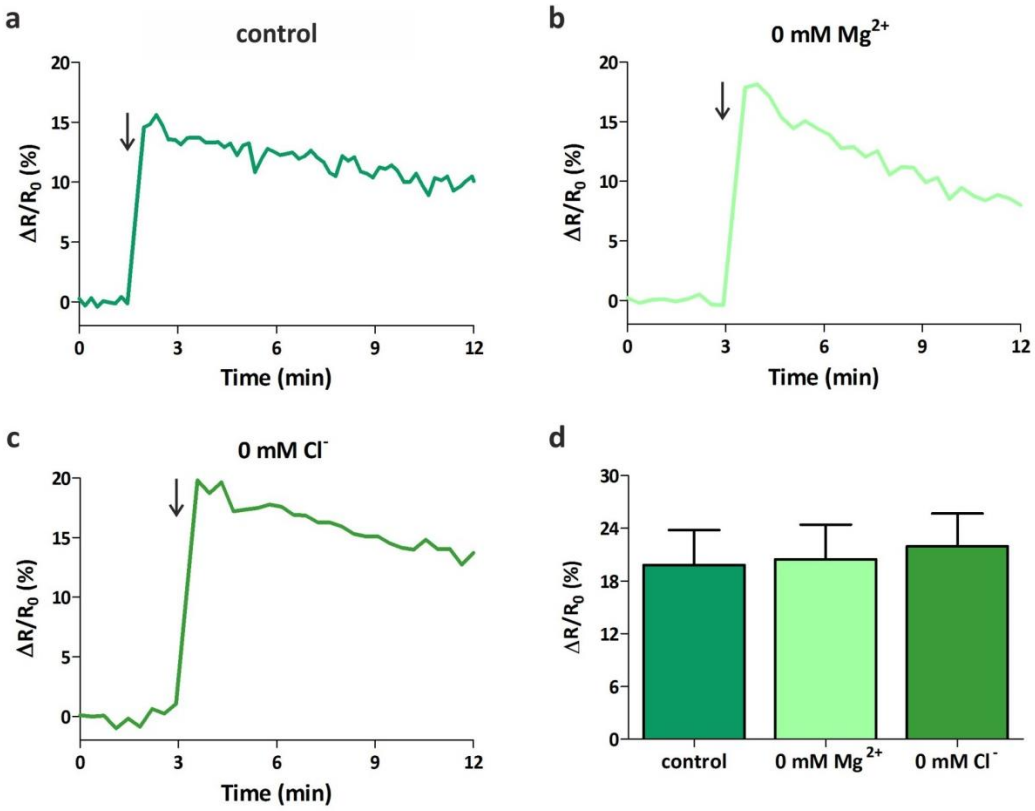

Fig. 3.38: ZP3-evoked alkalization at high and low extracellular Mg^{2+} and Cl^-

(a,b,c) Change in pH_i evoked by 100 µg/ml hZP3 in capacitiated sperm bathed in **(a)** 1 mM $[Mg^{2+}]_o$/ 145 mM $[Cl^-]_o$ (control), **(b)** 0 mM $[Mg^{2+}]_o$, or **(c)** 0 mM $[Cl^-]_o$, representative mesurement. The arrow indicates the time point of stimulus stimulation. **(d)** Mean signal amplitudes; error bars indicate + SD (n = 5).

Moreover, the ZP-induced alkalization was similar at a pH_o of 6.9, 7.4, and 7.9; with increasing pH_o, the amplitude of the NH_4Cl response increased, because the action of weak bases is enhanced at alkaline pH_o (Fig. 3.39).

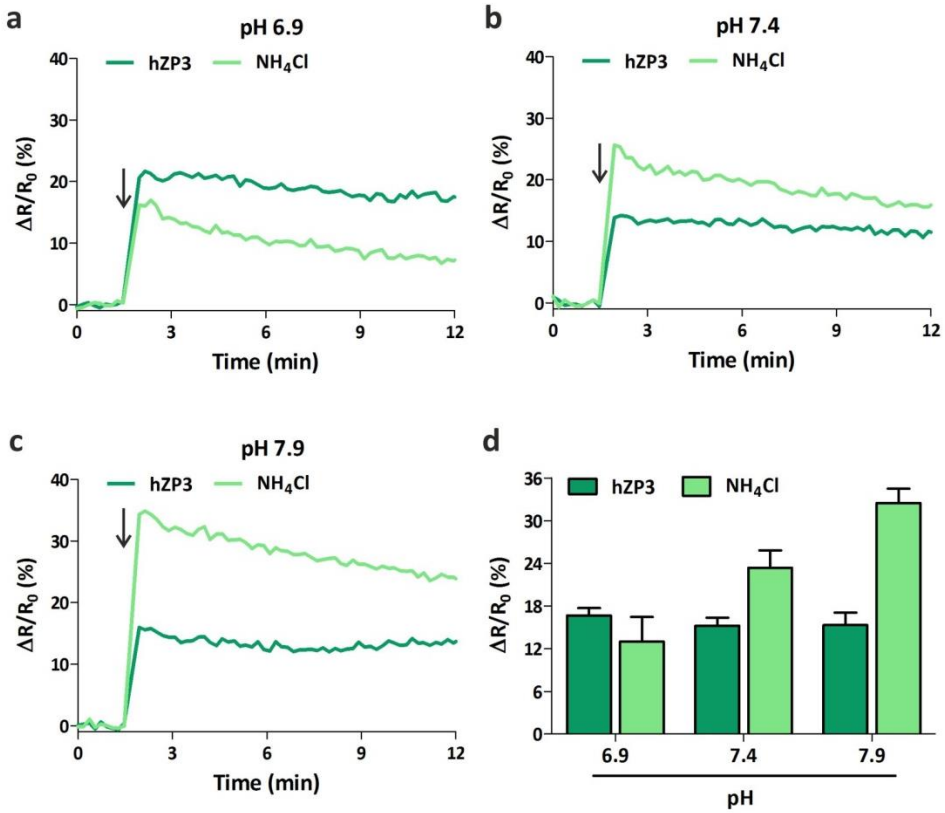

Fig. 3.39: ZP3-evoked alkalization at high and low extracellular pH

(a,b,c) Change in pH_i evoked by 100 µg/ml hZP3 (dark green) or 20 mM NH_4Cl (light green) in capacitated human sperm incubated in buffer with pH **(a)** 6.9, **(b)** 7.4 or **(c)** 7.9, representative measurement. The arrow indicates the time point of stimulus stimulation. **(d)** Mean signal amplitudes; error bars indicate + SD (n = 4).

Finally, I studied the action of ZP3 at 0, 4, and 25 mM extracellular HCO_3^- (Fig. 3.40). The amplitude of the ZP-induced alkalization decreased with increasing $[HCO_3^-]_o$. Thus, the ZP-induced alkalization might involve a HCO_3^- dependent transport mechanism. Taken together, this shows that although similar to mouse, ZP-evoked alkalization in human also requires a polarized V_M, ZP-evoked alkalization is mediated by different proteins in mouse and human sperm.

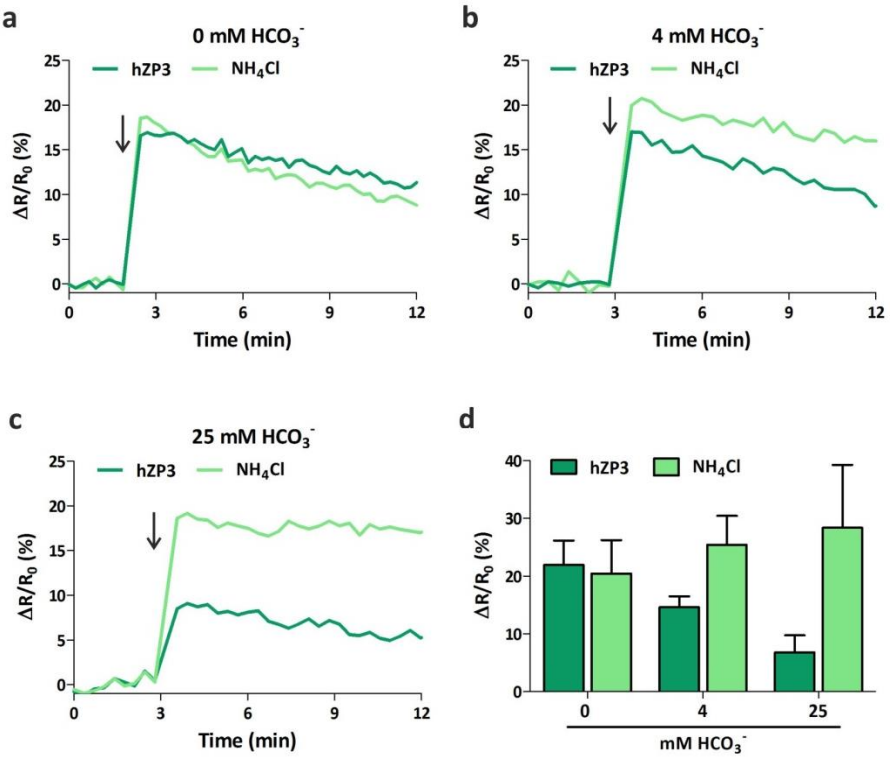

Fig. 3.40: ZP3-evoked pH_i response at high and low extracellular bicarbonate

(a,b,c) Change in pH_i evoked by 100 µg/ml hZP3 (dark green) or 20 mM NH_4Cl (light green) in capacitated human sperm incubated in **(a)** 0 mM, **(b)** 4 mM or **(c)** 25 mM $[HCO_3^-]_o$, representative measurement. The arrow indicates the time point of stimulus stimulation. **(d)** Mean signal amplitudes; error bars indicate + SD (n = 3).

3.2.6 ZP glycoproteins directly activate human CatSper

Next, I investigated whether the ZP-induced pH_i increase is required for Ca^{2+} influx via CatSper. To this end, I studied ZP3-induced Ca^{2+} responses in sperm bathed in high $[K^+]_o$ (Fig. 3.41); at high $[K^+]_o$, the ZP-evoked pH_i increase was abolished. The ZP3-evoked Ca^{2+} increase was however similar at high and low $[K^+]_o$, demonstrating that in human sperm, in contrast to mouse sperm, the ZP-evoked alkalization is not required for the Ca^{2+} influx via CatSper.

To scrutinize that hZP3 activates CatSper, whole cell patch-clamp recordings from human sperm were performed by Dr. Christoph Brenker (CeRA, Münster) (Fig. 3.42). CatSper is highly selective for Ca^{2+}. However, due to the long dwell time of Ca^{2+} in the pore (Kirichok *et al.*, 2006), Ca^{2+} currents carried by CatSper are very small and below the detecting limit of the patch-clamp technique. Therefore, measurements were performed in divalent-free intra- and extracellular

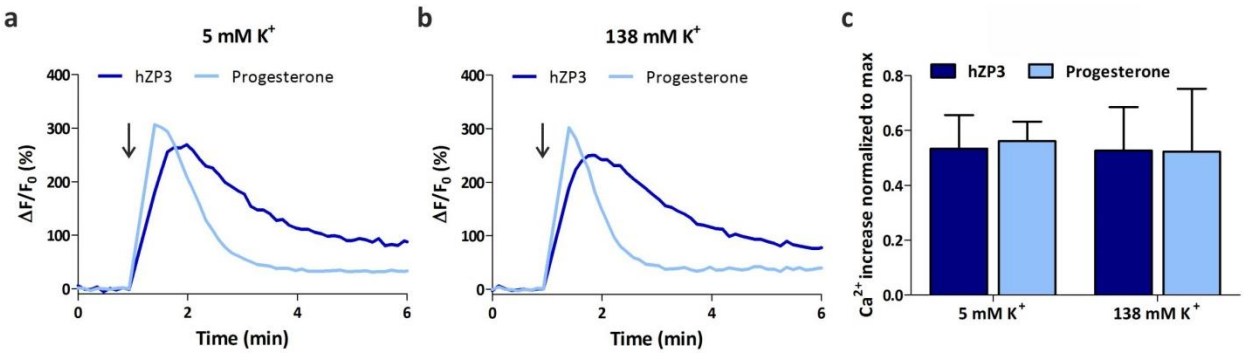

Fig. 3.41: ZP3-evoked Ca^{2+} responses at high and low extracellular K^+

(a,b) Change in $[Ca^{2+}]_i$ evoked by 100 µg/ml hZP3 (dark blue) or 2 µM progesterone (light blue) in capacitated sperm bathed in **(a)** 5 mM (control) or **(b)** 138 mM K^+ buffer, representative measurement. The arrow indicates the time point of stimulus stimulation. **(c)** Mean signal amplitudes normalized to the maximal response evoked by ionomycin; error bars indicate + SD (n = 3).

solutions (NaDVF). Under these conditions, CatSper is permeable for monovalent ions like Cs^+ and Na^+ and the monovalent CatSper current ($I_{CatSper}$) is readily detectable. Perfusion of sperm with ZP3 evoked a sizeable increase of the monovalent CatSper current. These results

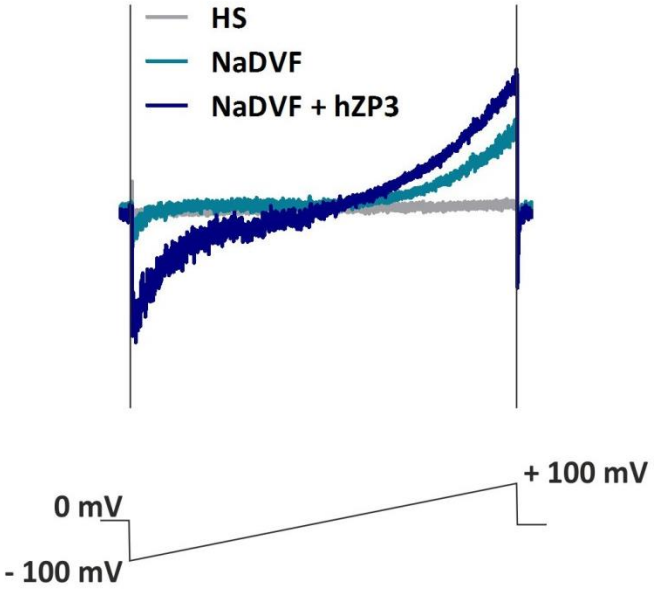

Fig. 3.42: ZP3 potentiates monovalent CatSpers current in human sperm

Control current in extracellular solution containing Mg^{2+} and Ca^{2+} (HS, grey). Representative monovalent whole-cell CatSper currents recorded in divalent-free Na^+-based bath solution (NaDVF, teal). Perfusion with 0.5 ZP/µl potentiated monovalent currents (NaDVF + hZP3, blue). Currents were recorded at pH_i 7.3 by running a ramp protocol from - 100 mV to + 100 mV in 1 s using a holding potential of 0 mV.

demonstrate that ZPs directly activate CatSper and that the activation of the channel does not require an increase of pH_i or diffusible intracellular signaling molecules.

Finally, I tested whether human ZP glycoproteins compete with progesterone or prostaglandine E1 (PGE1) for the activation of CatSper (Fig. 3.43). To this end, sperm were stimulated with a saturating concentration of progesterone or PGE1. Progesterone and PGE1 evoked a rapid, transient Ca^{2+} increase. In a second step, in the presence of progesterone or PGE1, sperm were stimulated with ZP3 (100 µg/ml). The ZP3-evoked Ca^{2+} response was similar in the absence and presence of progesterone or PGE1, demonstrating that ZP3 employs a distinct binding site to activate CatSper.

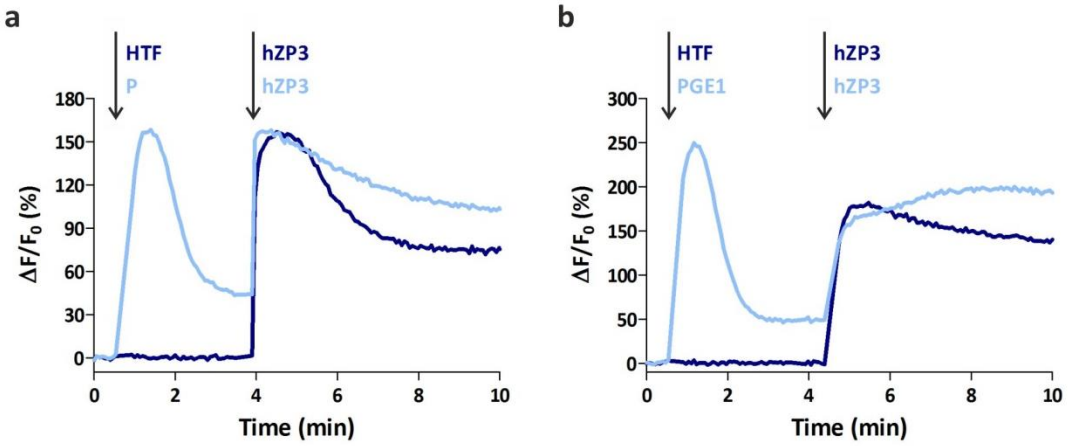

Fig. 3.43: ZP3 does not compete with progesterone and prostaglandine for CatSper activation

(a,b) Representative cross-desensitization experiment between hZP3 and **(a)** progesterone (P) or **(b)** prostaglandine E1 (PGE1) in capacitated human sperm. The arrow indicates the time point of stimulus stimulation.

4 Discussion

This thesis provides new insights into the signaling pathways underlying the action of ZP glycoproteins in sperm. Based on my results, I propose the following model (Fig. 4.1): In mouse sperm, activation of an unknown ZP-binding protein activates Na^+/H^+ exchange and, thereby, increases pH_i. The Na^+/H^+ exchange is mediated by NHA1 and other, yet, unknown Na^+/H^+ exchangers. The pH_i increase activates CatSper, resulting in a Ca^{2+} influx. This action of ZPs requires a polarized V_M set by the Slo3 channel and the second messenger cAMP. However, the ZP-binding protein and the additional Na^+/H^+ exchanger(s), the role of V_M and cAMP, and the mechanism of NHA1 activation remain elusive.

In human sperm, ZPs evoke a rapid increase of pH_i that does not involve Na^+/H^+ exchange or H^+ efflux via H_v1 and requires a polarized V_M. Remarkably, in humans, the ZP-induced alkalization is not required for the ZP-induced Ca^{2+} influx mediated by CatSper; ZPs do however not compete with progesterone or prostaglandins for CatSper activation, indicating that ZPs employ a different binding site and mechanism (Fig. 4.1). Altogether, these results demonstrate that the mechanism of ZP action is distinctively different in mouse and human sperm. However, the mechanism and role of the ZP-induced alkalization in human sperm is unknown.

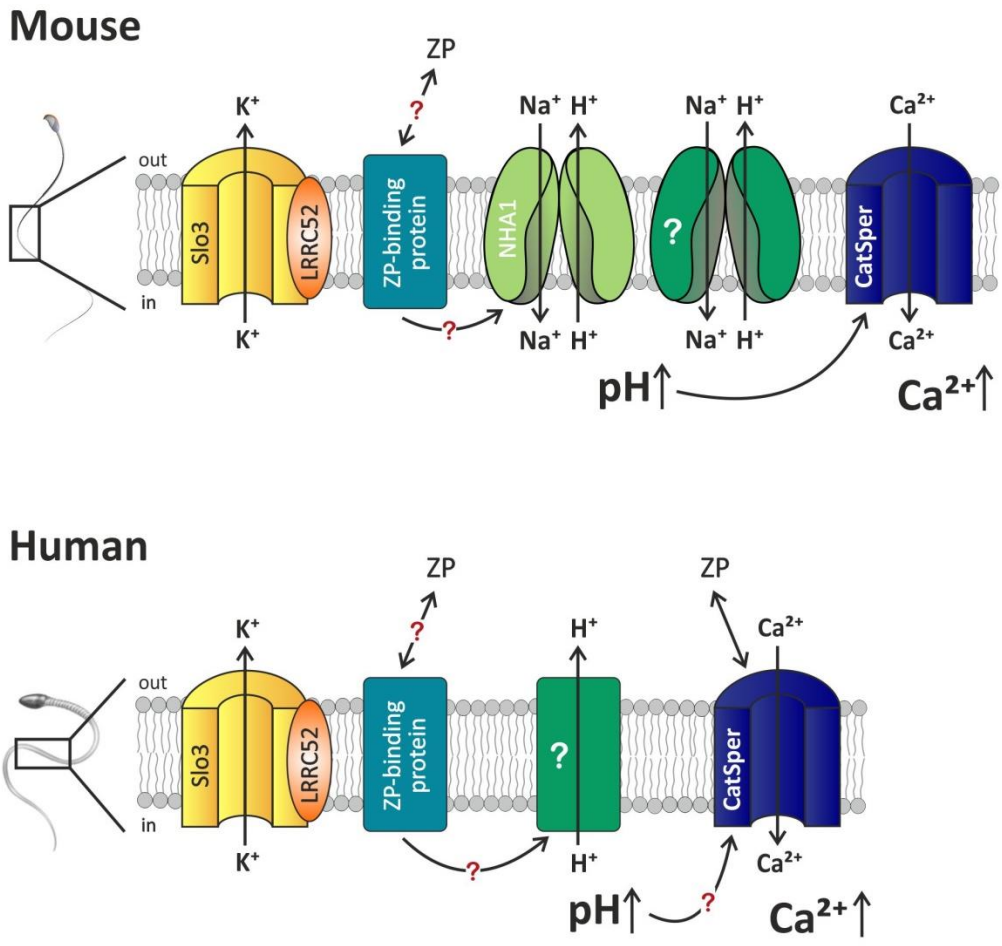

Fig. 4.1: Model for ZP signaling in mouse and human sperm

Mouse: Interaction of an unknown ZP-binding protein with the ZP activates NHA1 and another protein of the NHE family, resulting in proton export and an increase in sperm pH_i. Sperm alkalization activates CatSper, resulting in a Ca^{2+} influx. A polarized V_M set by Slo3 and the second messenger cAMP are required for the ZP-induced increase in pH_i and $[Ca^{2+}]_i$. **Human:** Activation of CatSper by ZPs does not require an alkalization. A polarized V_M is required for the ZP-induced increase in pH_i. The underlying molecular mechanism and a potential role in CatSper activation still have to be elucidated. Question marks indicate hypothetical signaling pathways that have not been confirmed experimentally.

4.1 ZP signaling in mouse and human sperm

Most of the knowledge in reproductive biology comes from work with mice. Initial studies on human gametes revealed many similarities between humans and mice, suggesting that mice serve as a good model to study human reproduction. However, a more detailed analysis of sperm signaling pathways revealed fundamental differences between mouse and human sperm, demonstrating that fertilization is controlled by species-specific mechanisms. My studies concerning ZP signaling provide another interesting twist concerning the difference between mammalian species.

First, CatSper activation by ZPs in human sperm does not require a change in pH_i. In line with this observation, other studies have shown that in human, but not in mouse sperm, CatSper mediates a ligand- rather than a pH-dependent Ca^{2+} influx (Brenker *et al.*, 2012; Lishko *et al.*, 2011; Strünker *et al.*, 2011). This might explain why a more direct activation by ZPs has evolved in humans. In contrast, mouse CatSper has developed a higher sensitivity towards changes in pH_i (Lishko & Kirichok, 2010), which might allow for activation by ZP-evoked alkalization Supporting this notion, Xia and Ren excluded a direct CatSper activation by ZPs in mouse (Xia & Ren, 2009).

Second, the ZP-evoked alkalization is mediated by different proteins in mouse and human sperm. In mouse sperm, the alkalization is predominantly mediated by the NHA1, whereas in human sperm, Na^+/H^+ exchange is not involved in the pH_i response. In fact, the ZP-evoked pH response was attenuated at high extracellular HCO_3^- concentrations, suggesting that it involves a HCO_3^--dependent transport mechanism. Indeed, HCO_3^--transporting proteins have been identified in the human sperm head and midpiece (Chávez *et al.*, 2012; Holappa *et al.*, 1999; Parkkila *et al.*, 1993; Xu *et al.*, 2007). However, these candidates belong to the Cl^-/HCO_3^- exchanger family that utilize the electrochemical gradient of Cl^-. The ZP-evoked alkalization was, however, independent of the extracellular Cl^- concentration, arguing against that Cl^-/HCO_3^- exchange is involved. In fact, the attenuation of the ZP-evoked alkalization at high extracellular HCO_3^- concentrations might rather reflect an enhanced pH_i buffering capacity: an increase of the extracellular HCO_3^- concentration increases also the HCO_3^- concentration inside the cell. This

increases the intracellular pH buffering capacity, which might dampen the ZP-induced alkalization. Other candidate proteins in human sperm, which could underlie the ZP-evoked alkalization, are the voltage-dependent phosphoinositide-phosphatase paralogs TPTE and TPTE2 (transmembrane phosphatase with tensin homology). TPTE and TPTE2 are expressed in sperm precursor cells in the human testis, but have not yet been detected in mature sperm (Chen *et al.*, 1999; Tapparel *et al.*, 2003; Walker *et al.*, 2001). It has been proposed that both TPTE and TPTE2 carry voltage-activated H^+ currents (Sutton *et al.*, 2012); thus, TPTEs might be involved in the ZP-evoked pH response.

In my thesis, I could also attribute a physiological function to the NHA1, which underlies the ZP-evoked alkalization in mouse sperm. This suggests that the subfertility of NHA1-deficient male mice is caused by impaired ZP penetration. This notion should be scrutinized by i*n vitro* fertilization experiment with NHA1-deficient sperm.
However, NHA1-deficient sperm also display a motility defect, namely stiffness of the sperm midpiece. A similar phenotype has been described after inhibition of the Ca^{2+}-dependent phosphatase calcineurin and knockout of CatSper ζ (Chung *et al.*, 2017; Miyata *et al.*, 2015). In these mouse models, the rigidity of the midpiece can be explained by a defect in Ca^{2+} signaling: In CatSper ζ sperm, the Ca^{2+} signaling platform along the flagellum is disturbed (Chung *et al.*, 2017), whereas blocking calcineurin activity removes a crucial component of the Ca^{2+} signaling platform (Chung *et al.*, 2014). However, the ultrastructure of the quadrilateral Ca^{2+} signaling domains is not affected in NHA1-deficient sperm.
In contrast to my results, Chen *et al*. describe a much stronger motility defect in their NHA1 knockout mouse-model, which they relate to attenuated SACY-cAMP signaling (Chen *et al.*, 2016). I failed to reproduce these results: In fact, SACY function is not impaired in NHA1-knockout sperm. The reason for this discrepancy is unclear. However, Chen *et al*. used a different buffer for sperm isolation and the tools to analyze sperm motility were also different. Another explanation could be that the stiff midpiece of NHA1-deficient sperm was mistakenly considered as an immotility phenotype

So far, my work does not provide insights how NHA1 is activated. The sNHE in sea urchin sperm is regulated by hyperpolarization and cAMP (Florian Windler, unpublished data). The NHA1 does not contain a cyclic nucleotide-binding domain or a voltage-sensor domain (Liu *et al.*, 2010), arguing against an activation by cyclic nucleotides or by changes in V_M. Alternatively, the NHA1 might be directly activated by ZP glycoproteins. Other members of the NHE family are indeed regulated by protein-protein interaction. The human NHE1 is for example activated by binding of calmodulin (Bertrand *et al.*, 1994), carbonic anhydrase II (Li *et al.*, 2006b) or the actin binding proteins ezrin, radixin, and moesin (Denker *et al.*, 2000). Patch-clamp experiments with heterologously expressed NHA1 might provide further insights into the activation mechanism of the exchanger.

4.2 Regulation of ZP-evoked acrosome reaction

My results indicate that ZP-evoked alkalization regulates acrosomal exocytosis. Reportedly, the acrosome reaction is triggered by Ca^{2+} release from intracellular stores (O'Toole *et al.*, 2000; Rossato *et al.*, 2001). It has been suggested that binding of IP3 to its receptor is pH-dependent (Worley *et al.*, 1987), since alkalization decreases the IP3-concentration required for half-maximal Ca^{2+} store depletion by ~50 fold (O'Toole *et al.*, 2000). To scrutinize that the alkalization is crucial for the ZP-induced acrosome reaction, experiments using NHA1-deficient sperm should be performed. Moreover, it could be tested if an increase in intracellular pH, for example induced by NH_4Cl, is already sufficient to evoke acrosomal exocytosis in mouse sperm. For human, my work does not provide conclusive insights whether acrosomal exocytosis is controlled by ZP-evoked alkalization or by the CatSper-mediated Ca^{2+} influx. In sperm preincubated with the CatSper inhibitor, high levels of spontaneous acrosome reaction were detected in the non-stimulated control so it was not possible to draw any conclusion (Fig. 4.2). Progesterone evoked acrosomal exocytosis in human sperm (Fig. 4.2). The action of progesterone in human sperm does not involve a change in pH_i (Strünker *et al.*, 2011), suggesting that the acrosome reaction in human sperm is not controlled by alkalization but rather by CatSper-mediated Ca^{2+} influx. However, further experiments are required to confirm this hypothesis.

The fact that ZP glycoproteins evoke acrosomal exocytosis suggests that *in* vivo, sperm undergo the acrosome reaction only upon binding to the zona pellucida. However, this is challenged by studies demonstrating that the acrosome reaction in mouse and human sperm is already

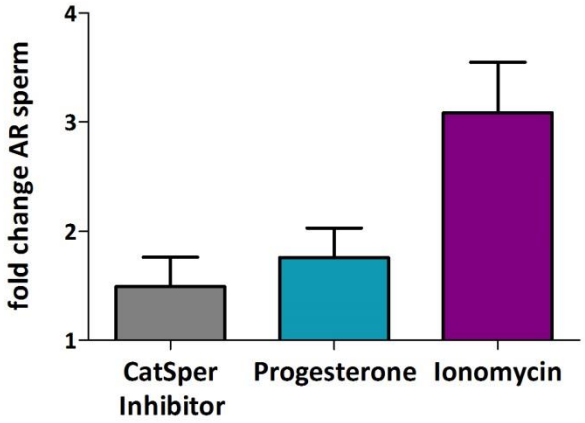

Fig. 4.2: CatSper inhibitor- and progesterone-evoked acrosome reaction

Acrosome reaction in capacitated human sperm induced by 30 µM RU1968F1, 1 µM progesterone or 2 µM ionomycin. Data are shown as mean + SD percentage of acrosome-reacted (AR) sperm normalized to the buffer-treated control, error bars indicate + SD; (n = 4).

initiated while sperm pass through the cumulus oophorus (Jin *et al.*, 2011; Pereda & Coppo, 1985) or even prior to reaching the oocyte (La Spina *et al.*, 2016). In line with this observation, acrosome-reacted sperm are able to bind and penetrate the ZP (Inoue *et al.*, 2011; Morales *et al.*, 1989), indicating that undergoing the acrosome reaction directly at the ZP surface is not required to fertilize the oocyte. It might be possible that ZPs are secreted from the oocyte into the uterus and interact with the approaching sperm before they reach the oocyte. This would require that ZP glycoproteins are shed from the ZP. However, experimental evidence supporting this hypothesis is lacking. Alternatively, ZP glycoproteins might act in concert with other factors in the female genital tract. Similar to ZPs, progesterone and prostaglandin have been implicated in human sperm acrosomal exocytosis (Baldi *et al.*, 2009; Harper *et al.*, 2003; Oren-Benaroya *et al.*, 2008; Publicover *et al.*, 2008; Schaefer *et al.*, 1998; Tamburrino *et al.*, 2014; Tamburrino *et al.*, 2015). In mice, other physiological stimuli of acrosomal exocytosis have not been identified. Since only acrosome-reacted sperm are able to fuse with the oocyte`s plasma membrane, sperm have to undergo the acrosome reaction prior to fertilization. A redundancy of the site of acrosome reaction might therefore be beneficial for fertilization success. The cumulus oophorus, for instance, dissipates over time (Chang & Pincus, 1951) so that sperm arriving late after ovulation rely on interactions with the ZP to induce acrosomal exocytosis (Avella & Dean, 2011).

4.3 Which roles play different ZP glycoproteins in ZP signaling?

Another goal of my PhD thesis was to reveal, which of the different ZP glycoproteins evokes a signaling response in sperm. To this end, I established a heterologous eukaryotic expression system, which allowed to express functional human and mouse ZP glycoproteins. In human, ZP3 evoked larger Ca^{2+} and pH_i responses than ZP2 and only ZP3 evoked acrosomal exocytosis, in line with other studies using different heterologous expression systems (Chiu *et al.*, 2008a; Ganguly *et al.*, 2010; Gupta, 2015). This suggests that the Ca^{2+} or pH_i increase induced by ZP2 was not sufficient to evoke a behavioral response. In mouse, the relative potency of the individual ZP glycoproteins to evoke a Ca^{2+} and pH_i response, as well as acrosomal exocytosis, was ZP3 > ZP2 >> ZP1. A study using purified native mouse ZP glycoproteins reported similar results (Bleil & Wassarman, 1983).

In both mouse and human, ZP2 was identified as the primary sperm binding protein (Avella *et al.*, 2014; Avella & Dean, 2011). Results from my thesis demonstrate that binding of sperm to ZP2 is not sufficient to evoke a behavioral response. Instead, the interaction with ZP3 seems to be required to evoke acrosomal exocytosis. These results suggest that the primary interaction with the ZP and induction of acrosomal exocytosis are two distinctly regulated events. This is in line with the finding that sperm-oocyte interaction is characterized by two phases, an initial loose attachment followed by tight binding between the gametes (Shur & Neely, 1988). Studies analyzing the binding between sperm and oocyte should, therefore, not be used to draw a

conclusion about the regulation of sperm behavior, e.g. acrosomal exocytosis. Moreover, the distinct regulation of sperm binding and induction of acrosomal exocytosis provides an additional control point to exclude cross-species fertilization. Although mouse sperm are able to bind to human ZP, acrosomal exocytosis is not evoked, presumably because sperm only interact with ZP2. The secondary ZP interaction might exclusively be established with sperm from the same species, ensuring species-specific fertilization.

What`s the molecular basis for the species-specificity of the sperm-oocyte interaction? ZPs lacking posttranscriptional glycosylation do not evoke acrosomal exocytosis (Chakravarty *et al.*, 2008; Dell *et al.*, 1999), suggesting that the carbohydrate residues of ZP glycoproteins mediate the secondary interaction with sperm. Mouse and human ZP might contain species-specific glycan residues, whereby acrosomal exocytosis is evoked in species-specific fashion. Indeed, it has been shown for human ZP glycoproteins that they express a species-specific sequence of glycan residues called sialyl-Lewis^x (Pang *et al.*, 2011). In contrast, the synthesis of O-linked oligosaccharides with terminal α-galactosides is restricted to mouse oocytes (Larsen *et al.*, 1990). One way to test this hypothesis would be to perform acrosome reaction assays with human ZP3 expressed in transgenic mouse oocytes, thereby modifying the human protein with glycan structures of mouse ZP3 due to post-transcriptional modification by the glycosyltransferases in the Golgi apparatus of mouse oocytes (Dell *et al.*, 2003). Another explanation could be a defined 3-dimensional species-specific presentation of highly branched glycans. Here, a difference in ZP ultrastructure between mouse and human ZP could account for the species-specific induction of acrosomal exocytosis. Furthermore, it is likely that also the male gametes contain regulatory mechanisms, which ensure that acrosomal exocytosis is only evoked when they bind to the ZP of the same species. Mouse and human sperm could, for example, express species-specific multimeric oocyte-binding complexes, which only allow a tight interaction with ZP glycoproteins from the same species.

4.4 Outlook

My thesis provides multiple important insights into the molecular mechanism of ZP signaling; however, a plethora of questions still have to be addressed. It is still unknown how ZP glycoproteins activate CatSper in human sperm. Do they bind to one of the four pore-forming subunits, to one of the five accessory subunits, or, act like progesterone via ABHD2 (Miller *et al.*, 2016)? Furthermore, the binding partner of ZP glycoproteins on the mouse sperm surface remains elusive, although numerous candidates have been proposed (Bleil & Wassarman, 1990; Cheng *et al.*, 1994; Ensslin & Shur, 2003; Maldera *et al.*, 2014; Petit *et al.*, 2013). However, so far, no candidate could be experimentally verified because in the respective knockout sperm, the binding and penetration of the zona pellucida was not impaired (Baba *et al.*, 2002; Lin *et al.*, 2007; Lu & Shur, 1997). There is increasing evidence that the sperm-ZP interaction involves multiple recognition sites (Nixon & Aitken, 2009; Redgrove *et al.*, 2011; van Gestel *et al.*, 2007),

indicating that gamete interaction is not mediated by a single receptor-ligand pair. The differentiation between primary sperm binding and induction of acrosomal exocytosis is in line with this finding, indicating that different sperm proteins might be involved in these two events, which further complicates the hunt for the ZP receptor. The only potential ZP receptor that has been assigned with acrosome reaction-inducing properties is the β1,4-galactosyltransferase (GalTase). When GalTase was heterologously expressed in *Xenopus* oocytes and when the oocytes were stimulated with ZP3, cortical granules were released (Shi *et al.*, 2001). However, exocytotic signaling is controlled very differently in amphibians and mammals, which questions the physiological significance of this finding. A possibility, which has not yet been considered is that ZP glycoproteins might directly activate an ion channel or exchanger in the flagellum of mouse sperm. To identify the ZP binding site on CatSper in human sperm and the ZP binding partner in mouse sperm, a crosslinking experiment could be performed, similar to the approach used for identifying the progesterone receptor in human sperm (Miller *et al.*, 2016). Here, ZP glycoprotein derivates containing a photoactivatable cross-linker have to be synthesized. Using UV-light, these derivates could then be covalently attached to their sperm receptor. Subsequently, the cross-linked proteins could be purified and identified via mass spectrometry. However, ZP glycoproteins in quantities over 1 mg would be required for the synthesis, which is out of reach for the established heterologous expression system using HEK293T cells.

The role of cAMP for ZP signaling is also enigmatic. One study analyzing the possible interplay between ZP and cAMP signaling suggested that ZPs stimulate the activity of transmembrane adenylate cyclases (tmACs) (Leclerc & Kopf, 1995). However, the presence of tmACs and their role in mammalian sperm is controversial. The knockout of tmACs does not impair fertility (Iwamoto *et al.*, 2003; Li *et al.*, 2006a; Livera *et al.*, 2005), a well-established tmAC activator does not increase the intracellular cAMP concentration in mouse sperm and human sperm (Brenker *et al.*, 2012; Mukherjee *et al.*, 2016), and total cAMP levels in SACY-deficient sperm are below the detection limit (Xie *et al.*, 2006). Taken together, this rules out a dominant role for tmACs in controlling cAMP levels in the sperm flagellum. In addition, I measured cAMP levels in transgenic sperm expressing a novel FRET-based bio-sensor (Mukherjee *et al.*, 2016); stimulation of sperm with ZPs did not evoke an increase in intracellular cAMP (Fig. 4.3). Therefore, my results suggest that ZPs do not stimulate cAMP synthesis. However, cAMP is unequivocally involved in the ZP-evoked signaling pathway. cAMP orchestrates different aspects of sperm function, which makes it difficult to identify its precise function for ZP signaling. For example, cAMP is essential for protein phosphorylation during sperm epididymal maturation and capacitation (Alvau *et al.*, 2016; Baker *et al.*, 2006; Battistone *et al.*, 2014; Varano *et al.*, 2009). Thus, one explanation would be that the phosphorylation primes the NHA1 activation by ZPs. For NHE1 it has been shown that phosphorylation greatly increases carbonic anhydrase II binding (Li *et al.*, 2006b). To scrutinize this hypothesis, the phosphorylation of NHA1 in wildtype and SACY-deficient sperm could be compared.

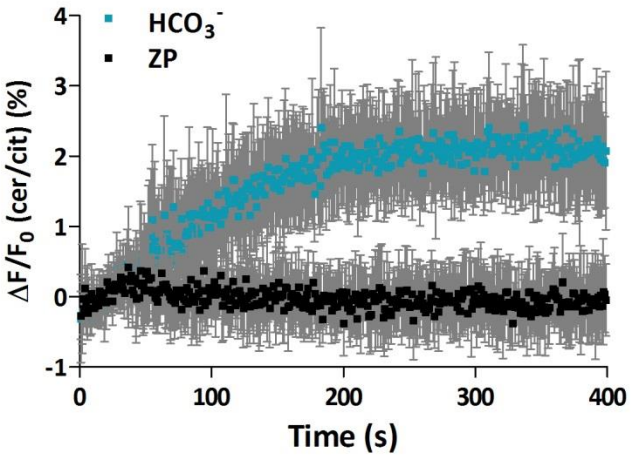

Fig. 4.3: ZPs do not evoke a cAMP increase in mouse sperm

Changes in FRET after stimulation of a mlCNBD-FRET sperm with 0.5 ZP/µl or 25 mM bicarbonate. FRET has been measured using a spectrofluorometer. Data is shown as mean ± SD; n = 3.

Finally, it should be addressed why a polarized V_M is a prerequisite for ZP signaling. One possible explanation might be that the activity of SACY is voltage-dependent. Adenylate cyclases in sea urchin sperm have been shown to be controlled by the V_M (Beltrán *et al.*, 1996). In line with this observation, SACY in mouse sperm might not produce cAMP at a depolarized V_M so that ZP signaling cannot be evoked. To scrutinize this hypothesis, SACY activity should be analyzed at depolarized and polarized V_M. Moreover, one might be able to rescue the loss of ZP signaling in sperm with polarized V_M by preincubation with cAMP.

5 References

Adham, I. M., Nayernia, K.,Engel, W. (1997) "Spermatozoa lacking acrosin protein show delayed fertilization." *Molecular reproduction and development* 46, 370 - 376

Alvau, A., Battistone, M. A., Gervasi, M. G., Navarrete, F. A., Xu, X., Sánchez-Cárdenas, C., De la Vega-Beltran, J. L., Da Ros, V. G., Greer, P. A., Darszon, A., Krapf, D., Salicioni, A. M., Cuasnicu, P. S.,Visconti, P. E. (2016) "The tyrosine kinase FER is responsible for the capacitation-associated increase in tyrosine phosphorylation in murine sperm." *Dev* 143, 2325 - 2333

Arnoult, C., Cardullo, R. A., Lemos, J. R., Florman, H. M. (1996a) "Activation of mouse sperm T-type Ca2+ channels by adhesion to the egg zona pellucida" *Proceedings of the National Academy of Sciences of the United States of America* 93, 13004-13009

Arnoult, C., Cardullo, R. A., Lemos, J. R., Florman, H. M. (1996b) "Activation of mouse sperm T-type Ca2+ channels by adhesion to the egg zona pellucida." *Proc Natl Acad Sci U S A.* 93, 13004 - 13009

Arnoult, C., Kazam, I. G., Visconti, P. E., Kopf, G. S., Villaz, M., Florman, H. M. (1999) "Control of the low voltage-activated calcium channel of mouse sperm by egg ZP3 and by membrane hyperpolarization during capacitation" *Proceedings of the National Academy of Sciences of the United States of America* 96, 6757-6762

Arnoult, C., Zeng, Y.,Florman, H. M. (1996c) "ZP3-dependent activation of sperm cation channels regulates acrosomal secretion during mammalian fertilization" *The Journal of cell biology* 134, 637-645

Avella, M. A., Baibakov, B.,Dean, J. (2014) "A single domain of the ZP2 zona pellucida protein mediates gamete recognition in mice and humans." *The Journal of cell biology* 205, 801 - 809

Avella, M. A.,Dean, J. (2011) "Fertilization with acrosome-reacted mouse sperm: implications for the site of exocytosis." *PNAS* 108, 19843 - 19844

Avenarius, M. R., Hildebrand, M. S., Zhang, Y., Meyer, N. C., Smith, L. L., Kahrizi, K., Najmabadi, H.,Smith, R. J. (2009) "Human male infertility caused by mutations in the CATSPER1 channel protein." *Am J Hum Genet* 84, 505 - 510

Avidan, N., Tamary, H., Dgany, O., Cattan, D., Pariente, A., Thulliez, M.,Beckmann, J. S. (2003) "CATSPER2, a human autosomal nonsyndromic male infertility gene." *Eur J Hum Gen* 11, 497 - 502

Baba, D., Kashiwabara, S., Honda, A., Yamagata, K., Wu, Q., Ikawa, M., Okabe, M.,Baba, T. (2002) "Mouse sperm lacking cell surface hyaluronidase PH-20 can pass through the layer of cumulus cells and fertilize the egg" *J Biol Chem* 277, 30310-30314

Bahat, A., Tur-Kaspa, I., Gakamsky, A., Giojalas, L. C., Breitbart, H.,Eisenbach, M. (2003) "Thermotaxis of mammalian sperm cells: a potential navigation mechanism in the female genital tract." *Nat Med* 9, 49 - 50

Baibakov, B., Boggs, N. A., Yauger, B., Baibakov, G.,Dean, J. (2012) "Human sperm bind to the N-terminal domain of ZP2 in humanized zonae pellucidae in transgenic mice" *The Journal of cell biology* 197, 897-905

Baker, M. A., Hetherington, L.,Aitken, R. J. (2006) "Identification of SRC as a key PKA-stimulated tyrosine kinase involved in the capacitation-associated hyperactivation of murine spermatozoa." *Journal of cell science* 119, 3182 - 3192

Bałakier, H.,Casper, R. F. (1991) "A morphologic study of unfertilized oocytes and abnormal embryos in human in vitro fertilization." *J In Vitro Fert Embryo Transf.* 8, 73 - 79

Baldi, E., Casano, R., Falsetti, C., Krausz, C., Maggi, M.,Forti, G. (1991) "Intracellular calcium accumulation and responsiveness to progesterone in capacitating human spermatozoa" *J Androl* 12, 323-330

Baldi, E., Luconi, M., Muratori, M., Marchiani, S., Tamburrino, L.,Forti, G. (2009) "Nongenomic activation of spermatozoa by steroid hormones: facts and fictions." *Molecular and cellular endocrinology* 308, 39 - 46

Bastiaan, H.,Franken, D. (2007) "The influence of homogenous zona pellucida on human spermatozoa hyperactivation, acrosome reaction and zona binding" *Andrologia* 39, 7-11

Battistone, M. A., Alvau, A., Salicioni, A. M., Visconti, P. E., Da Ros, V. G.,Cuasnicú, P. S. (2014) "Evidence for the involvement of proline-rich tyrosine kinase 2 in tyrosine phosphorylation downstream of protein kinase A activation during human sperm capacitation." *Molecular human reproduction* 20, 1054 - 1066

Bauskin, A. R., Franken, D. R., Eberspaecher, U.,Donner, P. (1999) "Characterization of human zona pellucida glycoproteins" *Molecular human reproduction* 5, 534-540

Bedford, J. M. (1977) "Sperm/egg interaction: the specificity of human spermatozoa" *The Anatomical record* 188, 477-487

Beebe, S. J., Leyton, L., Burks, D., Ishikawa, M., Fuerst, T., Dean, J.,Saling, P. (1992) "Recombinant mouse ZP3 inhibits sperm binding and induces the acrosome reaction" *Developmental biology* 151, 48-54

Beltrán, C., Zapata, O.,Darszon, A. (1996) "Membrane potential regulates sea urchin sperm adenylylcyclase." *Biochem* 35, 7591 - 7598

Berger, T. K., Fußhöller, D. M., Goodwin, N., Bönigk, W., Müller, A., Khesroshahi, N. D., Brenker, C., Wachten, D., Krause, E., Kaupp, U. B.,Strünker, T. (2016) "Posttranslational cleavage of Hv1 in human sperm tunes pH- and voltage-dependent gating." *The Journal of physiology*

Bertrand, B., Wakabayashi, S., Ikeda, T., Pouysségur, J.,Shigekawa, M. (1994) "The Na+/H+ exchanger isoform 1 (NHE1) is a novel member of the calmodulin-binding proteins. Identification and characterization of calmodulin-binding sites.

Bertrand B1, Wakabayashi S, Ikeda T, Pouysségur J, Shigekawa M." *The Journal of biological chemistry* 269, 13703 - 13709

Bertrand, E., Van den Bergh, M.,Englert, Y. (1995) "Does zona pellucida thickness influence the fertilization rate?" *Human reproduction (Oxford, England)* 10, 1189 - 1192

Bianchi, E., Doe, B., Goulding, D.,Wright, G. J. (2014) "Juno is the egg Izumo receptor and is essential for mammalian fertilization." *Nature* 508, 483 - 487

Birnboim, H.,Doly, J. (1979) "A rapid alkaline extraction procedure for screening recombinant plasmid DNA." *Nucleic Acids Res.* 7, 1513 - 1523

Bleil, J. D., Greve, J. M.,Wassarman, P. M. (1988) "Identification of a secondary sperm receptor in the mouse egg zona pellucida: role in maintenance of binding of acrosome-reacted sperm to eggs" *Developmental biology* 128, 376-385

Bleil, J. D.,Wassarman, P. M. (1980) "Mammalian sperm-egg interaction: identification of a glycoprotein in mouse egg zonae pellucidae possessing receptor activity for sperm" *Cell* 20, 873-882

Bleil, J. D.,Wassarman, P. M. (1983) "Sperm-egg interactions in the mouse: sequence of events and induction of the acrosome reaction by a zona pellucida glycoprotein" *Developmental biology* 95, 317-324

Bleil, J. D.,Wassarman, P. M. (1990) "Identification of a ZP3-binding protein on acrosome-intact mouse sperm by photoaffinity crosslinking" *Proceedings of the National Academy of Sciences of the United States of America* 87, 5563-5567

Boerke, A., Tsai, P. S., Garcia-Gil, N., Brewis, I. A.,Gadella, B. M. (2008) "Capacitation-dependent reorganization of microdomains in the apical sperm head plasma membrane: functional relationship with zona binding and the zona-induced acrosome reaction." *Theriogenology* 70, 1188 - 1196

Boussif, O., Lezoualc'h, F., Zanta, M. A., Mergny, M. D., Scherman, D., Demeneix, B.,Behr, J. P. (1995) "A versatile vector for gene and oligonucleotide transfer into cells in culture and in vivo: polyethylenimine." *Proc Natl Acad Sci U S A.* 92, 7297 - 7301

Braden, A. W., Austin, C. R.,David, H. A. (1954) "The reaction of zona pellucida to sperm penetration." *Aust J Biol Sci.* 7, 391 - 409

Bray, C., Son, J. H., Kumar, P., Harris, J. D.,Meizel, S. (2002) "A role for the human sperm glycine receptor/Cl(-) channel in the acrosome reaction initiated by recombinant ZP3." *Biology of reproduction* 66, 91 - 97

Brenker, C., Goodwin, N., Weyand, I., Kashikar, N. D., Naruse, M., Krahling, M., Muller, A., Kaupp, U. B.,Strunker, T. (2012) "The CatSper channel: a polymodal chemosensor in human sperm" *The EMBO journal* 31, 1654-1665

Brenker, C., Zhou, Y., Müller, A., Echeverry, F. A., Trötschel, C., Poetsch, A., Xia, X. M., Bönigk, W., Lingle, C. J., Kaupp, U. B.,Strünker, T. (2014) "The Ca2+-activated K+ current of human sperm is mediated by Slo3." *Elife* 3, e01438

Brewis, I. A., Clayton, R., Barratt, C. L., Hornby, D. P.,Moore, H. D. (1996a) "Recombinant human zona pellucida glycoprotein 3 induces calcium influx and acrosome reaction in human spermatozoa" *Molecular human reproduction* 2, 583-589

Brewis, I. A., Clayton, R., Barratt, C. L., Hornby, D. P.,Moore, H. D. (1996b) "Recombinant human zona pellucida glycoprotein 3 induces calcium influx and acrosome reaction in human spermatozoa." *Molecular human reproduction* 2, 583-589

Brown, S. G., Publicover, S. J., Mansell, S. A., Lishko, P. V., Williams, H. L., Ramalingam, M., Wilson, S. M., Barratt, C. L., Sutton, K. A.,Da Silva, S. M. (2016) "Depolarization of sperm membrane potential is a common feature of men with subfertility and is associated with low fertilization rate at IVF." *Human reproduction (Oxford, England)* 31, 1147 - 1157

Buck, J., Sinclair, M. L., Schapal, L., Cann, M. J.,Levin, L. R. (1999) "Cytosolic adenylyl cyclase defines a unique signaling molecule in mammals." *PNAS* 96, 79 - 84

Burkart, A. D., Xiong, B., Baibakov, B., Jimenez-Movilla, M.,Dean, J. (2012) "Ovastacin, a cortical granule protease, cleaves ZP2 in the zona pellucida to prevent polyspermy" *The Journal of cell biology* 197, 37-44

Callebaut, I., Mornon, J. P.,Monget, P. (2007) "Isolated ZP-N domains constitute the N-terminal extensions of Zona Pellucida proteins" *Bioinformatics (Oxford, England)* 23, 1871-1874

Carlson, A. E., Quill, T. A., Westenbroek, R. E., Schuh, S. M., Hille, B.,Babcock, D. F. (2005) "Identical phenotypes of CatSper1 and CatSper2 null sperm" *The Journal of biological chemistry* 280, 32238-32244

Carlson, A. E., Westenbroek, R. E., Quill, T., Ren, D., Clapham, D. E., Hille, B., Garbers, D. L.,Babcock, D. F. (2003) "CatSper1 required for evoked Ca2+ entry and control of flagellar function in sperm" *Proceedings of the National Academy of Sciences of the United States of America* 100, 14864-14868

Catterall, W. A. (2000) "Structure and regulation of voltage-gated Ca2+ channels." *Annu Rev Cell Dev Biol* 16, 521 - 555

Chakravarty, S., Kadunganattil, S., Bansal, P., Sharma, R. K.,Gupta, S. K. (2008) "Relevance of glycosylation of human zona pellucida glycoproteins for their binding to capacitated human spermatozoa and subsequent induction of acrosomal exocytosis" *Molecular reproduction and development* 75, 75-88

Chang, H.,Suarez, S. S. (2012) "Unexpected flagellar movement patterns and epithelial binding behavior of mouse sperm in the oviduct." *Biology of reproduction* 86, 1-7

Chang, M.,Pincus, G. (1951) "Physiology of fertilization in mammals." *Physiol Rev* 31

Chávez, J. C., Ferreira, J. J., Butler, A., De La Vega Beltrán, J. L., Treviño, C. L., Darszon, A., Salkoff, L.,Santi, C. M. (2014) "SLO3 K+ channels control calcium entry through CATSPER channels in sperm." *The Journal of biological chemistry* 289, 32266 - 32275

Chávez, J. C., Hernández-González, E. O., Wertheimer, E., Visconti, P. E., Darszon, A.,Treviño, C. L. (2012) "Participation of the Cl-/HCO(3)- exchangers SLC26A3 and SLC26A6, the Cl- channel CFTR, and the regulatory factor SLC9A3R1 in mouse sperm capacitation." *Biology of reproduction* 86, 1 - 14

Chen, H., Rossier, C., Morris, M. A., Scott, H. S., Gos, A., Bairoch, A.,Antonarakis, S. E. (1999) "A testis-specific gene, TPTE, encodes a putative transmembrane tyrosine phosphatase and maps to the pericentromeric region of human chromosomes 21 and 13, and to chromosomes 15, 22, and Y." *Hum Genet* 105, 399 - 409

Chen, S. R., Chen, M., Deng, S. L., Hao, X. X., Wang, X. X.,Liu, Y. X. (2016) "Sodium-hydrogen exchanger NHA1 and NHA2 control sperm motility and male fertility." *Cell Death Dis.* 24, e2152

Cheng, A., Le, T., Palacios, M., Bookbinder, L. H., Wassarman, P. M., Suzuki, F.,Bleil, J. D. (1994) "Sperm-egg recognition in the mouse: characterization of sp56, a sperm protein having specific affinity for ZP3." *The Journal of cell biology* 125, 867 - 878

Cheng, Y., Zhon, Z.,Latham, K. (2012) "Strain-specific spontaneous activation during mouse oocyte maturation" *Feril Steril.* 98, 200 - 206

Chiu, P. C., Wong, B. S., Chung, M. K., Lam, K. K., Pang, R. T., Lee, K. F., Sumitro, S. B., Gupta, S. K.,Yeung, W. S. (2008a) "Effects of native human zona pellucida glycoproteins 3 and 4 on acrosome reaction and zona pellucida binding of human spermatozoa." *Biology of reproduction* 79, 869 - 877

Chiu, P. C., Wong, B. S., Lee, C. L., Lam, K. K., Chung, M. K., Lee, K. F., Koistinen, R., Koistinen, H., Gupta, S. K., Seppala, M.,Yeung, W. S. (2010) "Zona pellucida-induced acrosome reaction in human spermatozoa is potentiated by glycodelin-A via down-regulation of extracellular signal-regulated kinases and up-regulation of zona pellucida-induced calcium influx" *Human reproduction (Oxford, England)* 25, 2721-2733

Chiu, P. C., Wong, B. S., Lee, C. L., Pang, R. T., Lee, K. F., Sumitro, S. B., Gupta, S. K.,Yeung, W. S. (2008b) "Native human zona pellucida glycoproteins: purification and binding properties" *Human reproduction (Oxford, England)* 23, 1385-1393

Chung, J. J., Miki, K., Kim, D., Shim, S. H., Shi, H. F., Hwang, J. Y., Cai, X., Iseri, Y., Zhuang, X.,Clapham, D. E. (2017) "CatSperζ regulates the structural continuity of sperm Ca2+ signaling domains and is required for normal fertility." *Elife* e23082

Chung, J. J., Navarro, B., Krapivinsky, G., Krapivinsky, L.,Clapham, D. E. (2011) "A novel gene required for male fertility and functional CATSPER channel formation in spermatozoa" *Nature communications* 2, 153

Chung, J. J., Shim, S. H., Everley, R. A., Gygi, S. P., Zhuang, X.,Clapham, D. E. (2014) "Structurally distinct Ca(2+) signaling domains of sperm flagella orchestrate tyrosine phosphorylation and motility." *Cell* 157, 808 - 822

Dacheux, J. L.,Dacheux, F. (2013) "New insights into epididymal function in relation to sperm maturation." *Reproduction (Cambridge, England)* 147, 27-42

De La Vega-Beltran, J. L., Sánchez-Cárdenas, C., Krapf, D., Hernandez-González, E. O., Wertheimer, E., Treviño, C. L., Visconti, P. E.,Darszon, A. (2012) "Mouse sperm membrane potential hyperpolarization is necessary and sufficient to prepare sperm for the acrosome reaction." *The Journal of biological chemistry* 287, 44384 - 44393

Dell, A., Chalabi, S., Easton, R. L., Haslam, S. M., Sutton-Smith, M., Patankar, M. S., Lattanzio, F., Panico, M., Morris, H. R.,Clark, G. F. (2003) "Murine and human zona pellucida 3 derived from mouse eggs express identical O-glycans." *PNAS* 100, 15631 - 15636

Dell, A., Morris, H. R., Easton, R. L., Patankar, M.,Clark, G. F. (1999) "The glycobiology of gametes and fertilization" *Biochimica et biophysica acta* 1473, 196-205

Demarco, I. A., Espinosa, F., Edwards, J., Sosnik, J., De La Vega-Beltran, J. L., Hockensmith, J. W., Kopf, G. S., Darszon, A.,Visconti, P. E. (2003) "Involvement of a Na+/HCO-3 cotransporter in mouse sperm capacitation.

Demarco IA1, Espinosa F, Edwards J, Sosnik J, De La Vega-Beltran JL, Hockensmith JW, Kopf GS, Darszon A, Visconti P" *The Journal of biological chemistry* 278, 7001 - 7009

Demott, R. P.,Suarez, S. S. (1992) "Hyperactivated sperm progress in the mouse oviduct." *Biology of reproduction* 46, 779 - 785

Denker, S. P., Huang, D. C., Orlowski, J., Furthmayr, H.,Barber, D. L. (2000) "Direct binding of the Na--H exchanger NHE1 to ERM proteins regulates the cortical cytoskeleton and cell shape independently of H(+) translocation." *Mol Cell* 6, 1425 - 1436

Ensslin, M. A.,Shur, B. D. (2003) "Identification of mouse sperm SED1, a bimotif EGF repeat and discoidin-domain protein involved in sperm-egg binding" *Cell* 114, 405-417

Epifano, O., Liang, L. F., Familari, M., Moos, M. C.,Dean, J. (1995) "Coordinate expression of the three zona pellucida genes during mouse oogenesis." *Dev* 121, 1947 - 1956

Esposito, G., Jaiswal, B. S., Xie, F., Krajnc-Franken, M. A., Robben, T. J., Strik, A. M., Kuil, C., Philipsen, R. L., van Duin, M., Conti, M.,Gossen, J. A. (2004) "Mice deficient for soluble adenylyl cyclase are infertile because of a severe sperm-motility defect." *Proc Natl Acad Sci U S A.* 101, 2993 - 2998

Ficarro, S., Chertihin, O., Westbrook, V. A., White, F., Jayes, F., Kalab, P., Marto, J. A., Shabanowitz, J., Herr, J. C., Hunt, D. F.,Visconti, P. E. (2003) "Phosphoproteome analysis of capacitated human sperm. Evidence of tyrosine phosphorylation of a kinase-anchoring protein 3 and valosin-containing protein/p97 during capacitation." *The Journal of biological chemistry* 278, 11579 - 11589

Flesch, F. M., Brouwers, J. F., Nievelstein, P. F., Verkleij, A. J., van Golde, L. M., Colenbrander, B.,Gadella, B. M. (2001) "Bicarbonate stimulated phospholipid scrambling induces cholesterol redistribution and enables cholesterol depletion in the sperm plasma membrane." *Journal of cell science* 114

Florman, H. M. (1994) "Sequential focal and global elevations of sperm intracellular Ca2+ are initiated by the zona pellucida during acrosomal exocytosis" *Developmental biology* 165, 152-164

Florman, H. M., Arnoult, C., G., K., C., L.,C.B., O. T. (1999) "An Intimate Biochemistry: Egg-Regulated Acrosome Reactions of Mammalian Sperm" *Advances in Developmental Biochemistry* 5, 199-233

Florman, H. M., Tombes, R. M., First, N. L.,Babcock, D. F. (1989) "An adhesion-associated agonist from the zona pellucida activates G protein-promoted elevations of internal Ca2+ and pH that mediate mammalian sperm acrosomal exocytosis" *Dev Biol* 135, 133-146

Fukami, K., Yoshida, M., Inoue, T., Kurokawa, M., Fissore, R. A., Yoshida, N., Mikoshiba, K.,Takenawa, T. (2003) "Phospholipase Cdelta4 is required for Ca2+ mobilization essential for acrosome reaction in sperm." *The Journal of cell biology* 161, 79 - 88

Gadella, B. M.,Harrison, R. A. (2000) "The capacitating agent bicarbonate induces protein kinase A-dependent changes in phospholipid transbilayer behavior in the sperm plasma membrane." *Dev* 127, 2407 - 2420

Ganguly, A., Bukovsky, A., Sharma, R. K., Bansal, P., Bhandari, B.,Gupta, S. K. (2010) "In humans, zona pellucida glycoprotein-1 binds to spermatozoa and induces acrosomal exocytosis." *Human reproduction (Oxford, England)* 25, 1643 - 1656

Garcia, M. A.,Meizel, S. (1999) "Regulation of intracellular pH in capacitated human spermatozoa by a Na^+/H^+ exchanger" *Molecular reproduction and development* 52, 189-195

Goudet, G., Mugnier, S., Callebaut, I.,Monget, P. (2008) "Phylogenetic analysis and identification of pseudogenes reveal a progressive loss of zona pellucida genes during evolution of vertebrates." *Biology of reproduction* 78, 796 - 806

Green, D. P. (1997) "Three-dimensional structure of the zona pellucida" *Rev Reprod* 2, 147-156

Griffin, J., Emery, B. R., Huang, I., Peterson, C. M.,Carrell, D. T. (2006) "Comparative analysis of follicle morphology and oocyte diameter in four mammalian species (mouse, hamster, pig, and human)." *J Exp Clin Assist Reprod* 3

Grynkiewicz, G., Poenie, M.,Tsien, R. Y. (1985) "A new generation of Ca^{2+} indicators with greatly improved fluorescence properties" *The Journal of biological chemistry* 260, 3440-3450

Gupta, S. K. (2015) "Role of zona pellucida glycoproteins during fertilization in humans." *J Reprod Immunol.* 108, 90 - 97

Gupta, S. K.,Bhandari, B. (2011) "Acrosome reaction: relevance of zona pellucida glycoproteins" *Asian journal of andrology* 13, 97-105

Hanada, A.,Chang, M. C. (1978) "Penetration of the zona-free or intact eggs by foreign spermatozoa and the fertilization of deer mouse eggs in vitro." *J Exp Zool.* 203, 277 - 285

Harper, C. V., Kirkman-Brown, J. C., Barratt, C. L.,Publicover, S. J. (2003) "Encoding of progesterone stimulus intensity by intracellular [Ca2+] ([Ca2+]i) in human spermatozoa." *The Biochemical journal* 372, 407 - 417

Harrison, R. A. (2003) "Cyclic AMP signalling during mammalian sperm capacitation--still largely terra incognita" *Reprod Domest Anim.* 38, 102 - 110

Hess, K. C., Jones, B. H., Marquez, B., Chen, Y., Ord, T. S., Kamenetsky, M., Miyamoto, C., Zippin, J. H., Kopf, G. S., Suarez, S. S., Levin, L. R., Williams, C. J., Buck, J.,Moss, S. B. (2005) "The "soluble" adenylyl cyclase in sperm mediates multiple signaling events required for fertilization." *Dev Cell.* 9, 249 - 259

Holappa, K., Mustonen, M., Parvinen, M., Vihko, P., Rajaniemi, H.,Kellokumpu, S. (1999) "Primary structure of a sperm cell anion exchanger and its messenger ribonucleic acid expression during spermatogenesis." *Biology of reproduction* 61, 981 - 986

Hong, L., Pathak, M. M., Kim, I. H., Ta, D.,Tombola, F. (2013) "Voltage-sensing domain of voltage-gated proton channel Hv1 shares mechanism of block with pore domains" *Neuron* 77, 274 - 287

Huang, H. L., Lv, C., Zhao, Y. C., Li, W., He, X. M., Li, P., Sha, A. G., Tian, X., Papasian, C. J., Deng, H. W., Lu, G. X.,Xiao, H. M. (2014) "Mutant ZP1 in familial infertility." *N Engl J Med* 370, 1220 - 1226

Huang, Z.,Wells, D. (2010) "The human oocyte and cumulus cells relationship: new insights from the cumulus cell transcriptome" *Molecular human reproduction* 16, 715-725

Inoue, N., Ikawa, M., Isotani, A.,Okabe, M. (2005) "The immunoglobulin superfamily protein Izumo is required for sperm to fuse with eggs." *Nature* 434, 234 - 238

Inoue, N., Satouh, Y., Ikawa, M., Okabe, M.,Yanagimachi, R. (2011) "Acrosome-reacted mouse spermatozoa recovered from the perivitelline space can fertilize other eggs." *PNAS* 108, 20008 - 20011

Ishijima, S. (2011) "Dynamics of flagellar force generated by a hyperactivated spermatozoon." *Reprod* 142, 409 - 415

Ishikawa, Y., Usui, T., Yamashita, M., Kanemori, Y.,Baba, T. (2016) "Surfing and Swimming of Ejaculated Sperm in the Mouse Oviduct." *Biology of reproduction* 94, 89

Iwamoto, T., Okumura, S., Iwatsubo, K., Kawabe, J., Ohtsu, K., Sakai, I., Hashimoto, Y., Izumitani, A., Sango, K., Ajiki, K., Toya, Y., Umemura, S., Goshima, Y., Arai, N., Vatner, S. F.,Ishikawa, Y. (2003) "Motor dysfunction in type 5 adenylyl cyclase-null mice." *The Journal of biological chemistry* 278, 16936 - 16940

Jansen, V., Alvarez, L., Balbach, M., Strünker, T., Hegemann, P., Kaupp, U. B.,Wachten, D. (2015) "Controlling fertilization and cAMP signaling in sperm by optogenetics." *Elife* 4

Jiménez-Movilla, M., Avilés, M., Gómez-Torres, M. J., Fernández-Colom, P. J., Castells, M. T., de Juan, J., Romeu, A.,Ballesta, J. (2004) "Carbohydrate analysis of the zona pellucida and cortical granules of human oocytes by means of ultrastructural cytochemistry." *Human reproduction (Oxford, England)* 19, 1842 - 1855

Jin, J., Jin, N., Zheng, H., Ro, S., Tafolla, D., Sanders, K. M.,Yan, W. (2007) "Catsper3 and Catsper4 are essential for sperm hyperactivated motility and male fertility in the mouse." *Biology of reproduction* 77, 37 - 44

Jin, M., Fujiwara, E., Kakiuchi, Y., Okabe, M., Satouh, Y., Baba, S. A., Chiba, K.,Hirohashi, N. (2011) "Most fertilizing mouse spermatozoa begin their acrosome reaction before contact with the zona pellucida during in vitro fertilization." *PNAS* 108, 4892 - 4896

Johnson, K. A. (1986) "Rapid kinetic analysis of mechanochemical adenosinetriphosphatases" *Methods in enzymology* 134, 677-705

Jovine, L., Darie, C. C., Litscher, E. S.,Wassarman, P. M. (2005) "Zona pellucida domain proteins" *Annu Rev Biochem* 74, 83-114

Jovine, L., Qi, H., Williams, Z., Litscher, E.,Wassarman, P. M. (2002) "The ZP domain is a conserved module for polymerization of extracellular proteins" *Nature cell biology* 4, 457-461

Jungnickel, M. K., Marrero, H., Birnbaumer, L., Lémos, J. R.,Florman, H. M. (2001) "Trp2 regulates entry of Ca^{2+} into mouse sperm triggered by egg ZP3." *Nature cell biology* 3, 499 - 502

Jungnickel, M. K., Sutton, K. A., Wang, Y.,Florman, H. M. (2007) "Phosphoinositide-dependent pathways in mouse sperm are regulated by egg ZP3 and drive the acrosome reaction." *Developmental biology* 304, 116 - 126

Kantsler, V., Dunkel, J., Blayney, M.,Goldstein, R. E. (2014) "Rheotaxis facilitates upstream navigation of mammalian sperm cells." *Elife* 3

Kaupp, U. B., Kashikar, N. D.,Weyand, I. (2008) "Mechanisms of sperm chemotaxis." *Annu Rev Biochem* 70, 93 - 117

Kawano, N., Kang, W., Yamashita, M., Koga, Y., Yamazaki, T., Hata, T., Miyado, K.,Baba, T. (2010) "Mice lacking two sperm serine proteases, ACR and PRSS21, are subfertile, but the mutant sperm are infertile in vitro." *Biology of reproduction* 83, 359 - 369

Kiefer, S. M.,Saling, P. (2002) "Proteolytic processing of human zona pellucida proteins." *Biology of reproduction* 66, 407 - 414

Kimura, M., Kim, E., Kang, W., Yamashita, M., Saigo, M., Yamazaki, T., Nakanishi, T., Kashiwabara, S.,Baba, T. (2009) "Functional roles of mouse sperm hyaluronidases, HYAL5 and SPAM1, in fertilization." *Biology of reproduction* 81, 939 - 947

Kirichok, Y., Navarro, B.,Clapham, D. E. (2006) "Whole-cell patch-clamp measurements of spermatozoa reveal an alkaline-activated Ca2+ channel" *Nature* 439, 737-740

La Spina, F. A., Puga Molina, L. C., Romarowski, A., Vitale, A. M., Falzone, T. L., Krapf, D., Hirohashi, N.,Buffone, M. G. (2016) "Mouse sperm begin to undergo acrosomal exocytosis in the upper isthmus of the oviduct." *Developmental biology* 411, 172 - 182

Laemmli, U. K. (1970) "Cleavage of structural proteins during the assembly of the head of bacteriophage T4." *Nature* 227, 680 - 685

Larsen, R. D., Rivera-Marrero, C. A., Ernst, L. K., Cummings, R. D.,Lowe, J. B. (1990) "Frameshift and nonsense mutations in a human genomic sequence homologous to a murine UDP-Gal:beta-D-Gal(1,4)-D-GlcNAc alpha(1,3)-galactosyltransferase cDNA." *The Journal of biological chemistry* 265, 7055-7061

Leclerc, P.,Kopf, G. S. (1995) "Mouse sperm adenylyl cyclase: general properties and regulation by the zona pellucida." *Biol Reprod.* 52, 1227 - 1233

Lee, S. Y., Letts, J. A.,R., M. (2008) "Dimeric subunit stoichiometry of the human voltage-dependent proton channel Hv1." *Proc Natl Acad Sci U S A.* 105, 7692 - 7695

Lefievre, L., Conner, S. J., Salpekar, A., Olufowobi, O., Ashton, P., Pavlovic, B., Lenton, W., Afnan, M., Brewis, I. A., Monk, M., Hughes, D. C.,Barratt, C. L. (2004) "Four zona pellucida glycoproteins are expressed in the human" *Human reproduction (Oxford, England)* 19, 1580-1586

Li, S., Lee, M. L., Bruchas, M. R., Chan, G. C., Storm, D. R.,Chavkin, C. (2006a) "Calmodulin-stimulated adenylyl cyclase gene deletion affects morphine responses." *Mol Pharmacol* 70, 1742 - 1749

Li, X., Liu, Y., Alvarez, B. V., Casey, J. R.,Fliegel, L. (2006b) "A novel carbonic anhydrase II binding site regulates NHE1 activity." *Biochemistry* 45, 2414 - 2424

Lin, Y. N., Roy, A., Yan, W., Burns, K. H.,Matzuk, M. M. (2007) "Loss of zona pellucida binding proteins in the acrosomal matrix disrupts acrosome biogenesis and sperm morphogenesis." *Mol Cell Biol* 27, 6794 - 6805

Lishko, P. V., Botchkina, I. L., Fedorenko, A.,Kirichok, Y. (2010) "Acid extrusion from human spermatozoa is mediated by flagellar voltage-gated proton channel." *Cell* 140, 327 - 337

Lishko, P. V., Botchkina, I. L.,Kirichok, Y. (2011) "Progesterone activates the principal Ca2+ channel of human sperm" *Nature* 471, 387-391

Lishko, P. V.,Kirichok, Y. (2010) "The role of Hv1 and CatSper channels in sperm activation" *The Journal of physiology* 588, 4667-4672

Litscher, E. S., Qi, H.,Wassarman, P. M. (1999) "Mouse zona pellucida glycoproteins mZP2 and mZP3 undergo carboxy-terminal proteolytic processing in growing oocytes." *Biochemistry* 38, 12880 - 12887

Liu, C., Litscher, E. S., Mortillo, S., Sakai, Y., Kinloch, R. A., Stewart, C. L.,Wassarman, P. M. (1996) "Targeted disruption of the mZP3 gene results in production of eggs lacking a zona pellucida and infertility in female mice" *Proceedings of the National Academy of Sciences of the United States of America* 93, 5431-5436

Liu, D. Y., Liu, M. L., Clarke, G. N.,Baker, H. W. (2007a) "Hyperactivation of capacitated human sperm correlates with the zona pellucida-induced acrosome reaction of zona pellucida-bound sperm" *Human reproduction (Oxford, England)* 22, 2632-2638

Liu, J., Xia, J., Cho, K. H., Clapham, D. E.,Ren, D. (2007b) "CatSperbeta, a novel transmembrane protein in the CatSper channel complex" *The Journal of biological chemistry* 282, 18945-18952

Liu, T., Huang, J. C., Zuo, W. L., Lu, C. L., Chen, M., Zhang, X. S., Li, Y. C., Cai, H., Zhou, W. L., Hu, Z. Y., Gao, F.,Liu, Y. X. (2010) "A novel testis-specific Na+/H+ exchanger is involved in sperm motility and fertility." *Front Biosci (Elite Ed).* 2, 566 - 581

Livera, G., Xie, F., Garcia, M. A., Jaiswal, B., Chen, J., Law, E., Storm, D. R.,Conti, M. (2005) "Inactivation of the mouse adenylyl cyclase 3 gene disrupts male fertility and spermatozoon function." *Mol Endrocrinol* 19, 1277 - 1290

Lu, Q.,Shur, B. D. (1997) "Sperm from beta 1,4-galactosyltransferase-null mice are refractory to ZP3-induced acrosome reactions and penetrate the zona pellucida poorly" *Development (Cambridge, England)* 124, 4121-4131

Lybaert, P., Danguy, A., Leleux, F., Meuris, S.,Lebrun, P. (2009) "Improved methodology for the detection and quantification of the acrosome reaction in mouse spermatozoa." *Histol Histopathol.* 24, 999 - 1007

Mahaut-Smith, M. P. (1989) "The effect of zinc on calcium and hydrogen ion currents in intact snail neurones." *J Exp biol.* 145, 455 - 464

Maldera, J. A., Weigel Muñoz, M., Chirinos, M., Busso, D., G E Raffo, F., Battistone, M. A., Blaquier, J. A., Larrea, F.,Cuasnicu, P. S. (2014) "Human fertilization: epididymal hCRISP1 mediates sperm-zona pellucida binding through its interaction with ZP3." *Molecular human reproduction* 20, 341 - 349

Mannowetz, N., Naidoo, N. M., Choo, S. A., Smith, J. F.,Lishko, P. V. (2013) "Slo1 is the principal potassium channel of human spermatozoa." *Elife* 2

Mbizvo, M. T., Burkman, L. J.,Alexander, N. J. (1990) "Human follicular fluid stimulates hyperactivated motility in human sperm." *Feril Steril.* 54, 708 - 712

Miki, K.,Clapham, D. E. (2013) "Rheotaxis guides mammalian sperm." *Current biology : CB* 23, 443 - 452

Miller, M. R., Mannowetz, N., Iavarone, A. T., Safavi, R., Gracheva, E. O., Smith, J. F., Hill, R. Z., Bautista, D. M., Kirichok, Y.,Lishko, P. V. (2016) "Unconventional endocannabinoid signaling governs sperm activation via the sex hormone progesterone." *Science (New York, N.Y.)* 352, 555 - 559

Minta, A., Kao, J. P.,Tsien, R. Y. (1989) "Fluorescent indicators for cytosolic calcium based on rhodamine and fluorescein chromophores" *The Journal of biological chemistry* 264, 8171-8178

Miyata, H., Satouh, Y., Mashiko, D., Muto, M., Nozawa, K., Shiba, K., Fujihara, Y., Isotani, A., Inaba, K.,Ikawa, M. (2015) "Sperm calcineurin inhibition prevents mouse fertility with implications for male contraceptive." *Sciene* 350, 442 - 445

Moller, C. C.,Wassarman, P. M. (1989) "Characterization of a proteinase that cleaves zona pellucida glycoprotein ZP2 following activation of mouse eggs." *Developmental biology* 132, 103 - 112

Morales, P., Cross, N. L., Overstreet, J. W.,Hanson, F. W. (1989) "Acrosome intact and acrosome-reacted human sperm can initiate binding to the zona pellucida." *Developmental biology* 133, 385 - 392

Morales, P., Overstreet, J. W.,Katz, D. F. (1988) "Changes in human sperm motion during capacitation in vitro" *Journal of reproduction and fertility* 83, 119-128

Mukherjee, S., Jansen, V., Jikeli, J. F., Hamzeh, H., Alvarez, L., Dombrowski, M., Balbach, M., Strünker, T., Seifert, R., Kaupp, U. B.,Wachten, D. (2016) "A novel biosensor to study cAMP dynamics in cilia and flagella." *Elife* 5, e14052

Mullis, K., Faloona, F., Scharf, S., Saiki, R., Horn, G.,Erlich, H. (1986) "Specific enzymatic amplification of DNA in vitro: the polymerase chain reaction." *Cold Spring Harb Symp Quant Biol.* 51, 263 - 273

Navarro, B., Kirichok, Y., Chung, J. J.,Clapham, D. E. (2008) "Ion channels that control fertility in mammalian spermatozoa" *The International journal of developmental biology* 52, 607-613

Navarro, B., Kirichok, Y.,Clapham, D. E. (2007) "KSper, a pH-sensitive K+ current that controls sperm membrane potential" *Proceedings of the National Academy of Sciences of the United States of America* 104, 7688-7692

Nixon, B.,Aitken, R. J. (2009) "The biological significance of detergent-resistant membranes in spermatozoa" *Journal of reproductive immunology* 83, 8-13

Nolan, M. A., Babcock, D. F., Wennemuth, G., Brown, W., Burton, K. A.,McKnight, G. S. (2004) "Sperm-specific protein kinase A catalytic subunit Calpha2 orchestrates cAMP signaling for male fertility." *PNAS* 101, 13483 - 13488

O'Toole, C. M., Arnoult, C., Darszon, A., Steinhardt, R. A.,Florman, H. M. (2000) "Ca(2+) entry through store-operated channels in mouse sperm is initiated by egg ZP3 and drives the acrosome reaction" *Mol Biol Cell* 11, 1571-1584

Okamura, N., Tajima, Y., Soejima, A., Masuda, H.,Sugita, Y. (1985) "Sodium bicarbonate in seminal plasma stimulates the motility of mammalian spermatozoa through direct activation of adenylate cyclase." *The Journal of biological chemistry* 260, 9699 - 9705

Oliveira, R. G., Tomasi, L., Rovasio, R. A.,Giojalas, L. C. (1999) "Increased velocity and induction of chemotactic response in mouse spermatozoa by follicular and oviductal fluids." *Journal of reproduction and fertility* 115, 23 - 27

Oren-Benaroya, R., Orvieto, R., Gakamsky, A., Pinchasov, M.,Eisenbach, M. (2008) "The sperm chemoattractant secreted from human cumulus cells is progesterone." *Human reproduction (Oxford, England)* 23, 2339 - 2345

Osheroff, J. E., Visconti, P. E., Valenzuela, J. P., Travis, A. J., Alvarez, J.,Kopf, G. S. (1999) "Regulation of human sperm capacitation by a cholesterol efflux-stimulated signal transduction pathway leading to protein kinase A-mediated up-regulation of protein tyrosine phosphorylation." *Molecular human reproduction* 5, 1017 - 1026

Pacey, A. A., Davies, N., Warren, M. A., Barratt, C. L.,Cooke, I. D. (1995) "Hyperactivation may assist human spermatozoa to detach from intimate association with the endosalpinx." *Human reproduction (Oxford, England)* 10, 2603 - 2609

Pang, P. C., Chiu, P. C., Lee, C. L., Chang, L. Y., Panico, M., Morris, H. R., Haslam, S. M., Khoo, K. H., Clark, G. F., Yeung, W. S.,Dell, A. (2011) "Human sperm binding is mediated by the sialyl-Lewis(x) oligosaccharide on the zona pellucida" *Science (New York, N.Y.)* 333, 1761-1764

Parkkila, S., Rajaniemi, H.,Kellokumpu, S. (1993) "Polarized expression of a band 3-related protein in mammalian sperm cells." *Biology of reproduction* 49, 326 - 331

Patrat, C., Auer, J., Fauque, P., Leandri, R. L., Jouannet, P.,Serres, C. (2006) "Zona pellucida from fertilised human oocytes induces a voltage-dependent calcium influx and the acrosome reaction in spermatozoa, but cannot be penetrated by sperm" *BMC Dev Biol* 6

Pereda, J.,Coppo, M. (1985) "An electron microscopic study of sperm penetration into the human egg investments." *Anat Embryol* 173, 247 - 252

Petit, F. M., Serres, C., Bourgeon, F., Pineau, C.,Auer, J. (2013) "Identification of sperm head proteins involved in zona pellucida binding" *Human reproduction (Oxford, England)* 28, 852-865

Publicover, S., Harper, C. V.,Barratt, C. (2007) "[Ca2+]i signalling in sperm--making the most of what you've got." *Nat Cell Biol.* 9, 235 - 242

Publicover, S. J., Giojalas, L. C., Teves, M. E., de Oliveira, G. S., Garcia, A. A., Barratt, C. L.,Harper, C. V. (2008) "Ca2+ signalling in the control of motility and guidance in mammalian sperm." *Front Biosci.* 1, 5623 - 5637

Qi, H., Moran, M. M., Navarro, B., Chong, J. A., Krapivinsky, G., Krapivinsky, L., Kirichok, Y., Ramsey, I. S., Quill, T. A.,Clapham, D. E. (2007) "All four CatSper ion channel proteins are required for male fertility and sperm cell hyperactivated motility" *Proceedings of the National Academy of Sciences of the United States of America* 104, 1219-1223

Qi, H., Williams, Z.,Wassarman, P. M. (2002) "Secretion and assembly of zona pellucida glycoproteins by growing mouse oocytes microinjected with epitope-tagged cDNAs for mZP2 and mZP3." *Mol Biol Cell* 13, 530 - 541

Qui, F., Chamberlin, A., Noskov, S.,Larsson, H. P. (2015) "Molecular Mechanism of Zinc Inhibition on Voltage-Gated Proton Channel Hv1" *Biophysical Journal* 108, 367

Quill, T. A., Ren, D., Clapham, D. E.,Garbers, D. L. (2001) "A voltage-gated ion channel expressed specifically in spermatozoa" *Proceedings of the National Academy of Sciences of the United States of America* 98, 12527-12531

Quill, T. A., Sugden, S. A., Rossi, K. L., Doolittle, L. K., Hammer, R. E.,Garbers, D. L. (2003) "Hyperactivated sperm motility driven by CatSper2 is required for fertilization." *PNAS* 100, 14869 - 14874

Ralt, D., Manor, M., Cohen-Dayag, A., Tur-Kaspa, I., Ben-Shlomo, I., Makler, A., Yuli, I., Dor, J., Blumberg, S., Mashiach, S.,al., e. (1994) "Chemotaxis and chemokinesis of human spermatozoa to follicular factors." *Biology of reproduction* 50, 774 - 785

Ramsey, I. S., Mokrab, Y., Carvacho, I., Sands, Z. A., Sansom, M. S.,Clapham, D. E. (2010) "An aqueous H+ permeation pathway in the voltage-gated proton channel Hv1." *Nat Struct Mol Biol.* 17, 869 - 875

Ramsey, I. S., Ruchti, E., Kaczmarek, J. S.,Clapham, D. E. (2009) "Hv1 proton channels are required for high-level NADPH oxidase-dependent superoxide production during the phagocyte respiratory burst." *PNAS* 106, 7642-7647

Rankin, T., Familari, M., Lee, E., Ginsberg, A., Dwyer, N., Blanchette-Mackie, J., Drago, J., Westphal, H.,Dean, J. (1996) "Mice homozygous for an insertional mutation in the Zp3 gene lack a zona pellucida and are infertile." *Dev* 122, 2903 - 2910

Rankin, T., Talbot, P., Lee, E.,Dean, J. (1999) "Abnormal zonae pellucidae in mice lacking ZP1 result in early embryonic loss" *Development (Cambridge, England)* 126, 3847-3855

Rankin, T. L., O'Brien, M., Lee, E., Wigglesworth, K., Eppig, J.,Dean, J. (2001) "Defective zonae pellucidae in Zp2-null mice disrupt folliculogenesis, fertility and development" *Development (Cambridge, England)* 128, 1119-1126

Redgrove, K. A., Anderson, A. L., Dun, M. D., McLaughlin, E. A., O'Bryan, M. K., Aitken, R. J.,Nixon, B. (2011) "Involvement of multimeric protein complexes in mediating the capacitation-dependent binding of human spermatozoa to homologous zonae pellucidae." *Developmental biology* 356, 460 - 474

Ren, D., Navarro, B., Perez, G., Jackson, A. C., Hsu, S., Shi, Q., Tilly, J. L.,Clapham, D. E. (2001) "A sperm ion channel required for sperm motility and male fertility" *Nature* 413, 603-609

Rossato, M., Di Virgilio, F., Rizzuto, R., Galeazzi, C.,Foresta, C. (2001) "Intracellular calcium store depletion and acrosome reaction in human spermatozoa: role of calcium and plasma membrane potential." *Molecular human reproduction* 7, 119 - 128

Ruknudin, A.,Silver, I. A. (1990) "Ca2+ uptake during capacitation of mouse spermatozoa and the effect of an anion transport inhibitor on Ca2+ uptake" *Molecular reproduction and development* 26, 63-68

Saling, P. M., Sowinski, J.,Storey, B. T. (1979) "An ultrastructural study of epididymal mouse spermatozoa binding to zonae pellucidae in vitro: sequential relationship to the acrosome reaction." *J Exp Zool.* 209, 229 - 238

Santi, C. M., Martínez-López, P., de la Vega-Beltrán, J. L., Butler, A., Alisio, A., Darszon, A.,Salkoff, L. (2010) "The SLO3 sperm-specific potassium channel plays a vital role in male fertility." *FEBS letters* 584, 1041 - 1046

Sasaki, M., Takagi, M.,Okamura, Y. (2006) "A voltage sensor-domain protein is a voltage-gated proton channel" *Science (New York, N.Y.)* 312, 589-592

Sauerbrun-Cutler, M. T., Vega, M., Breborowicz, A., Gonzales, E., Stein, D., Lederman, M.,Keltz, M. (2015) "Oocyte zona pellucida dysmorphology is associated with diminished in-vitro fertilization success." *J Ovarian Res* 8

Schaefer, M., Hofmann, T., Schultz, G.,Gudermann, T. (1998) "A new prostaglandin E receptor mediates calcium influx and acrosome reaction in human spermatozoa." *Proc Natl Acad Sci U S A.* 95, 3008 - 3013

Schiffer, C., Müller, A., Egeberg, D. L., Alvarez, L., Brenker, C., Rehfeld, A., Frederiksen, H., Wäschle, B., Kaupp, U. B., Balbach, M., Wachten, D., Skakkebaek, N. E., Almstrup, K.,Strünker, T. (2014) "Direct action of endocrine disrupting chemicals on human sperm." *EMBO Rep.* 15, 758 - 765

Schreiber, M., Wei, A., Yuan, A., Gaut, J., Saito, M.,Salkoff, L. (1998) "Slo3, a novel pH-sensitive K+ channel from mammalian spermatocytes." *J Biol Chem.* 273, 3509 - 3516

Shi, X., Amindari, S., Paruchuru, K., Skalla, D., Burkin, H., Shur, B. D.,Miller, D. J. (2001) "Cell surface beta-1,4-galactosyltransferase-I activates G protein-dependent exocytotic signaling." *Development (Cambridge, England)* 128, 645 - 654

Shur, B. D.,Neely, C. A. (1988) "Plasma membrane association, purification, and partial characterization of mouse sperm beta 1,4-galactosyltransferase" *The Journal of biological chemistry* 263, 17706-17714

Soler, C., Yeung, C. H.,Cooper, T. G. (1994) "Development of sperm motility patterns in the murine epididymis." *Int J Androl* 17, 271 - 278

Sonawane, N. D., Szoka, F. C. J.,Verkman, A. S. (2003) "Chloride accumulation and swelling in endosomes enhances DNA transfer by polyamine-DNA polyplexes." *J Biol Chem.* 278, 44826 - 44831

Strünker, T., Goodwin, N., Brenker, C., Kashikar, N. D., Weyand, I., Seifert, R.,Kaupp, U. B. (2011) "The CatSper channel mediates progesterone-induced Ca2+ influx in human sperm" *Nature* 471, 382-386

Sutton, K. A., Jungnickel, M. K., Jovine, L.,Florman, H. M. (2012) "Evolution of the voltage sensor domain of the voltage-sensitive phosphoinositide phosphatase VSP/TPTE suggests a role as a proton channel in eutherian mammals." *Mol Biol Evol* 29, 2147 - 2155

Tamburrino, L., Marchiani, S., Minetti, F., Forti, G., Muratori, M.,Baldi, E. (2014) "The CatSper calcium channel in human sperm: relation with motility and involvement in progesterone-induced acrosome reaction." *Human reproduction (Oxford, England)* 29, 418 - 428

Tamburrino, L., Marchiani, S., Vicini, E., Muciaccia, B., Cambi, M., Pellegrini, S., Forti, G., Muratori, M.,Baldi, E. (2015) "Quantification of CatSper1 expression in human spermatozoa and relation to functional parameters" *Human reproduction (Oxford, England)* 30, 1532 - 1544

Tapparel, C., Reymond, A., Girardet, C., Guillou, L., Lyle, R., Lamon, C., Hutter, P.,Antonarakis, S. E. (2003) "The TPTE gene family: cellular expression, subcellular localization and alternative splicing." *Gene* 323, 189 - 199

Thaler, C. D.,Cardullo, R. A. (1996) "The initial molecular interaction between mouse sperm and the zona pellucida is a complex binding event." *The Journal of biological chemistry* 271, 23289 - 23297

Tombola, F., Ulbrich, M. H.,Isacoff, E. Y. (2008) "The voltage-gated proton channel Hv1 has two pores, each controlled by one voltage sensor." *Neuron* 58, 546 - 556

Toyoda, Y.,Chang, M. C. (1974) "Capacitation of epididymal spermatozoa in a medium with high K-Na ratio and cyclic AMP for the fertilization of rat eggs in vitro." *J Reprod Fertil.* 36, 125 - 134

Tsien, R. Y. (1981) "A non-disruptive technique for loading calcium buffers and indicators into cells" *Nature* 290, 527-528

Tsubamoto, H., Hasegawa, A., Nakata, Y., Naito, S., Yamasaki, N.,Koyama, K. (1999) "Expression of recombinant human zona pellucida protein 2 and its binding capacity to spermatozoa" *Biology of reproduction* 61, 1649-1654

van den Hurk, R.,Zhao, J. (2005) "Formation of mammalian oocytes and their growth, differentiation and maturation within ovarian follicles." *Theriogenology* 63, 1717 - 1751

van Gestel, R. A., Brewis, I. A., Ashton, P. R., Brouwers, J. F.,Gadella, B. M. (2007) "Multiple proteins present in purified porcine sperm apical plasma membranes interact with the zona pellucida of the oocyte" *Molecular human reproduction* 13, 445-454

Van Soom, A., Tanghe, S., De Pauw, I., Maes, D.,de Kruif, A. (2002) "Function of the cumulus oophorus before and during mammalian fertilization" *Reproduction in domestic animals = Zuchthygiene* 37, 144-151

Varano, G., Lombardi, A., Cantini, G., Forti, G., Baldi, E.,Luconi, M. (2009) "Src activation triggers capacitation and acrosome reaction but not motility in human spermatozoa." *Human reproduction (Oxford, England)* 23, 2652 - 2662

Visconti, P. E., Moore, G. D., Bailey, J. L., Leclerc, P., Connors, S. A., Pan, D., Olds-Clarke, P.,Kopf, G. S. (1995) "Capacitation of mouse spermatozoa. II. Protein tyrosine phosphorylation and capacitation are regulated by a cAMP-dependent pathway" *Development* 121, 1139-1150

Visconti, P. E., Ning, X., Fornés, M. W., Alvarez, J. G., Stein, P., Connors, S. A.,Kopf, G. S. (1999) "Cholesterol efflux-mediated signal transduction in mammalian sperm: cholesterol release signals an increase in protein tyrosine phosphorylation during mouse sperm capacitation." *Developmental biology* 214, 429 - 443

Vredenburgh-Wilberg, W. L.,Parrish, J. J. (1995) "Intracellular pH of bovine sperm increases during capacitation" *Molecular reproduction and development* 40, 490-502

Walker, S. M., Downes, C. P.,Leslie, N. R. (2001) "TPIP: a novel phosphoinositide 3-phosphatase." *The Biochemical journal* 360, 277 - 283

Wandernoth, P. M., Raubuch, M., Mannowetz, N., Becker, H. M., Deitmer, J. W., Sly, W. S.,Wennemuth, G. (2010) "Role of carbonic anhydrase IV in the bicarbonate-mediated activation of murine and human sperm." *PloS one* 5, e15061

Wang, D., Hu, J., Bobulescu, I. A., Quill, T. A., McLeroy, P., Moe, O. W.,Garbers, D. L. (2007) "A sperm-specific Na+/H+ exchanger (sNHE) is critical for expression and in vivo bicarbonate regulation of the soluble adenylyl cyclase (sAC)" *Proceedings of the National Academy of Sciences of the United States of America* 104, 9325-9330

Wang, D., King, S. M., Quill, T. A., Doolittle, L. K.,Garbers, D. L. (2003) "A new sperm-specific Na+/H+ exchanger required for sperm motility and fertility" *Nature cell biology* 5, 1117-1122

Wang, H., Liu, J., Cho, K. H.,Ren, D. (2009) "A novel, single, transmembrane protein CATSPERG is associated with CATSPER1 channel protein" *Biology of reproduction* 81, 539-544

Wassarman, P. M. (1988) "Zona pellucida glycoproteins" *Annu Rev Biochem* 57, 415-442

Wassarman, P. M. (2008) "Zona pellucida glycoproteins" *The Journal of biological chemistry* 283, 24285-24289

Wassarman, P. M., Jovine, L.,Litscher, E. S. (2001) "A profile of fertilization in mammals" *Nature cell biology* 3, E59-64

Wassarman, P. M., Liu, C., Chen, J., Qi, H.,Litscher, E. S. (1998) "Ovarian development in mice bearing homozygous or heterozygous null mutations in zona pellucida glycoprotein gene mZP3" *Histol Histopathol* 13, 293-300

Wassarman, P. M.,Mortillo, S. (1991) "Structure of the mouse egg extracellular coat, the zona pellucida" *Int Rev Cytol* 130, 85-110

Williams, Z.,Wassarman, P. M. (2001) "Secretion of mouse ZP3, the sperm receptor, requires cleavage of its polypeptide at a consensus furin cleavage-site." *Biochem* 40, 929 - 937

Wolf, D. P.,Hamada, M. (1977) "Induction of zonal and egg plasma membrane blocks to sperm penetration in mouse eggs with cortical granule exudate." *Biology of reproduction* 17, 350 - 354

Worley, P. F., Baraban, J. M., Supattapone, S., Wilson, V. S.,Snyder, S. H. (1987) "Characterization of inositol trisphosphate receptor binding in brain. Regulation by pH and calcium." *The Journal of biological chemistry* 262, 12132 - 12136

Wuttke, M. S., Buck, J.,Levin, L. R. (2001) "Bicarbonate-regulated soluble adenylyl cyclase." *JOP.* 2, 154 - 158

Xia, J., Reigada, D., Mitchell, C. H.,Ren, D. (2007) "CATSPER channel-mediated Ca2+ entry into mouse sperm triggers a tail-to-head propagation" *Biology of reproduction* 77, 551-559

Xia, J.,Ren, D. (2009) "Egg coat proteins activate calcium entry into mouse sperm via CATSPER channels" *Biology of reproduction* 80, 1092-1098

Xie, F., Garcia, M. A., Carlson, A. E., Schuh, S. M., Babcock, D. F., Jaiswal, B. S., Gossen, J. A., Esposito, G., van Duin, M.,Conti, M. (2006) "Soluble adenylyl cyclase (sAC) is indispensable for sperm function and fertilization." *Developmental biology* 296, 153 - 362

Xu, W. M., Shi, Q. X., Chen, W. Y., Zhou, C. X., Ni, Y., Rowlands, D. K., Yi, G., Zhu, H., Ma, Z. G., Wang, X. F., Chen, Z. H., Zhou, S. C., Dong, H. S., Zhang, X. H., Chung, Y. W., Yuan, Y. Y., Yang, W. X.,Chan, H. C. (2007) "Cystic fibrosis transmembrane conductance regulator is vital to sperm fertilizing capacity and male fertility." *PNAS* 104, 9816 - 9821

Yanagimachi, R. (1994) "Fertility of mammalian spermatozoa: its development and relativity" *Zygote (Cambridge, England)* 2, 371-372

Yanagimachi, R., Yanagimachi, H.,Rogers, B. J. (1976) "The use of zona-free animal ova as a test-system for the assessment of the fertilizing capacity of human spermatozoa." *Biology of reproduction* 15, 471 - 476

Yang, C., Zeng, X. H., Zhou, Y., Xia, X. M.,Lingle, C. J. (2011) "LRRC52 (leucine-rich-repeat-containing protein 52), a testis-specific auxiliary subunit of the alkalization-activated Slo3 channel." *Proc Natl Acad Sci U S A.* 108, 19419 - 19424

Ye, G., Chen, C., Han, D., Xiong, X., Kong, Y., Wan, B.,Yu, L. (2006) "Cloning of a novel human NHEDC1 (Na+/H+ exchanger like domain containing 1) gene expressed specifically in testis." *Mol Biol Rep* 33, 175 - 180

Yeung, C. H., Cooper, T. G., Oberpenning, F., Schulze, H.,Nieschlag, E. (1993) "Changes in movement characteristics of human spermatozoa along the length of the epididymis." *Biology of reproduction* 49, 274 - 280

Zeng, X. H., Navarro, B., Xia, X. M., Clapham, D. E.,Lingle, C. J. (2013) "Simultaneous knockout of Slo3 and CatSper1 abolishes all alkalization- and voltage-activated current in mouse spermatozoa." *The Journal of general physiology* 42, 305 - 313

Zeng, X. H., Yang, C., Kim, S. T., Lingle, C. J.,Xia, X. M. (2011) "Deletion of the Slo3 gene abolishes alkalization-activated K+ current in mouse spermatozoa." *Proc Natl Acad Sci U S A.* 108, 5879 - 5884

Zeng, X. H., Yang, C., Xia, X. M., Liu, M.,Lingle, C. J. (2015) "SLO3 auxiliary subunit LRRC52 controls gating of sperm KSPER currents and is critical for normal fertility." *Proc Natl Acad Sci U S A. 2015* 112, 2599 - 2604

Zeng, Y., Clark, E. N.,Florman, H. M. (1995) "Sperm membrane potential: hyperpolarization during capacitation regulates zona pellucida-dependent acrosomal secretion." *Dev Biol.* 171, 554 - 563

Zeng, Y., Oberdorf, J. A.,Florman, H. M. (1996) "pH regulation in mouse sperm: identification of Na(+)-, Cl(-)-, and HCO3(-)-dependent and arylaminobenzoate-dependent regulatory mechanisms and characterization of their roles in sperm capacitation" *Developmental biology* 173, 510-520

Zhao, M., Gold, L., Ginsberg, A. M., Liang, L. F.,Dean, J. (2002) "Conserved furin cleavage site not essential for secretion and integration of ZP3 into the extracellular egg coat of transgenic mice." *Mol Cell Biol* 22, 3111 - 3120

6 Appendix

Table 14: Primer sequences

Primer	5` → 3` sequence	Construct
#C2399	GGCGAATTCAAGCTTGCCACCATGGGG	pHLsec-mZP1intHis pHLsec-mZP2intHis pHLsec-mZP3intHis
#C2400	ACAAAGCCAGGTTCCAGATGCAGACGC	pHLsec-mZP1intHis
#C4001	AGCGTCTGCATCTGGAACCTGGCTTTG	pHLsec-mZP1intHis
#C2402	CCTGTGATGGTGATGGTGTGGTGCATCTCCATGCACACTGAGAG	pHLsec-mZP1intHis
#C2403	GCACACCACCATCACCATCACAGGCGTCGACGATCCTCTGGTC	pHLsec-mZP1intHis
#C2404	AGTCTCGAGTTACTAATATCTGATGCCTTCCCAGAG CTTC	pHLsec-mZP1intHis
#C2405	CTGTGATGGTGATGGTGGTGCAGTGATGCAGGGCAAGTCACAG	pHLsec-mZP2intHis
#C2406	CTGCACCACCATCACCA TCACAGGAGCAAACGAGAGGCCAACAAAG	pHLsec-mZP2intHis
#C2407	AGTCTCGAGTTACTAGTGATTGAACCTTATAGTTCTTTTCTTATAC	pHLsec-mZP2intHis
#C2408	CGGTGA TGGTGATGGTGGTGAGAAACTAGCTTGGACCACTGGCG	pHLsec-mZP3intHis
#C2409	TTCTCACCACCATCACCATCACCGAAACCGCAGGCACGTGACC	pHLsec-mZP3intHis
#C2410	AGTCTCGAGTTACTATTGCGGAAGGGATACAAGGTAGGAAG	pHLsec-mZP3intHis
#C2566	TATACCGGTATGGCGTGCAGGCAGAGAGGAG	pHLsec-hZP2intHis
#C2567	CCTGTGATGGTGATGGTGGTGAGAGGACACAGGGCAGGTCAC	pHLsec-hZP2intHis
#C2568	CTCACC ACCATCACCATCACAGGCACAGGCGAGCCACAGG	pHLsec-hZP2intHis
#C2569	ATACTCGAGCTATTAGTGATTTGACACAGTCCTTTTCTC	pHLsec-hZP2intHis
#C2578	TATACCGGTATGGAGCTGAGCTATAGGCTCTTC	pHLsec-hZP3intHis
#C2579	CGGTGATGGTGATGGTGGTGGGAAGCAGACCTGGACCACTG	pHLsec-hZP3intHis
#C2580	CCCACCACCATCACCATCACCGTAACCGCAGGCATGTGACAG	pHLsec-hZP3intHis
#C2581	ATACTCGAGCTATTCGGAAGCAGACACAGGGTG	pHLsec-hZP3intHis
C2939	GCCATAAAAGCTTGTCACCTTTAGG	Slc9b1-HA
C2940	GATGATGGCAAGCTTTTTAATGATGG	Slc9b1-HA
C2942	AGTCTGTCTGCGCTTGTCATTTGG	Slc9b1-HA
C2943	GTGAAGCTTCCACCATGAGTGAGCACGACGTAGAATCAAAC	Slc9b1-HA
C2944	GTCTCTCCTGCTGTTGTCGTCCCC	Slc9b1-HA
C2945	GGGGACGACAACAGCAGGAGAGAC	Slc9b1-HA
C2946	GTAGTCGGGCACGTCGTAGGGGTAATGATGGAAGTTCGAGAGCTCAAC	Slc9b1-HA

```
        10          20          30          40          50          60
MSEHDVESNK KDDGFQSSVT VEMSKDPDSF HEETVEPKPE LKEPEPKEPE PKEPERKEPE
        70          80          90         100         110         120
RKEPERKEPE RKEPERKVPG RRETQTKETQ TTEIERKETK KKRGTNSYCP PQGTINKTIT
       130         140         150         160         170         180
DGAALIALWT LLWALIGQEV LPGGNLFGLV VIFYSAFLGG KILEFIKIPV VPPLPPLIGM
       190         200         210         220         230         240
LLAGFTIRNV PIIYEFVHIP TTWSSALRNT ALTIILVRAG LGLDPQALKH LKGVCLRLSF
       250         260         270         280         290         300
GPCFLEACSA ALFSHFIMNF PWQWGFLLGF VLGAVSPAVV VPNMLMLQEN GYGVEKGIPT
       310         320         330         340         350         360
LLVAASSMDD IVAITGFNTF LSIVFSSGSV ISNILSSLRD VLIGVLVGIV MGVFVQYFPS
       370         380         390         400         410         420
GDQERLTQRR AFLVLSMCIS AVLGCQHIGL HGSGGLVTLV LSFMAAKRWA EEKVGIQKIV
       430         440         450         460         470         480
ANTWNVFQPL LFGLVGTEVS VESLESKTIG MCLATLGLAL SVRILSTFVL MSFANFRFKE
       490         500         510         520         530         540
KVFIALSWIP KATVQAVLGP LALETARVMA PHLEGYAKAV MTVAFLAILI TAPNGALLIG
       550         560
ILGPKILEQS EVTFPLKVEL SNFHH
```

Fig. 6.1: Mass spectrometry detection of NHA1 in mouse sperm

Ten unique peptides for NHA1 (indicated in blue) were identified in mouse sperm.

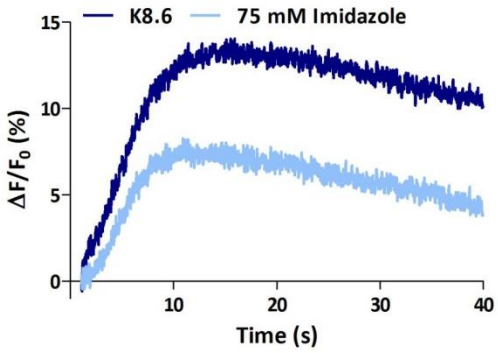

Fig. 6.2: Imidazole evokes a Ca^{2+} response in mouse sperm

(a) $[Ca^{2+}]_i$ increase evoked by K8.6 (dark blue) and 75 mMimidazole (light blue) in capacitated mouse sperm. Representative stopped-flow measurement.

7 Acknowledgement

This thesis was prepared in the department Molecular Sensory Systems at the research center caesar in Bonn. I would like to express my sincere gratitude to all colleagues for their help, cooperation and for the friendly working atmosphere. In particular, I would like to thank

- Prof. Dr. Dagmar Wachten and Prof. Dr. Timo Strünker for their scientific advice and general support in all phases of this thesis, lively discussions, constructive criticism, constant encouragement, patience, many fun moments and assistance in writing down this thesis.

- Prof. Dr. U.B. Kaupp for giving me the opportunity to work in his group and to spend a summer in Woods Hole. It was a very instructive and exciting experience.

- Dr. Jan Jikeli, Dr. Christoph Brenker, and Hussein Hamzeh for performing exeriments for my thesis and Dr. Wolfgang Bönigk for his help with cloning.

- Jessica Hierer for her indispensable help with cell culture as well as Sybille Wolf-Kümmeth, Anne Bücker and Jens-Henning Krause for their general assistance in the lab.

- Isabel Lux, Dana Herborn and Mona Völker for their assistance in everything relating to mice.

- Dr. Heinz Körschen and Dr. Luis Alvarez for their scientific support and many stimulating discussions.

- Heike Krause for taking care of all the administrative details.

- All my fellow PhD students and Postdocs for their friendship, a pleasant working atmosphere, much appreciated help, and a lot of fun. Special thanks goes to all members of the Molecular Physiology and former Sperm Physiology group.

- My family and friends for their unreserved love, faith, and support.